2012

ASSESSMENT OF CONDUCTIVITY SENSORS PERFORMANCE FOR MONITORING MINED LAND DISCHARGED WATERS AND AN EVALUATION OF THE HYDROLOGIC PERFORMANCE OF THE GUY COVE STREAM RESTORATION PROJECT

Travis Pritchard Maupin
University of Kentucky, travis.maupin@gmail.com

STUDENT AGREEMENT:

I represent that my thesis or dissertation and abstract are my original work. Proper attribution has been given to all outside sources. I understand that I am solely responsible for obtaining any needed copyright permissions. I have obtained and attached hereto needed written permission statements(s) from the owner(s) of each third-party copyrighted matter to be included in my work, allowing electronic distribution (if such use is not permitted by the fair use doctrine).

I hereby grant to The University of Kentucky and its agents the non-exclusive license to archive and make accessible my work in whole or in part in all forms of media, now or hereafter known. I agree that the document mentioned above may be made available immediately for worldwide access unless a preapproved embargo applies.

I retain all other ownership rights to the copyright of my work. I also retain the right to use in future works (such as articles or books) all or part of my work. I understand that I am free to register the copyright to my work.

REVIEW, APPROVAL AND ACCEPTANCE

The document mentioned above has been reviewed and accepted by the student's advisor, on behalf of the advisory committee, and by the Director of Graduate Studies (DGS), on behalf of the program; we verify that this is the final, approved version of the student's dissertation including all changes required by the advisory committee. The undersigned agree to abide by the statements above.

Travis Pritchard Maupin, Student

Dr. Carmen T. Agouridis, Major Professor

Dr. Dwayne R. Edwards, Director of Graduate Studies

ASSESSMENT OF CONDUCTIVITY SENSORS PERFORMANCE FOR MONITORING MINED LAND DISCHARGED WATERS AND AN EVALUATION OF THE HYDROLOGIC PERFORMANCE OF THE GUY COVE STREAM RESTORATION PROJECT

THESIS

A thesis submitted in partial fulfillment of the
requirements for the degree of Master of Science in
Biosystems and Agricultural Engineering in the College
of Engineering at the University of Kentucky

By

Travis Pritchard Maupin

Lexington, Kentucky

Director: Dr. Carmen T. Agouridis, Assistant Professor of Biosystems and Agricultural Engineering

Lexington, Kentucky

2012

ABSTRACT OF THESIS

ASSESSMENT OF CONDUCTIVITY SENSORS PERFORMANCE FOR MONITORING MINED LAND DISCHARGED WATERS AND AN EVALUATION OF THE HYDROLOGIC PERFORMANCE OF THE GUY COVE STREAM RESTORATION PROJECT

The surface mining method of mountaintop removal has been shown to adversely affect the water quality and hydrologic characteristics of downstream regions. Based on recent scientific literature, the U.S. EPA issued guidance on the specific conductivity (EC_{25^oC}) of waters discharged from mined lands in the Appalachian Coal Belt Region stating that these waters should have an EC_{25^oC} less than 300-500 $\mu S\ cm^{-1}$. Hence, accurately measuring EC_{25^oC} levels of mine discharged waters has significant implications. Furthermore, the development of reclamation techniques that positively impact the hydrological and water quality aspects of valley fill (VF) discharge is needed. To tackle these questions, a two-part study was conducted. First, a detailed study comparing sensor performance under controlled and field conditions was performed. Second, the hydrologic parameters (storm flow only) of a stream restoration project constructed atop a retrofitted valley fill were compared to a headwater stream with no mining as well as one influenced by mining with no restoration. Results indicated that significant differences were noted between four conductivity sensors with errors positively correlated with increases in EC_{25^oC}. For storm events, the restored stream section atop the VF is performing similar to the unminded, forested watershed for some hydrologic parameters.

Keywords: coal mining, Appalachia, water quality, electrical conductivity, Hydrology

Travis Prichard Maupin
Signature

June 8, 2012
Date

ASSESSMENT OF CONDUCTIVITY SENSORS PERFORMANCE FOR MONITORING MINED LAND DISCHARGED WATERS AND AN EVALUATION OF THE HYDROLOGIC PERFORMANCE OF THE GUY COVE STREAM RESTORATION PROJECT

By

Travis Pritchard Maupin

Carmen T. Agouridis
Director of Thesis

Dwayne R. Edwards
Director of Graduate Studies

June 8, 2012
Date

for my family

ACKNOWLEDGEMENTS

My educational and research experiences were greatly enhanced by my family, advisors, committee members, and fellow graduate students. Without their help and support this project would not have been possible. I would also like to thank all the faculty and staff in the Biosystem and Agricultural Engineering Department for always having their door open for questions or equipment needs and for their added encouragement and assistance throughout the project.

A special thanks to Alex Fogle and Otto Hoffman for their help with field equipment and installation. The tips and tricks learned from their experiences made data evaluation and organization much less time consuming and efficient. My committee members, Dr. Richard Warner and Dr. Chris Barton were always open for questions and provided valuable insight to many aspects of the project.

I would especially like to thank my advisor, Dr. Carmen Agouridis, for the opportunity and mentoring. I was able to learn many valuable engineering concepts that will transition directly to industry. Without her direction and countless hours of editing help this thesis would not have been possible.

TABLE OF CONTENTS

LIST OF TABLES

LIST OF FIGURES

CHAPTER 1: INTRODUCTION

The surface mining method of mountaintop removal is commonly used to extract coal in the mountainous terrain of the Appalachian Coal Belt Region (Peng, 2000). The excess spoil or overburden that results from this practice is placed in valleys adjacent to its point of extraction. This spoil placement creates valley fills (VFs) that often cover existing streams. Alterations to the hydrologic and water quality characteristics in downstream regions are a result of covering the existing steam systems (Hartman et al., 2005). Precipitation and groundwater permeate through the overburden picking up contaminates, which are subsequently discharged from the toe of the fill as surface water (Pond et al., 2008). Research has shown that the water quality downstream of valley fills exhibits increased levels of electrical conductivity, suspended sediments, and dissolved minerals (USEPA 2005; Fritz et al., 2008). Traditional surface mine reclamation practices have resulted in high compaction rates with ground cover that is largely composed of grasses. This reclamation practice has resulted in lands with low infiltration rates, increased discharge, and poor reforestation potential (Angel et al., 2009; Burger et al., 2005). Recent interest in improving the quality of waters discharged from valley fills has promoted research into various new reclamation techniques to improve hydrological, water quality, and ultimately ecological aspects of watersheds that have been impacted by mining operations.

Past reclamation techniques were largely dictated by the Surface Mining Control and Reclamation Act (SMCRA) that was enacted by Congress in 1977. The legislation endorsed mining and reclamation practices that would better benefit the environment. The Act required returning the landscape to its approximate original contour and planting vegetation to reduce sedimentation. To meet the standards of the SMCRA relating to land stability and reduced erosion many of the reclamation methods were characterized by high compaction rates and the use of dense ground covers such as grasses and legumes (Burger and Evans, 2010). Tree growth and survival in these areas was found to be poor due to the high compaction of soils and tenacious vegetation used as ground cover (Angel et al., 2009).

To increase the reforestation potential of mined lands, Burger et al., (2005) proposed guidelines known as the Forestry Reclamation Approach (FRA). The FRA promotes the use of a non-compacted suitable growth medium. This medium shall be loosely applied with

limited compaction to allow for increased water infiltration, root penetration and gas exchange (Angel et al., 2009). This approach can be summarized in five steps:

1. The top 4 to six feet should be comprised of topsoil to create a suitable growth medium,
2. The growth medium should be loosely graded to create a non-compacted layer,
3. Ground covers that are planted should be compatible with growing trees,
4. Two types of trees should be planted to promote early successional species for wildlife and soil stability, and
5. Use proper tree planting techniques (Burger et al., 2005).

Research conducted by the University of Kentucky and Virginia Tech has shown that productive forestland can be created on reclaimed mine land by using the FRA (Burger et al., 2005; Graves et al., 2000).

The U.S. Environmental Protection Agency (USEPA) has recently issued guidance specifying a range of acceptable specific conductivity levels for Appalachian streams within mined watersheds. The USEPA (2010a) states that in order to protect 95 percent of aquatic life, stream systems need to have specific conductivity values less than 300 $\mu S\ cm^{-1}$ but will allow for values up to 500 $\mu S\ cm^{-1}$. New mine permits will require in-stream water quality and biological monitoring to ensure compliance with permit conditions. Preliminary studies by the USEPA have not specified precise timeframes for sites to successfully return to acceptable levels. There is also very little guidance as to what monitoring practices and methods should be followed to ensure results are consistent and representative of the true water quality in the stream systems. How often should specific conductance samples be taken? When should sampling occur or be avoided? What, if any, other parameters should be monitored in conjunction with specific conductance?

In light of the USEPA guidance, understanding and evaluating reclamation techniques, specifically with regards to water quality, is a necessary step in the development of guidelines for mined land reclamation practices and monitoring methods. Agouridis et al. (2012) demonstrated that the FRA positively impacts water quality of discharged waters with specific conductance levels under 500 $\mu S\ cm^{-1}$ within a two-year period. Stream restoration used in conjunction with FRA holds promise a way to further reduce the impacts of mining. The Guy Cove stream restoration project was the first of its kind to demonstrate that a

stream could be constructed on a valley fill. Results from the third year monitoring period show the stream to be stable with salamanders and macroinvertebrates colonizing the site (Agouridis et al., 2011). By comparing the Guy Cove stream restoration project to an unmined reference location and an unrestored valley fill, knowledge will be gained regarding the impacts of this project on the hydrology and water quality of a valley fill.

OBJECTIVES

Research was conducted to evaluate specific conductance sensors and to characterize the hydrology of the Guy Cove stream restoration project. Data acquisition and analysis focused on accomplishing the following three objectives:

1. Evaluate the accuracy and temporal consistency of four continuously recording conductivity sensors in a laboratory setting (Chapter 2).
2. Evaluate the temporal consistency of four continuously recording conductivity sensors in a field setting (Chapter 3).
3. Characterize the hydrology of the restored intermittent stream in Guy Cove.

ORGANIZATION OF THESIS

Chapter 1 provides an overview of the research problem and objectives. Chapters 2, 3, and 4 provide a detailed description of work done to satisfy the objectives of the thesis. Chapter 5 discusses conclusions of the research. Chapter 6 highlights potential future work.

CHAPTER 2: LABORATORY EVALUATION OF CONDUCTIVITY SENSOR ACCURACY AND TEMPORAL CONSISTENCY

Electrical conductivity (EC) is the measure of the ability of water to pass an electric current (Hayashi, 2003) and is a function of the both types and quantities of dissolved substances or ions (e.g. calcium, magnesium, sodium, potassium, sulfate, bicarbonate, chloride) in solution (Chapman et al., 2000; Wagner et al., 2006). Increases in EC are linked to increases in the concentration of ions. For this reason combined with the fact that EC measurements can be taken rapidly and inexpensively, EC serves a common surrogate for total dissolved solids (TDS) concentrations (Tchobanoglous et al., 2003). Equation 2.1 can be used to estimate the TDS concentration for a wide spectrum of water samples given an EC value.

(2.1)

In addition to ion concentrations, EC is largely dependent on temperature, and thus needs to be corrected to a common temperature (25°C) to allow for comparison of values across sites and times (Hayashi, 2004). Such temperature corrected EC is termed specific conductance ($EC_{25°C}$).

The composition of ions comprising TDS is affected by a number of factors such as geology, land use, and precipitation (Kimmel and Argent, 2010; Barton, 2011). Presently, no national water-quality criterion exists for TDS (USEPA, 2012). The issue of TDS, and hence EC, is particularly relevant to the Central Appalachia Coal Fields of the U.S. This region includes portions of Kentucky, Tennessee, Virginia, and West Virginia. Within this Appalachian Coal Fields, coal is commonly extracted via mountain top mining (MTM) (USEPA, 2011a). The process of MTM involves the removal of rock and soil from the mountain top through the use of explosives in order to reach the underlying coal seams. Part of the overburden is used to regrade the surface to the approximate premining contour. Since all of the overburden cannot be used in the regarding process due to volumetric expansion from the extraction process, the excess is placed in adjacent valleys (Barton, 2011; Lindberg et al., 2011; USEPA, 2011a). From 1985 to 2001, the USEPA (2005) reports that valley fills buried an estimated 1,165 km of streams in the Central Appalachian Coal Fields.

As noted by Barton (2011), the process of extracting coal via MTM or other surface mining techniques produces high levels of TDS due to the blasting of consolidated rock into smaller rocks. Smaller sized rock fragments mean that water can come into contact with a greater amount of surface area thus increasing the rate at which the particles dissolve. More rapid dissolution of particles means greater levels of dissolved constituents entering headwater streams. Research has shown that elevated levels of TDS, and hence EC, can negatively impact aquatic life (Black, 1977; Pond et al., 2008); however, what is likely more important is the combination and concentration of ions within the water (Chapman et al., 2000). As noted by Barton (2011), two streams can have good water quality and high biodiversity but very different conductivity levels. He noted that stream in central Kentucky with high aquatic diversity typically had and average EC_{25^oC} of 500 $\mu S\ cm^{-1}$ while similar high aquatic diversity streams in eastern Kentucky has an average EC_{25^oC} of 50 $\mu S\ cm^{-1}$ – a ten-fold difference.

Pond et al. (2008) explored the effects of MTM on downstream aquatic communities in the Central Appalachians of West Virginia. A total of 27 small streams down-gradient of MTM operations and 10 small streams in unmined watersheds were examined. The authors found a negative correlation between biologic condition and EC_{25^oC}. Results showed that significantly fewer taxa and a lower percentage of insects belonging to the Ephemeroptera family were found in these streams when EC_{25} levels were greater than 500 $\mu S\ cm^{-1}$. Other studies conducted in the region, outlined by the USEPA (2011a), point to a similar degraded biological condition in streams influenced by MTM. However, in large response to the Pond et al. (2008), the USEPA issued guidance in April 2010 (final guidance memo issued in July 2011) indicating that waters discharged from mines in Appalachia should have EC_{25^oC} levels not to exceed 300-500 $\mu S\ cm^{-1}$ (Barton, 2011; USEPA, 2011b). Such a standard is challenging, and in order for mining operators to meet it, new mining and reclamation techniques are required. Presently, research is ongoing at the University of Kentucky to evaluate reforestation using the Forestry Reclamation Approach (Agouridis et al., 2012) as well as other mining best management practices related to source reduction and stream restoration in an effort to achieve the conductivity levels set forth by the USEPA (Agouridis et al., 2009; Warner and Agouridis, 2010).

Being able to accurately determine specific conductance levels of mine discharge waters has significant implications for the USEPA as well as mine operators particularly as specific conductance levels approach the designated thresholds. As a parallel, laboratory and field research into soil moisture sensors has demonstrated that performance among those sensors can differ significantly (Yoder et al., 1998; Leib et al., 2003) causing one to speculate that a similar situation is likely present for electrical conductivity sensors. Presently, a number of conductivity sensors are available on the market; however, a detailed study comparing sensor performance under controlled conditions has not been performed.

This study was conducted to compare the performance of four commercially available continuously recording conductivity sensors. Although the USEPA does not specify the collection of continuous $EC_{25^{o}C}$ readings for permitting, continuously recording sensors were selected because they provide the greatest insight into $EC_{25^{o}C}$ fluctuations which can be quite notable (Ahearn et al., 2005) particularly during storm events (Kobayashi et al., 1990). The objectives of the study were to: (1) evaluate sensor measurement stability over time (i.e. consistency); and (2) evaluate sensor accuracy at known specific conductivity levels.

METHODS

EXPERIMENTAL PROCEDURE

A laboratory experiment was conducted in 2010 at the University of Kentucky Biosystems and Agricultural Engineering Water Quality Laboratory in Lexington, Kentucky. Four commercially available conductivity sensors, capable of continuous monitoring, were evaluated: YSI 6600 V2-4 data sonde, HOBO U-24-001, Solinst Model 3001 LTC Levelogger Junior, and In-situ Aqua TROLL 100. Henceforth, the sensors will be referred to as YSI, HOBO, Solinst, and Aqua TROLL, respectively. A total of six YSI, six HOBO, three Solinst, and three Aqua TROLL sensors were tested. The difference in the number of each type of sensor tested was due to budgetary constraints. Each sensor was tested at seven temperature levels (5, 10, 15, 20, 25, 30 and 35°C) for six National Institute of Standards and Technology (NIST) traceable EC_{25} standards (5.66, 10.08, 98.9, 999, 1,411 and 9,986 $\mu S\ cm^{-1}$) resulting in 42 temperature and EC_{25} combinations. The NIST standards used potassium chloride. With the exception of the 9,986 $\mu S\ cm^{-1}$, the NIST standards were selected to represent the wide range of temperatures and EC_{25} values expected at streams in forested watersheds as well as streams down-gradient of MTM operations (Fritz et al., 2010). The

9,986 μS cm^{-1} NIST standard was chosen because it is closest to $EC_{25°C}$ values measured at coal processing effluent (Kennedy et al., 2003). Conductivity and temperature data were recorded at 15 second intervals for a 15 minute period for the YSI, HOBO, and Solinst sensors yielding 60 observations per temperature and $EC_{25°C}$ combination. For the Aqua TROLL sensors, the minimum sampling interval was one-minute, so 15 observations were obtained for each temperature and $EC_{25°C}$ combination.

All testing occurred in a Lauda Ecoline Staredition RE 220 water bath (Lauda-Königshofen, Germany) to allow for precise temperature control. Conductivity sensors were placed in the respective standards, and the temperature in the water bath was allowed to equilibrate at each tested temperature for 45 minutes prior to data collection. Hollow polypropylene balls were placed on the water surface of the water bath, in all unoccupied locations, to prevent evaporation and to help maintain a constant temperature in the water bath by providing a thermal insulation barrier between the water and the surrounding air. For the YSI and Aqua TROLLs, the sensors were placed in their respective calibration cups. Calibration cups were not provided for the Solinst and HOBO conductivity sensors. As such, conductivity standards were placed in 200 mL beakers, and the tops of the beakers were covered with parafilm to prevent evaporation. In all instances, a sufficient volume of conductivity standard was added to ensure both the temperature and conductivity components of the sensors were fully submerged.

SENSOR DESCRIPTION

A brief description of each sensor evaluated in the study follows. The descriptions include information on operating parameters, calibration technique, and the manufacturer of the sensors.

YSI

The YSI data sonde is equipped with a 6560 conductivity and temperature probe to discretely or continuously record data. The YSI measures conductivity using four pure nickel electrodes: two electrodes are current driven while the other two measure voltage drop, which is converted into a conductance value. The full conductivity range of the sensor is 0 to 100,000 μS cm^{-1} with a reported accuracy of ±0.5 percent of the reading plus 1 μS cm^{-1}. Resolution of the conductivity sensor is range dependent and varies from 1 to 100 μS cm^{-}

[1]. The conductivity sensor is very linear over the full conductivity range. Specific conductance is determined using Equation 2.2.

(2.2)

The variable $EC_{25°C}$ is specific conductance (conductivity corrected to 25ºC), µS cm^{-1}; EC is the raw conductivity value (non-temperature corrected conductivity), µS cm^{-1}; TC is temperature coefficient (0.0191 per degree Celsius); and T is the raw temperature value. Temperature is measured using a thermistor with a range of -5 to 50ºC and an accuracy of ±0.15ºC. Resolution of the temperature sensor is 0.01ºC.

Calibration of the conductivity sensor was performed per manufacturer's specifications. The manufacturer supplied calibration cups were filled with manufacturer recommended NIST traceable calibration solution (9,986 µS cm^{-1}) ensuring the sensor was fully submerged. Next, the YSI was shaken vigorously to expel any bubbles from the conductivity sensor. No calibration of the temperature sensor was required. The YSI was manufactured by YSI Incorporated, Yellow Springs, OH, USA. (www.ysi.com).

HOBO

The HOBO U24-001 is a continuous conductivity and temperature data logger designed for freshwater environments. The HOBO is a non-contact sensor meaning a magnetic field is used to determine conductivity (Rizzoni, 1993). The full-calibrated conductivity range for the sensor is 0 to 10,000 µS cm^{-1} with a full range accuracy of 3 percent of the reading or 20 µS cm^{-1}, whichever is greater. Resolution of the conductivity sensor is 1 µS cm^{-1}. Temperature is measured using a thermistor with a range of 5 to 35ºC and an accuracy of ±0.1ºC. Resolution of the temperature sensor is 0.01ºC. For the HOBO sensor, $EC_{25°C}$ can be calculated linearly using equation 2 with a default TC of 0.021 per degree Celsius though this value can be adjusted by the user. Specific conductance can also be calculated non-linearly using a natural water compensation per EN 27888 (*Determination of Electrical Conductivity*). This study used the non-linear method of determining $EC_{25°C}$.

Calibration of the conductivity sensors was performed per manufacturer's specifications. The manufacturer states that temperature and conductivity readings from a secondary source are required at the beginning and end of deployment to assist in post-processing of data and to help account for sensor drift that may occur during the deployment period. Temperature

readings were obtained from the water bath while the NIST specified $EC_{25°C}$ levels were used. The HOBO conductivity sensors were manufactured by Onset Computer Corporation, Cape Cod, MA, USA. (www.onsetcomp.com).

SOLINST

The Solinst Model 3001 Levelogger Junior continuously measures water level in addition to conductivity and temperature. The sensor measures conductivity using four platinum electrodes: two drive electrodes and two sensing electrodes. The full conductivity range of the sensor is 0 to 80,000 μS cm^{-1} with a reported accuracy of 2 percent of the reading or 20 μS cm^{-1}. Resolution of the conductivity sensor is 1 μS cm^{-1}. Temperature is measured using a platinum resistance temperature detector (RTD) with a range of 0 to 40°C and an accuracy of ±0.1°C. Resolution of the temperature sensor is 0.1°C. Specific conductance is also calculated using equation 2 but with a TC value of 0.02 per degree Celsius.

The Solinst sensors used in this study were factory calibrated and deployed for the first time during this study. Since the manufacturer states that the sensor requires minimal calibration (e.g. twice per year), the sensors were not recalibrated prior to the study. No calibration of the temperature sensor was required. The Solinst data loggers were manufactured by Solinst Canada Ltd., Georgetown, Ontario, Canada. (www.solinst.com).

AQUA TROLL

The Aqua TROLL 100 conductivity logger is a continuous conductivity and temperature data logger. Conductivity is measured using a balanced four-electrode conductivity cell: two electrodes are driven and two electrodes are sensing. The full conductivity range of the sensor is 5 to 100,000 μS cm^{-1} with a reported accuracy of ±0.5 percent of reading plus 1 μS cm^{-1} when less than 80,000 μS cm^{-1}; ±1.0 percent of reading when above 80,000 μS cm^{-1}. Temperature is measured using a thermistor with a range of -20 to 65°C and an accuracy of ±0.1°C. Resolution of the temperature sensor is 0.01°C. Specific conductance is also calculated using equation 2 with a TC value of 0.0191 per degree Celsius.

The Aqua TROLL data loggers used in this study were factory calibrated and deployed for the first time during this study. As recommended by the manufacture, the $EC_{25°C}$ readings were checked with the manufacturer supplied solution prior to use. As the reading were accurate, the manufacturer stated that no further calibration was required. No

calibration of the temperature sensor was required. The Aqua TROLL data loggers were manufactured by In-Situ Incorporated, Fort Collins, CO, USA (www.in-situ.com).

STATISTICAL ANALYSIS

The statistical analysis component of the project consisted of evaluating the temporal stability of the $EC_{25°C}$ readings produced by the sensors over time as well as the accuracy of these readings (i.e. how well did the measured conductivity readings match the NIST $EC_{25°C}$ standard values). A significance level of $p=0.05$ was used for all statistical analyses. All statistical analyses were performed using SAS version 9.2 (SAS Institute, Inc., 2008).

The first step in the data analysis was to examine the performance of each sensor type (YSI, HOBO, Solinst and Aqua TROLL) over time. For each sensor, linear mixed models (PROC MIXED) were used to examine the temporal stability (i.e. consistency) of the $EC_{25°C}$ measurements at each temperature level (5, 10, 15, 20, 25, 30 and 35°C) over all $EC_{25°C}$ standards combined. Wang and Goonewardene (2004) noted that the mixed model approach is preferred when dealing with repeated measures data because this model offers the user better capabilities with covariance structure modeling and missing observation management than traditional approaches such as AMOVA and MANOVA. Sensor readings were the response variable, $EC_{25°C}$ standard levels were the categorized variable, time was the continuous variable, and the interaction of the $EC_{25°C}$ standards levels and time were the fixed effects. The covariance structure used was AR(1) to account for autocorrelation resulting from repeated $EC_{25°C}$ measurements. The presence of a significant $EC_{25°C}$ standard level and time interactions indicated that, at the tested temperature, the $EC_{25°C}$ readings for all $EC_{25°C}$ standard levels combined fluctuated over time. The null hypothesis that the sensors did not exhibit temporal fluctuations in $EC_{25°C}$ measurements was evaluated using the *F* test.

If the sensors displayed temporal instability meaning a significant $EC_{25°C}$ standard level and time interaction was found, then pairwise comparisons between all $EC_{25°C}$ standard levels, for each sensor at each temperature level, were conducted. The pairwise comparisons offered insight into which $EC_{25°C}$ standard level and temperature level combinations resulted in the presence of significant fixed effects (e.g. $EC_{25°C}$ standard level and time interactions, time). For each $EC_{25°C}$ standard value at each temperature level, a slope of zero indicated that no significant temporal changes in $EC_{25°C}$ readings were present.

The null hypothesis that the slopes did not differ (i.e. the slopes were zero) was evaluated using the *F* test.

To test the ability of the sensors to accurately measure EC_{25^oC} at each temperature level, a second set of linear mixed models (PROC MIXED) were developed for each sensor. Sensor EC_{25^oC} readings were the response variable and EC_{25^oC} standard values were the continuous predictor variable. The 95 percent confidence intervals of the linear slopes were calculated for each sensor and each temperature level. The accuracy of each sensor at each temperature level was determined by comparing the estimated slope and intercept with one and zero, respectively.

RESULTS AND DISCUSSION

TEMPORAL PERFORMANCE

The results of the linear mixed models evaluating temporal stability of the EC_{25^oC} measurements at each temperature level are provided in Table 2.1 with the average slope of all sensors of a particular type as shown in Figure 2.1. For all figures, an EC_{25^oC} value of 1,411 $\mu S\ cm^{-1}$ and a temperature of 15°C were chosen for display as these values are closest, of the NIST standard levels and temperature intervals, to the mean EC_{25^oC} values and water temperatures recorded by Fritz et al. (2010) at valley fill sites in eastern Kentucky. Fritz et al. (2010) recorded average EC_{25^oC} values of about 2,500 $\mu S\ cm^{-1}$ and water temperatures of about 13°C.

If the sensors exhibited temporal stability, then slopes of EC_{25^oC} values over time should equal zero. Neither the YSI nor the Aqua TROLL sensors exhibited temporal fluctuations in EC_{25^oC} measurements for any of the temperature measurements. Figures 2.2-2.3 show the stability of the EC_{25^oC} readings over the 15-minute period for the YSI and Aqua TROLL sensors, respectively, at an EC_{25^oC} of 1,411 $\mu S\ cm^{-1}$ and a temperature of 15°C. Temporal fluctuations were noted for the Solinst sensors only for the 35°C temperature level. The reason the Solinst sensors had temporal fluctuations in EC_{25^oC} only at the 35°C temperature level is not known. While it was suspected that the temporal fluctuations in EC_{25} were due to the fact that the tested temperature of 35°C was near the temperature limit of the sensors (40°C), examination of temperature graphs did not reveal temporal fluctuations at 35°C. Otherwise, as seen in Figure 2.4, no significant temporal fluctuations were noted for the Solinst sensors.

Table 2.1 Performance of conductivity sensors with regards to temporal measurement stability (Ho = sensor does not exhibit temporal fluctuations in specific conductivity measurements).

Temperature (ºC)	YSI			HOBO			Solinst			Aqua TROLL		
	p-value[1]	F_{calc}	Reject H_o?	*p*-value	F_{calc}	Reject H_o?	*p*-value	F_{calc}	Reject H_o?	*p*-value	F_{calc}	*Reject H_o?*
5	1.0000	20.55	No	<0.0001	0.00	Yes	1.000	0.01	No	1.000	0.01	No
10	0.9999	14.25	No	<0.0001	0.01	Yes	1.000	0.00	No	1.000	0.00	No
15	1.0000	18.03	No	<0.0001	0.00	Yes	1.000	0.00	No	1.000	0.00	No
20	0.9736	30.89	No	<0.0001	0.17	Yes	1.000	0.00	No	1.000	0.00	No
25	1.0000	97.95	No	<0.0001	0.00	Yes	0.9192	0.29	No	1.000	0.00	No
30	1.0000	1.24	No	0.2878	0.00	No	0.1755	1.54	No	1.000	0.00	No
35	1.0000	0.77	No	0.5688	0.00	No	<0.0001	7.95	Yes	1.000	0.00	No

[1]Statistically significant at the p=0.05 level.

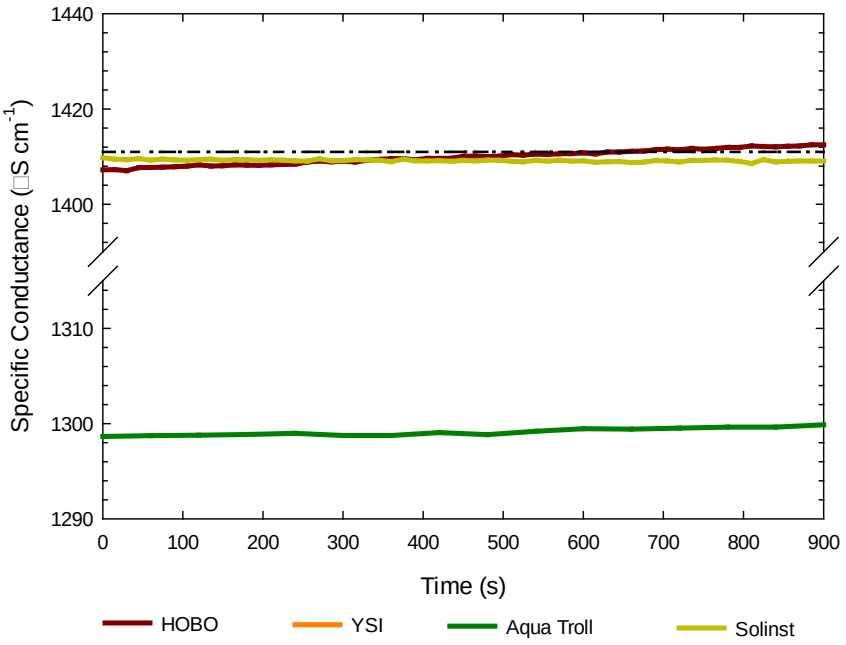

Figure 2.1 Temporal fluctuations associated with 1,411 µS cm^{-1} $EC_{25°C}$ and 15ºC temperature level for sensor type

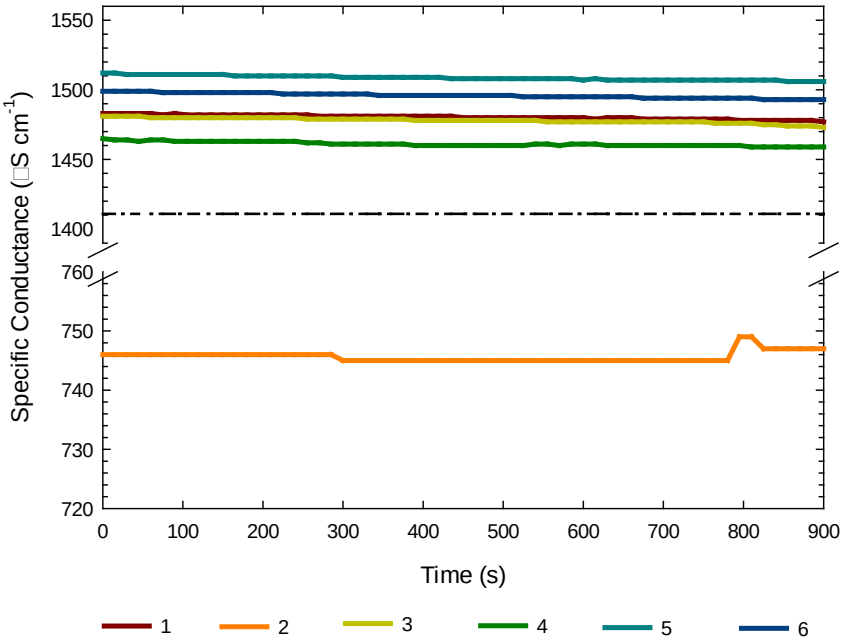

Figure 2.2 Fluctuations associated with 1,411 µS cm^{-1} $EC_{25°C}$ and 15ºC temperature level for YSI sensors

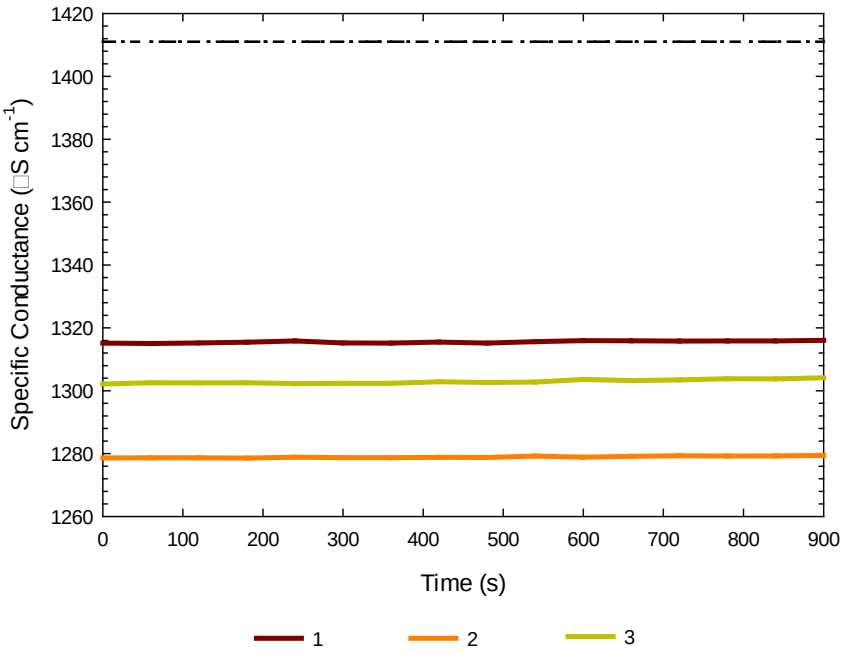

Figure 2.3 Temporal fluctuations associated with 1,411 µS cm^{-1} $EC_{25°C}$ and 15ºC temperature level for Aqua TROLL sensors

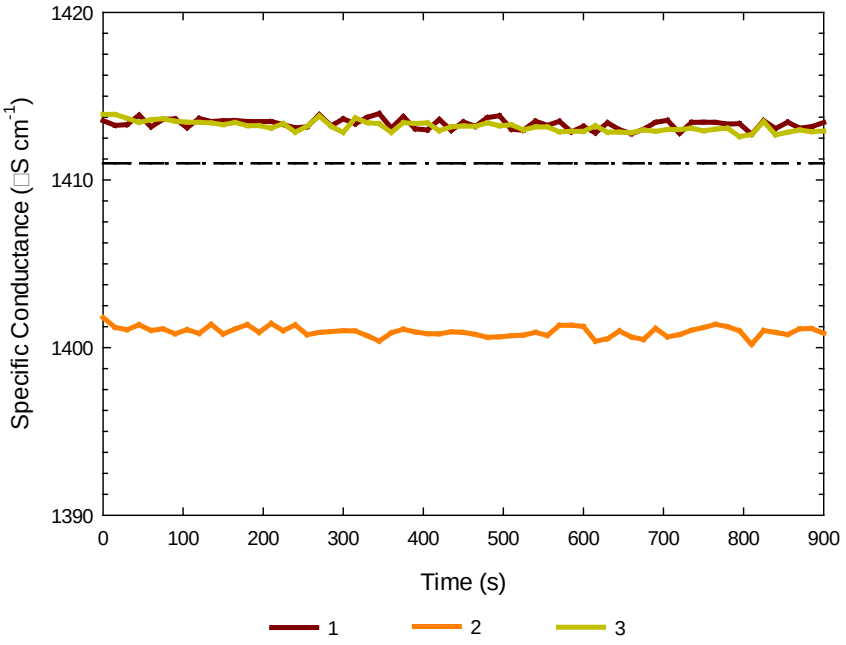

Figure 2.4 Temporal fluctuations associated with 1,411 µS cm^{-1} $EC_{25°C}$ and 15ºC temperature level for Solinst sensors

For the HOBO sensors, however, significant temporal fluctuations were noted for all of the temperature levels except 30 and 35°C. This result is surprising and the opposite of what was expected. As the HOBO sensors have a maximum rated temperature of 35°C, it was expected that these sensors would exhibit less temporal fluctuations at the lower temperatures that are well within the range of the sensor and not at higher temperatures at the limit of the range. Likewise with the HOBO sensors, temperature graphs did not reveal temporal fluctuations.

As seen in Figure 2.5 for a $EC_{25°C}$ of 1,411 μS cm^{-1} and a temperature of 15°C, the readings from the HOBO sensors tended to drift over the 15-minute monitoring period, in this case, upward. Important to note is that the presence of significant temporal fluctuations does not indicate the sensors performed in this manner for all temperature and $EC_{25°C}$ combinations. Instead, the

presence of significant temporal fluctuations means that for at least one $EC_{25°C}$ level, at the specified temperature level, the resulting slope of $EC_{25°C}$ versus time was significantly different than zero.

Results from the $EC_{25°C}$ pairwise comparisons provided insight into which $EC_{25°C}$ levels resulted in temporal fluctuations (i.e. slope ≠ 0) for the Solinst and HOBO sensors. At an $EC_{25°C}$ level of 9,986 μS cm^{-1}, the HOBO sensors consistently displayed temporal fluctuations (5, 10, 15, 20, and 25°C). These results are highlighted in Figure 2.6 for the HOBO sensors at 15°C. Like the HOBO sensors, the Solinst sensors exhibited temporal fluctuations at 9,986 μS cm^{-1} (35°C). These results were somewhat surprising for the Solinst sensors as they are rated for use up to 80,000 μS cm^{-1} and a temperature of up to 40°C. The $EC_{25°C}$ and temperature combination of 9,986 μS cm^{-1} and 35°C was within this range. However, for the HOBO sensors, the temporal fluctuations were less surprising as the $EC_{25°C}$ level for the test (9,986 μS cm^{-1}) was just under the stated full calibrated range of 10,000 μS cm^{-1} for these sensors.

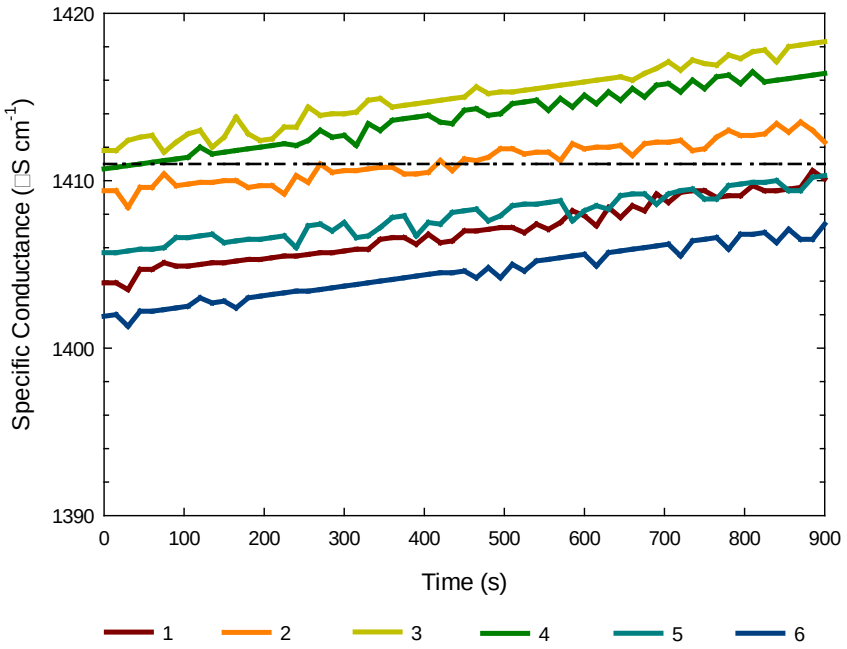

Figure 2.5 Temporal fluctuations associated with 1,411 µS cm^{-1} $EC_{25°C}$ and 15ºC temperature level for HOBO sensors

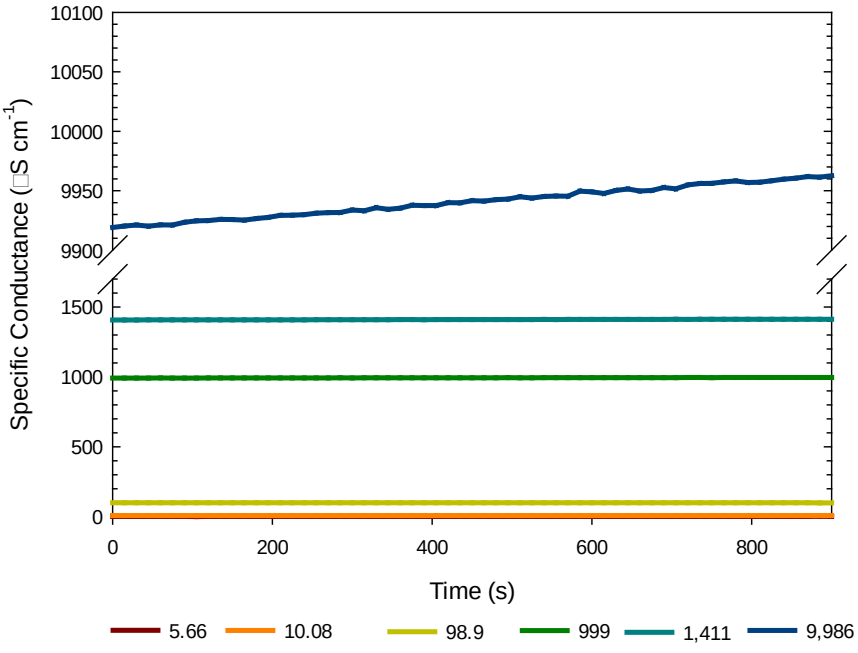

Figure 2.6 Pairwise comparisons for all $EC_{25°C}$ levels for HOBO sensor at 15ºC

ACCURACY

The results of the linear mixed models testing the ability of the sensors to accurately measure EC_{25^oC} at each temperature level are presented in Table 2.2. For all sensors at all temperature levels, the slopes of the lines generated from regressing measured EC_{25^oC} values on NIST standard EC_{25^oC} values (1:1 lines) differed statistically from one; however many of these values were quite close to one. For the YSI and Aqua Troll sensors, the slopes were consistently less than one for all temperature levels indicating that these sensors tended to under-predict or under-measure the true EC_{25} values (Figures 2.7-2.8). Except for the 5°C temperature level, the Solinst sensors also under-predicted the true EC_{25^oC} values (Figure 2.9). As for the HOBO sensors, both under- and over-prediction of true EC_{25^oC} values was seen (Figure 2.10). In all cases, the intercepts did not differ significantly from zero.

Table 2.2 Results of regressing measured specific conductivity versus specific conductivity standard values (Ho = slope equals one and intercept equals zero).

Temperature (ºC)	YSI		HOBO		Solinst		AquaTroll	
	Slope	Intercept	Slope	Intercept	Slope	Intercept	Slope	Intercept
5	0.947[r]	267.240	1.002[r]	0.166	1.008[r]	13.968	0.867[r]	36.436
10	0.926[r]	273.750	0.998[r]	0.841	0.974[r]	17.513	0.864[r]	39.788
15	0.891[r]	268.350	0.996[r]	0.345	0.953[r]	20.467	0.861[r]	42.713
20	0.867[r]	259.870	0.997[r]	-0.478	0.939[r]	24.012	0.861[r]	45.699
25	0.831[r]	280.020	1.002[r]	-1.971	0.932[r]	22.371	0.862[r]	53.588
30	0.848[r]	77.792	1.003[r]	0.250	0.937[r]	21.348	0.930[r]	4.705
35	0.850[r]	82.992	0.999[r]	-1.619	0.919[r]	29.944	0.931[r]	31.817

[1]Coefficient of determination (R^2) values for all regressed measured versus standard specific conductivity comparisons were greater than 0.999.
[2]The superscript r indicates that the null hypothesis was rejected at the p=0.05 level.

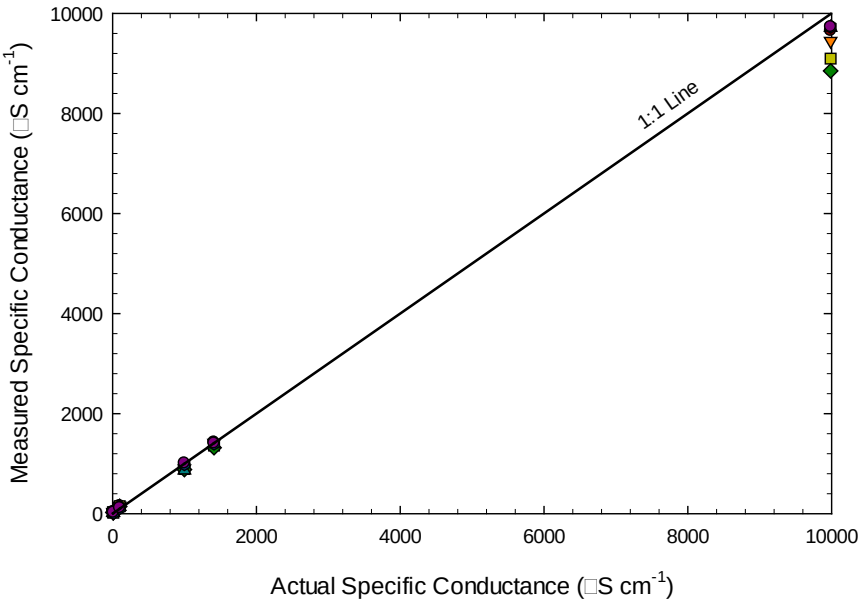

Figure 2.7 Actual $EC_{25^{o}C}$ plotted against measured $EC_{25^{o}C}$ of the YSI sensor

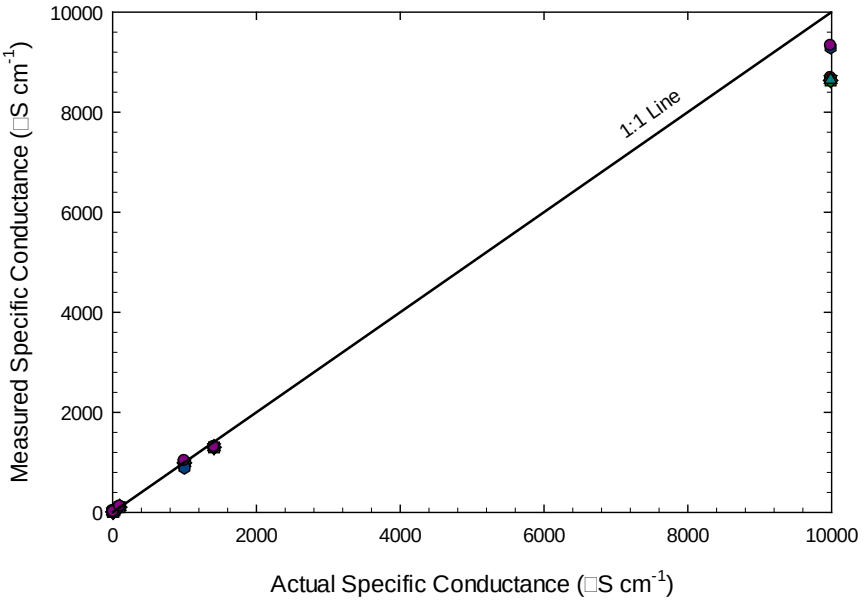

Figure 2.8 Actual $EC_{25^{o}C}$ plotted against measured $EC_{25^{o}C}$ of the Aqua TROLL sensor

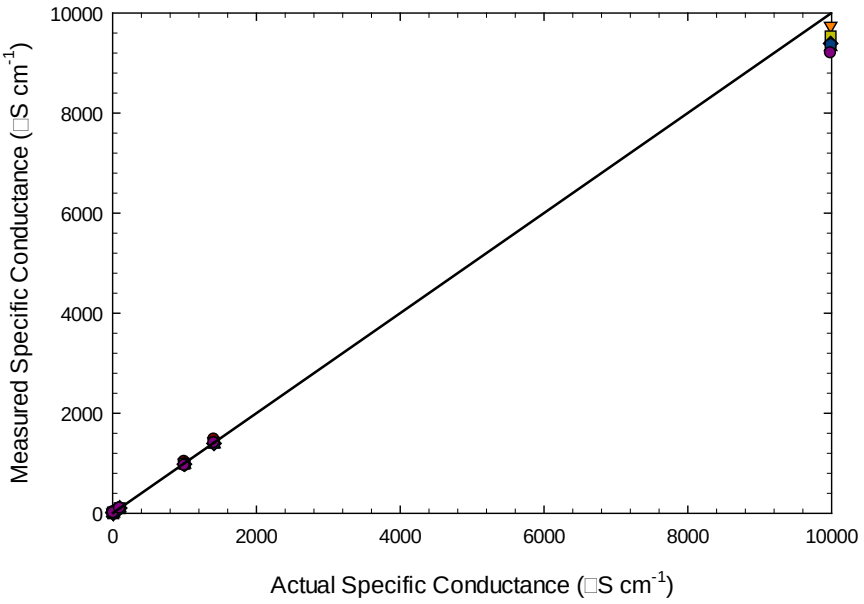

Figure 2.9 Actual $EC_{25°C}$ plotted against measured $EC_{25°C}$ of the Solinst sensor

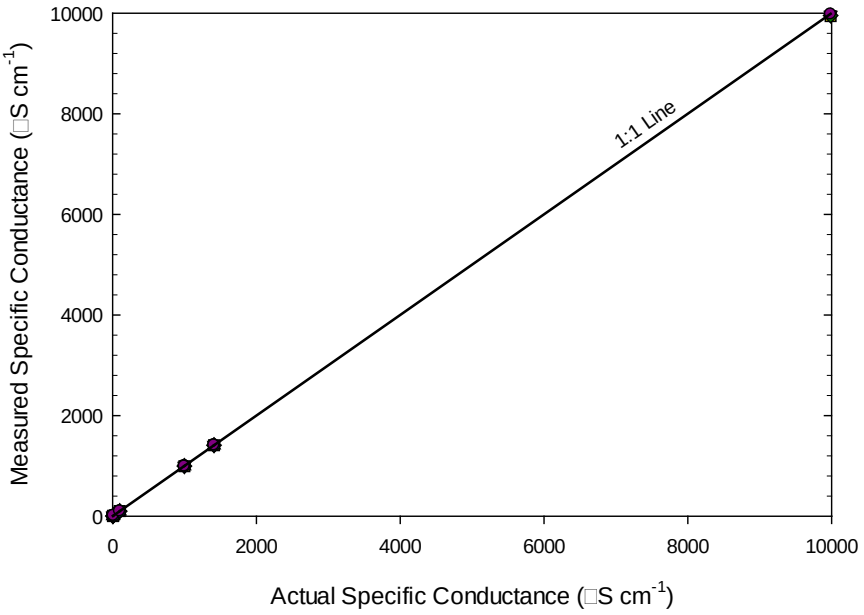

Figure 2.10 Actual $EC_{25°C}$ plotted against measured $EC_{25°C}$ of the HOBO sensor

As seen in Figures 2.7-2.10, the higher $EC_{25°C}$ level of 9,986 μS cm^{-1} was influential in evaluating sensor performance, particularly for the YSI, Solinst and Aqua TROLL sensors. Table 2.3 contains the results of rerunning the analysis without the standard value of 9,986 μS cm^{-1} (e.g. 5 to 1,411 μS cm^{-1}). As before, all slopes differed statistically from one while the intercepts did not differ from zero. No differences in over- or under-prediction trends were noted for the sensors with the exception of the YSIs. For the range of 5 to 1,411 μS cm^{-1}, the YSI sensors tended to over-predict for the temperature range of 5 to 25°C when the 9,986 μS cm^{-1} $EC_{25°C}$ level was excluded.

Though the slope of the 1:1 line for the HOBO sensors was statistically different than one, it had the best fit both with and without the inclusion of the 9,986 μS cm^{-1} standard. Excluding the 9,986 μS cm^{-1} standard, the Solinst sensors also had a comparable fit to the HOBO sensors. These results are somewhat surprising as the YSI, Solinst and Aqua TROLL sensors are rated for much higher $EC_{25°C}$ levels while the HOBO was operating near its limits.

Table 2.3 Results of regressing measured EC25ºC versus EC25ºC standard values excluding 9,986 standard value (Ho = slope equals one and intercept equals zero).[1, 2]

Temperature	YSI		HOBO		Solinst		Aqua TROLL	
(ºC)	Slope	Intercept	Slope	Intercept	Slope	Intercept	Slope	Intercept
5	1.32[r]	92.68	1.003[r]	-0.15	1.047[r]	-3.75	0.935[r]	4.83
10	1.31[r]	93.31	1.001[r]	-0.69	1.010[r]	-1.38	0.933[r]	7.60
15	1.29[r]	91.64	0.999[r]	-1.23	0.990[r]	0.68	0.934[r]	8.68
20	1.23[r]	89.48	0.999[r]	-1.38	0.984[r]	2.62	0.938[r]	9.92
25	1.26[r]	76.95	1.000[r]	-1.23	0.980[r]	0.60	0.934[r]	19.66
30	0.98[r]	16.28	1.005[r]	-0.75	0.980[r]	-0.18	0.904[r]	16.80
35	0.99[r]	19.25	0.996[r]	-0.45	0.980[r]	1.09	0.945[r]	25.48

[1]Coefficient of determination (R^2) values for all regressed measured versus standard specific conductivity comparisons were greater than 0.999.
[2]The superscript r indicates that the null hypothesis was rejected at the p=0.05 level.

INDIVIDUAL SENSOR VARIATION

Also of interest is the variation in individual sensor performance. Figures 2-5 display individual sensor $EC_{25°C}$ measurements at the 1,411 μS cm^{-1} $EC_{25°C}$ level and the 15°C temperature level. As seen in these figures, though temporal trends are the same for all sensors of a particular type, individual sensors can perform quite differently from one another. For the YSI sensors, five sensors over-predicted $EC_{25°C}$ by about 50 to 150 μS cm^{-1} while one sensor under-predicted by about 650 μS cm^{-1}. For the Aqua TROLL sensors, all three sensors under-predicted by about 100 to 140 μS cm^{-1}. The Solinst sensors were all quite close to the standard value of 1,411 μS cm^{-1}. The HOBO sensors, though displaying temporal fluctuations, were closely grouped with all sensors measuring within about 10 μS cm^{-1} of each other. These results highlight the importance of testing individual sensors prior to deployment. It should not be assumed that all sensors of a given type will perform in the same manner. Consideration should be given to the level of variation allowed amongst sensors.

CONCLUSIONS

Four $EC_{25°C}$ sensor types (six YSI, six HOBO, three Solinst, and three Aqua Troll) were evaluated at seven temperature levels (5, 10, 15, 20, 25, 30 and 35°C) and six NIST traceable $EC_{25°C}$ standards (5.66, 10.08, 98.9, 999, 1,411 and 9,986 μS cm^{-1}) to assess sensor performance with regards to temporal stability and accuracy. All sensors were factory calibrated or locally calibrated per manufacturer's recommendations. The YSI and Aqua TROLL sensors exhibited temporal stability over the $EC_{25°C}$ and temperature ranges evaluated while the Solinst and HOBO sensors did not. For the Solinst sensors, temporal fluctuations were found only at 35°C; such fluctuations were noted at 5, 10, 15, 20, and 25°C for the HOBO sensors. Results of pairwise comparisons for the sensors demonstrating temporal fluctuations found that the highest tested $EC_{25°C}$ of 9,986 μS cm^{-1} consistently had a different slope, and hence a different response. With regards to accuracy, regression of measured $EC_{25°C}$ values on NIST standard $EC_{25°C}$ values revealed that, for all sensor types, slopes differed from one regardless of whether the 9,986 μS cm^{-1} standard was included or excluded from the analysis. For conditions more frequently encountered in streams in eastern Kentucky (e.g. excluding the 9,986 μS cm^{-1} $EC_{25°C}$ level), the YSI tended to over-

predict and the Aqua TROLL tended to under-predict. The HOBO and Solinst sensors had the best fits.

Examination of the individual sensors within each sensor type revealed that in many instances at least one sensor performed quite differently than the others of the same type. For the examples presented herein for the EC_{25} and temperature combination of 1,411 μS cm^{-1} and 15°C, which are levels common for waters discharging mined lands (Frtiz et al., 2010), within sensor type differences could be relatively large (~150 μS cm^{-1} for the YSIs; ~140 μS cm^{-1} for the Aqua TROLLs) or small (~10 μS cm^{-1} for the HOBOs; ~5 μS cm^{-1} for the Solinsts). Careful attention should be paid to such differences in individual sensor performance, particularly when the sensor is used for regulatory enforcement. For the sensors tested, it is quite possible that one sensor could indicate a stream was in compliance with the 300-500 μS cm^{-1} threshold established by the USEPA (USEPA, 2011) while another sensor of the same type could indicate non-compliance. It is recommended that $EC_{25°C}$ sensors used in instances where the determination of regulatory compliance is done be regularly checked against NIST $EC_{25°C}$ standards.

In addition to performance, the choice of which $EC_{25°C}$ sensor to purchase also requires consideration of costs, both unit and fixed, as well as additional parameters that a particular sensor can monitor and calibration needs of the sensor. For the sensor types evaluated, costs varied considerably as seen in Table 2.4. The YSI had the largest initial cost at $7,000 U.S. (sensor and fixed software and communication costs); however, the YSI also had the capability of monitoring the largest number of parameters. Additional components can be added to the YSI to allow the simultaneous monitoring of rhodamine, turbidity, dissolved oxygen, water depth, pH, ORP, and blue-green algae in addition to $EC_{25°C}$ and temperature. The Solinst, at a cost of $1,385 U.S. (sensor and fixed software and communication costs) also measures water level. With regards to calibration, the HOBO sensors are the only ones examined in this study that require a secondary device to measure $EC_{25°C}$ and temperature at the beginning and ending of deployment to account for sensor drift.

As the results of this study provide insight into conductivity sensor performance with regards to temporal stability and accuracy in a controlled environment, care should be taken when extrapolating these results to field conditions. Under field conditions, natural conductivity levels can fluctuate widely and sensor fouling can occur. These factors are

Table 2.4 Cost comparison of tested specific conductivity sensors.

Sensor	Sensor Unit Cost ($U.S)	Software and Communications Fixed Cost ($U.S)[2]	Parameters Monitored
YSI	6,450[1]	550	$EC_{25°C}$, temperature[4]
HOBO	700	450[3]	$EC_{25°C}$, temperature
Solinst	1,200	185	$EC_{25°C}$, temperature, water level
Aqua Troll	1,800	500	$EC_{25°C}$, temperature

[1] $EC_{25°C}$ and temperature sensors are supplied with sonde. Measurement of additional parameters possible with the purchase of additional add-on sensors. These costs are for each site monitored.
[2]Includes software for managing data and download and communications cables. These costs are fixed regardless of the number of sites monitored.
[3]HOBO sensors require $EC_{25°C}$ and temperature measurements from a secondary device for data post-processing. Secondary measurements must be taken at the beginning and ending of deployment. The costs of a secondary device are not included in the table.
[4]Additional components can be added to sonde to measure rhodamine, turbidity, dissolved oxygen, water level, pH, ORP, and blue-green algae.

expected to affect sensor accuracy to a greater extent than what was recorded in this study where conductivity levels were steady and no fouling was present. Future work is required to evaluate the performance of conductivity sensors operating under a wide-range of field conditions (e.g. temperature and $EC_{25°C}$ variations).

CHAPTER 3: FIELD EVALUATION OF CONDUCTIVITY SENSOR PERFORMANCE

Water quality characteristics fluctuate in response to changes in environmental factors such as precipitation, land use, time of day (diurnal), and season or climate (Kobayashi et al., 1990; Fogle et al., 2003; Ahern et al., 2005; Pond et al., 2008). In order to adequately account for these variations in water quality, continuous water quality monitoring sensors are recommended (Wagner et al., 2006; Henjum et al., 2010). Such high frequency in-situ monitoring is best suited for capturing cyclical trends associated with seasons or diurnal fluctuations as well as rapid changes associated with storm events (Tomlinson and De Carlo, 2003; Kirchner et al., 2004). But which continuous water quality monitoring sensors to select becomes a challenging question. Sensor selection is dependent on a number of variables including project objectives, monitoring site conditions, sensor construction and ruggedness, accuracy and precision requirements, and budget (Wagner et al., 2006; Whelan and Regan, 2006). In some cases, data from water quality sensors can serve as a surrogate for another water quality parameter (Wagner et al., 2006). Turbidity and electrical conductivity (EC) are two such examples whereby a continuously recorded parameter is used to predict levels for variables that are more expensive and time-consuming to measure. Studies have demonstrated that turbidity is a viable surrogate for total suspended solids (Miguntanna eta l., 2010; Jones et al., 2011; Williamson and Crawford, 2011) and total phosphorus (Stubblefield et al., 2007; Jones et al., 2011) while EC can serve as a surrogate for total dissolved solids (TDS) (Tchobanoglous et al., 2003; Settle et al., 2007; Miguntanna et al, 2010).

Within the Appalachian Coal Belt Region of the United States, the issue of EC has gained importance due to the realized impact of coal mining on stream water quality and biotic composition. Research has demonstrated that elevated levels of TDS, and hence EC, negatively impact aquatic life. Pond et al. (2008) found that when specific conductance ($EC_{25°C}$) levels were greater than 500 $\mu S\ cm^{-1}$, Ephemeroptera communities were negatively impacted in the Appalachian Coal Belt Region. Pond (2012) also found a negative correlation between Plecoptera and Trichoptera communities and $EC_{25°C}$ in this region. Note that EC is temperature corrected to 25°C, and thus termed specific conductivity, so that values are comparable between locations and across time. The results of these studies

and others in the region (Pond, 2010; Lindberg et al., 2011; Merriam et al., 2011) prompted the USEPA to issue guidance stating that waters discharged from mines in the Appalachian Coal Belt Region should have EC_{25^oC} levels below 300-500 μS cm^{-1} (USEPA, 2011). Therefore, accurately determining the EC_{25^oC} levels of mine discharged water is of great importance to the USEPA and mine operators alike.

Research by Maupin et al. (2012) in a controlled laboratory study found variations in performance, between four types of continuous recording conductivity sensors (YSI 6600 V2-4 sonde, HOBO U-24-001, Solinst Model 3001 LTC Levelogger Junior, and In-Situ Aqua TROLL 100), with regards to temporal stability (i.e. consistency) and accuracy. Examining 42 temperature and EC_{25^oC} combinations, the authors found that only three of the four sensors output consistent EC_{25^oC} measurements over time with temporal fluctuations greatest at the highest EC_{25^oC} standard (10,000 μS cm^{-1}). With regards to accuracy, the HOBO tended to overestimate EC_{25^oC} while the other sensors tended to underestimate EC_{25^oC} for the range of 5-9,986 μS cm^{-1}. However, for the range of 5-1,411 μS cm^{-1} which represents conditions more frequently found in streams, the YSI tended to over-predict and the Aqua TROLL tended to under-predict. Furthermore, at least one sensor within each sensor type performed quite differently than the other sensors of the same type. This result indicates that individual sensors should be examined carefully before deployment.
But because the study by Maupin et al. (2012) was performed in a controlled environment, care must be taken when extrapolating results to field conditions as these are more harsh and variable than a laboratory setting. Though Wagner et al. (2006) notes that conductivity sensors are typically reliable and durable, they are susceptible to fouling from biofilms, sediment, and ion precipitants. Fritz et al. (2010) measured elevated levels of EC_{25^oC} and dissolved constituents in waters discharged from valley fills in the Appalachian Coal Belt Region. When compared to waters discharged from reference forested watersheds, average concentrations of SO_4^{2-}, Cl^-, Mn, Mg^{2-}, Fe, and Ca^{2+} in waters discharged from valley fills were about 108, 3, 145, 73, 69, and 9 times greater, respectively. In the presence of such elevated constituent concentrations, sensor fouling and thus sensor accuracy becomes a concern (Ramos et al., 2008). Furthermore, EC_{25^oC} levels in streams can change rapidly as discharges fluctuate with values of EC_{25^oC}; EC_{25^oC} levels tend to decrease with increasing discharge (Kobayashi et al., 1990; Ahern et al., 2005). This correlation is of importance in

mined areas where hydrographs associated with valley fills are more peaked than unmined sites (Messinger 2003; Wiley and Brogan 2003). This means that conductivity sensors must have the capability of accurately recording EC_{25^oC} levels under a wide range of water quality and flow conditions.

This purpose of this study was to compare the field performance of four commercially available continuously recording conductivity sensors in both mined and unmined locations. The objectives of this study were to: (1) calculate the white noise variance associated with each sensor type, and (2) evaluate white noise variance in relation to variations in EC_{25^oC} and flow.

METHODS

SENSOR DESCRIPTION

Four conductivity sensors were evaluated in this study: YSI 6600 V2-4 data sonde, HOBO U-24-001, Solinst Model 3001 LTC levelogger Junior, and In-Situ Aqua TROLL 100. Henceforth, these sensors will be referred to as YSI, HOBO, Solinst, and Aqua TROLL, respectively. For a description of the operating parameters, calibration techniques, and manufacturer information for each sensor, see Maupin et al. (2012).

STUDY SITES

The study sites are located within the University of Kentucky's Robinson Forest. Robinson Forest is a 6,100 ha second-growth forest located in Cumberland Plateau in southeastern Kentucky. In the mid-1990s, a portion of Robinson Forest was mined for coal resulting in the creation of valley fills. On one of these valley fills (Guy Cove), ephemeral, intermittent, and perennial stream channels were created totaling about 1-mile in length (Agouridis et al., 2009). As expected with multiple landscapes, water quality characteristics of streams flowing through Robinson Forest vary considerably. For 2011, EC_{25^oC} levels in forested reaches averaged about 40 $\mu S\ cm^{-1}$; those on the restored reach of Guy Cove varied from 450-850 $\mu S\ cm^{-1}$; and those at the outlet of valley fills averaged about 1,700 to 2,100 $\mu S\ cm^{-1}$ (Agouridis et al., 2011). Such variation is ideal for field-testing conductivity sensors.

Three locations of widely varying water quality and discharge were selected to test the conductivity sensors: Little Millseat (LMS), Guy Cove 01 (GC01), and Guy Cove 03 (GC03) (Agouridis et al., 2011). The average cation and anion concentrations at the sites in 2011 are

presented in Table 3.1. Table 3.2 contains average nutrient and metal concentrations in 2011 for the three sites.

The LMS location was at the outlet of a 90+ year old second-growth forested watershed that is about 75.7 ha in size. The GC01 and GC03 locations were located at the start and end of a stream creation project, respectively (Figure 3.1). Although the 9.2 ha watershed above the GC01 location was not mined, trees were harvested when the surrounded area was mined. The GC03 location is at the toe or outlet of the valley fill. This location receives waters from the primarily from the underdrain but also from the recreated streams. GC03 also receives runoff from 43.6 ha of lands that were mostly traditionally reclaimed though about 4 ha was reclaimed using the Forestry Reclamation Approach (FRA). The 43.6 ha watershed up-gradient of GC03 is strongly influence by discharge from the underdrain.

Table 3.1 Average Cation and Anion Concentrations in Water Samples from the 2011 Monitoring Year.[1]

Site[2]	$EC_{25°C}$	Cl^-	SO_4^{2-}	Mg	Ca^{2+}	K^+	Na^+
	$\mu S\ cm^{-1}$	----------mg L^{-1}----------					
LMS	43	1.3	15	1.7[3]	2.5	1.3	1.3
GC01	457	2.4	417	47	24	5.8	3.9
GC03	1,724	2.5	1,780	180	91	8.8	10.0

[1]Sample period: January 2011 to November 2011.
[2]LMS=Little Millseat; GC01=Guy Cove 01; GC03=Guy Cove 03.
[3]Mg values are for samples taken in 2010 only.

Table 3.2 Average Nutrient and Metal Concentrations in Water Samples from the 2011 Monitoring Year [1].

Site[2]	pH	NO_3^{2-}	NH_4^+		Alkalinity	Fe^{2+}	Mn
	su	----------mg L^{-1}----------					
Little Millseat	6.6	0.11	0.09		33	0.04	0.26
GC01	7.8	0.17	0.10		509	na[3]	0.24
GC03	6.6	0.01	0.15		91	na	3.58

[1]Sample period: January 2011 to November 2011.
[2]LMS=Little Millseat; GC01=Guy Cove 01; GC03=Guy Cove 03.
[3]na=sample results not available at the time of the report.

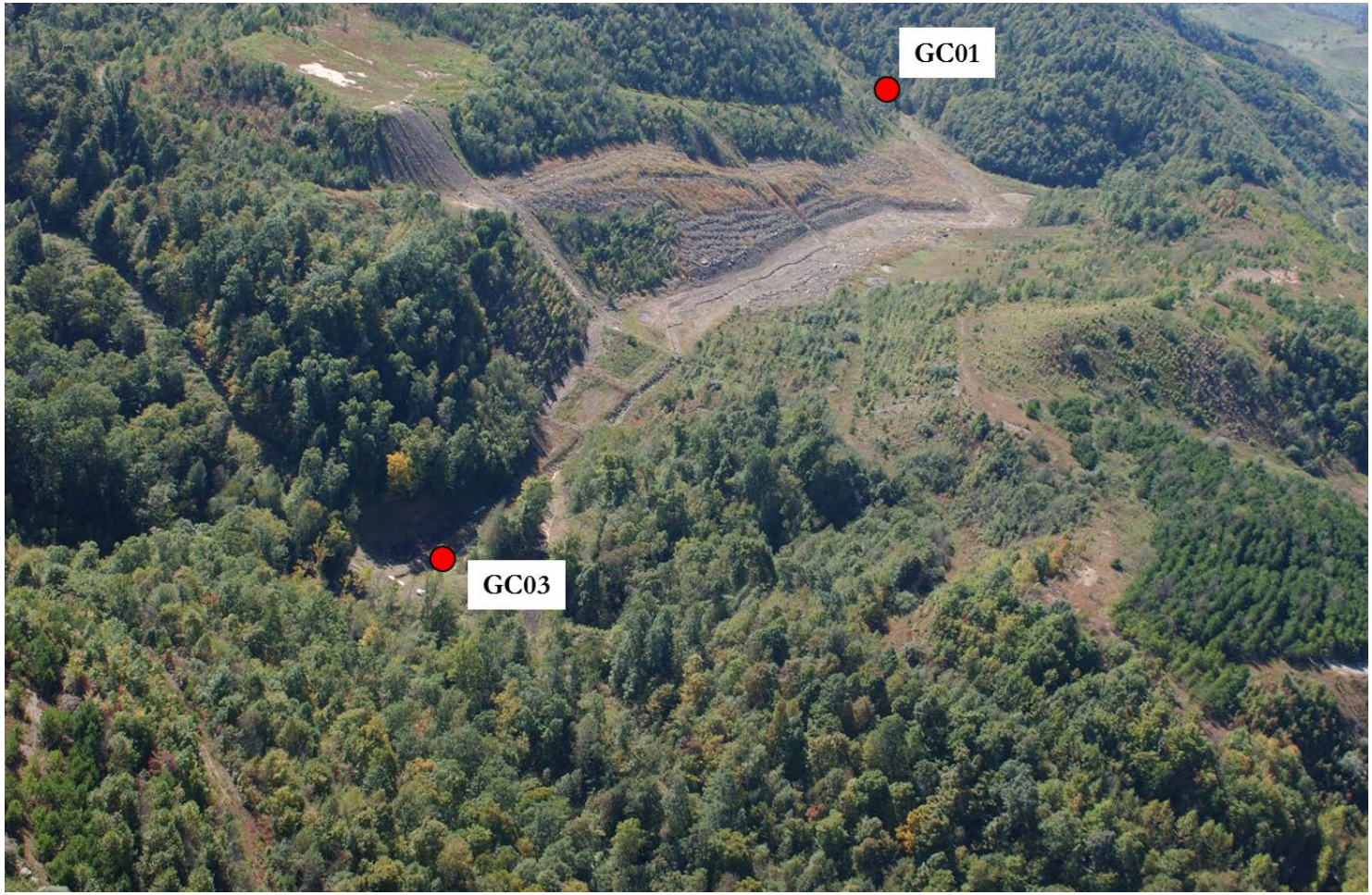

Figure 3.1 Conductivity Sensor Field Study Sites. *Locations identified with red circle. GC01 =Guy Cove 01; GC03=Guy Cove 03. Little Millseat (LMS) not shown.*

DATA COLLECTION

SPECIFIC CONDUCTIVITY

At each site, all conductivity sensors were deployed in riffles such that the sensors were fully submerged. The HOBO, Solinst, and Aqua TROLL sensors were each housed in their own 5-cm diameter PVC pipes for protection. The PCV pipes allowed flows to continuously circulate through the housing units and across the sensors. To avoid the potential for fouling due to metal contact, these sensors were secured in the PVC pipe using plastic zip-ties. The YSI sensors were protected in manufacturer supplied deployment cases.

DISCHARGE

Because of the expected influence of discharge on EC_{25^oC} levels, flow was measured at each of the three study sites. At GC01 and GC03, discharge was continuously measured using trapezoidal flumes (Grant, 1992) and In-Situ Level Trolls (5 psig) pressure transducers (Fort Collins, CO). Water level data were collected at 15-minute intervals and transformed into discharge. At LMS, discharge data were continuously recorded using a 3:1 side-sloped broad-crested combination weir and In-Situ Level Troll (5 psig) pressure transducer (Cherry, 2006).

During the project period, the conductivity sensors recorded EC_{25^oC} and temperature data for seven deployment periods. The length of the deployment periods varied, but generally encompassed a period of 2-3 weeks (range was 10 to 28 days with an average of 20 days). Data were collected at 15-minute intervals. Conductivity sensors were not rotated between sites but remained at the same site throughout the study. Between each deployment, conductivity sensors were cleaned and recalibrated, as required, per manufacturer's recommendations. Budgetary constraints and multi-project needs prevented the use of all conductivity sensors at all deployments. The Solinst and Aqua TROLL sensors were not deployed until period 4 as they were not purchased until the spring of 2011. Table 3.3 notes the location and deployment period of for each conductivity sensor used in the study.

Table 3.3 Conductivity Sensor Deployment Schedule.

Sensor	Deployment[1]						
	1	2	3	4	5	6	7
YSI							
LMS	X	X	X	X		X	
GC01	X			X			X
GC03	X	X	X	X			X
HOBO							
LMS	X	X	X	X	X	X	X
GC01	X	X	X	X	X	X	X
GC03	X	X	X	X	X	X	X
Solinst							
LMS				X	X	X	
GC01				X	X	X	X
GC03				X	X	X	X
Aqua TROLL							
LMS				X	X	X	X
GC01				X	X	X	X
GC03				X	X	X	X

[1]Deployment periods: 1=March 16, 2011 to April 1, 2011 (16 days); 2=April 14, 2011 to May 5, 2011 (20 days); 3=May 19, 2011 to May 29, 2011 (10 days); 4=June 23, 2011 to July 13, 2011 (20 days); 5=July 28, 2011 toAugust 17, 2011 (20 days); 6=September 8, 2011 to October 6, 2011 (28 days); and 7-October 28, 2011 to November 20, 2011 (23 days).

DATA ANALYSIS

WHITE NOISE

Because EC_{25^oC} values measured in the field could not be compared to known EC_{25^oC} standards, as was the case in the controlled laboratory study reported by Maupin et al. (2012), a white noise analysis was performed to assess temporal variations in the conductivity sensor readings (Haan, 1977). White noise is useful in modeling the impact of random disturbances, such as sensor noise and environmental disturbances (e.g. storm events, temperature changes), on sensor output (i.e. EC_{25^oC} readings). The goal of the analysis was to

determine if the variance of the white noise was related to $EC_{25°C}$ and discharge. Since variation in the white noise was desired, grouping of the data into time blocks was required to permit the computation of variance. For each study site and deployment period, a time block of three hours was used. A time block of three hours was chosen as it provided a representative time sample (e.g. enough data points) while maintaining a constant variance of $EC_{25°C}$ within the blocks. As $EC_{25°C}$ and flow data were collected at 15-minute intervals, each time block consisted of 12 data points.

Equation 3.1 was used to model white noise for each $EC_{25°C}$ data point.

(3.1)

The variable a(d) is the white noise associated with each data point, d ($\mu S\ cm^{-1}$); X'(d) is the detrended sensor output for each data point ($\mu S\ cm^{-1}$); and

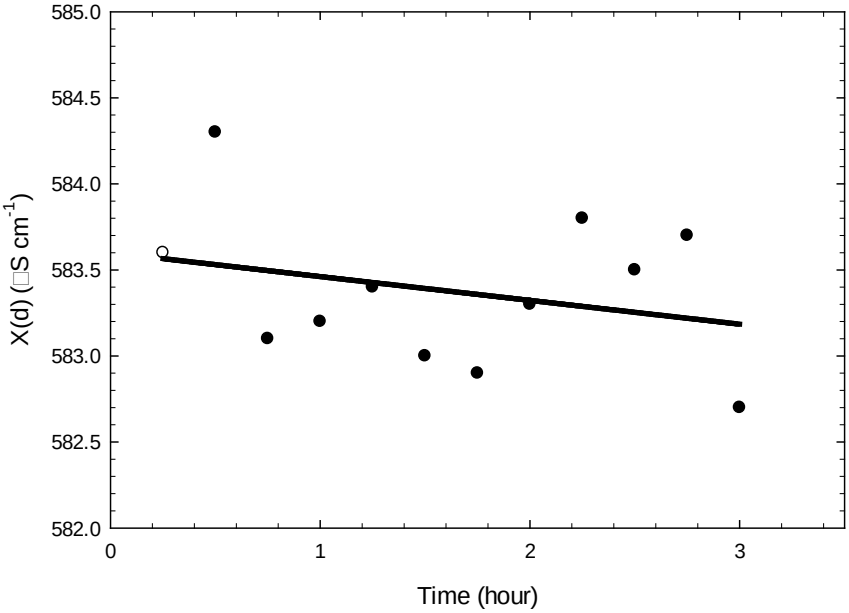

Figure 3.2. Raw $EC_{25^{o}C}$ data from time block 1 of the HOBO sensor at GC01 for deployment 3.

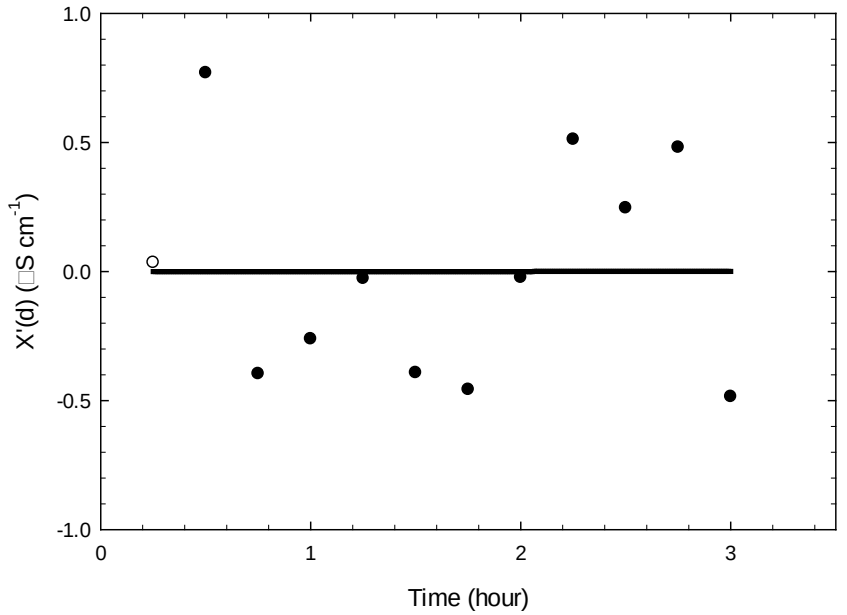

Figure 3.3. Detrended $EC_{25^{o}C}$ data from time block 1 of the HOBO sensor at GC01 for deployment 3.

Following computation of the white noise for each $EC_{25^{\circ}C}$ data point, the variance of the white noise for each 3-hour time block was computed using equation 3.4.

(3.4)

The variable S^2 is the variance of the white noise for the 3-hour time block ($\mu S^2\ cm^{-2}$); n is the number of data points within that time block; and

RESULTS AND DISCUSSION

STUDY SITE COMPARISONS

Tables3.4-3.5 contain non-detrended and non-transformed white noise variance and EC_{25^oC} means and standard deviations for each sensor, deployment, and location combination. Both white noise variance and EC_{25^oC} were smallest at LMS and highest at GC03. White noise variance at LMS was typically less than 2 $\mu S^2\ cm^{-2}$, across all sensors; similarly, EC_{25^oC} was generally less than 80 $\mu S\ cm^{-1}$ for the study period. Values for white noise variance were highest with the HOBO sensors as were EC_{25^oC} values. In a laboratory study, Maupin et al. (2012) found that the HOBO sensors tended to over-estimate EC_{25^oC} (5-9,986 $\mu S\ cm^{-1}$ range), which may be the case here as well. At GC01, white noise variance was also highest with the HOBO sensors; however, EC_{25^oC} values were similar to those of the other sensors. White noise variance values were generally low, like at LMS, with the exception of the HOBO sensors which posted values from about 1 $\mu S^2\ cm^{-2}$ up to about 50 $\mu S^2\ cm^{-2}$. At GC03, both white noise variance and EC_{25^oC} increased substantially. White noise variance was highest with the Solinst sensors averaging over 44,000 $\mu S^2\ cm^{-2}$ across the four deployment periods it was in use. The Aqua TROLL has the next highest white noise variance values with a mean of around 16,000 $\mu S^2\ cm^{-2}$. Both the YSI and HOBO sensors have similar white noise variance means with values of around 1,500 $\mu S^2\ cm^{-2}$. Mean EC_{25^oC} varied much less between sensors with values ranging from about 2,050 to 2,800 $\mu S\ cm^{-1}$.

Table 3.6 contains the non-detrended and non-transformed discharge means and standard deviations for each deployment and location combination. Mean discharge was lowest at GC01 (0.1 $m^3\ s^{-1}$) followed by GC03 (0.2 $m^3\ s^{-1}$) and then LMS (1.0 $m^3\ s^{-1}$). This order does not correspond to white noise variance and EC_{25^oC} values which increased in the order of LMS, GC01 and then GC03. Mean discharges were higher during deployments 2 and 3 which together encompassed mid-April through May of 2011.

Figures 3.4-3.6 show EC_{25^oC} measurements for all four sensor types at LMS, GC01, and GC03, respectively. At LMS, all four sensors recorded similar EC_{25^oC} values. The Solinst recorded EC_{25^oC} values about 20 $\mu S\ cm^{-1}$ lower than the other sensors at the beginning of the deployment period while the Aqua TROLL recorded values about 20 $\mu S\ cm^{-1}$ greater than the others for the latter part of the deployment period. The reason for this shift is not

Table 3.4 Mean (M) and Standard Errors (SE) of White Noise Variance ($\mu S^2\ cm^{-2}$).

Sensor[1]	Location		
	LMS	GC01	GC03
YSI			
1	0.4±0.1	0.7±0.1	2,127.5±211.5
2	3.1±1.2	--	1,911.8±799.7
3	0.2±0.1	--	2,398.3±1,644.2
4	0.4±0.1	8.4±5.1	1,206.5±524.1
5	--	--	--
6	0.4±0.2	--	--
7	--	2.5±0.4	776.7±371.7
M±SE	1.0±0.3	4.1±1.7	1,560.5±310.4
HOBO			
1	0.1±0.0	0.4±0.1	13.9±9.1
2	1.3±0.7	51.5±18.7	9,091.1±2016.7
3	0.1±0.0	31.6±17.7	1,478.1±1058.6
4	0.3±0.1	18.1±155.6	546.7±265.0
5	8.4±2.2	1.5±0.6	46.6±22.9
6	0.3±0.1	2.9±0.1	5.4±1.5
7	1.2±0.9	6.2±32.4	13.9±9.1
M±SE	1.7±0.4	14.8±113.7	1,586.2±333.3
Solinst			
1	--	--	--
2	--	--	--
3	--	--	--
4	0.2±0.1	2.5±1.5	48,218.5±14,387.6
5	1.9±0.4	0.3±.01	81,033.5±14,089.9
6	0.5±0.1	0.9±0.4	34,585.2±5,533.4
7	--	1.1±0.6	21,659.1±2,825.9
M±SE	0.8±0.1	1.2±0.4	44,323.1±4,819.1

Table 3.4 (continued)

Sensor[1]	Location		
	LMS	GC01	GC03
Aqua TROLL			
1	--	--	--
2	--	--	--
3	--	--	--
4	0.2±0.1	14.2±4.5	72,608.7±34,209.8
5	0.3±0.1	0.1±0.0	11.9±3.6
6	0.3±0.1	0.4±0.2	94.8±66.7
7	0.1±0.0	0.3±0.3	277.6±205.3
M±SE	0.2±0.1	3.3±1.1	16,036.8±7,571.9

[1]Deployment periods: 1=March 16, 2011 to April 1, 2011 (16 days); 2=April 14, 2011 to May 5, 2011 (20 days); 3=May 19, 2011 to May 29, 2011 (10 days); 4=June 23, 2011 to July 13, 2011 (20 days); 5=July 28, 2011 to August 17, 2011 (20 days); 6=September 8, 2011 to October 6, 2011 (28 days); and 7-October 28, 2011 to November 20, 2011 (23 days).

Table 3.5 Mean (M) and Standard Errors (SE) of $EC_{25^{o}C}$ ($\mu S\ cm^{-1}$).

Sensor[1]	Location		
	LMS	GC01	GC03
YSI			
1	42.8±0.2	301.4±1.4	1,930.1±3.8
2	39.4±0.4	--	1,571.3±25.9
3	41.1±0.1	--	2,069.1±21.1
4	58.1±0.3	570.1±2.1	2,338.6±15.3
5	--	--	--
6	67.1±1.0	--	--
7	--	498.3±14.1	2,325.3±34.7
M±SE	50.9±0.5	485.9±7.9	2,057.7±16.6
HOBO			
1	66.8±1.4	462.5±5.8	2,129.0±2.8
2	91.9±2.3	279.8±91.2	1,584.6±26.7
3	137.8±1.2	546.4±3.7	2,151.3±21.9
4	76.4±0.3	705.4±5.3	2,384.3±10.8
5	54.3±1.2	1,099.2±19.0	2,397.2±3.1
6	70.8±6.1	654.3±1.2	2,457.1±5.5
7	65.9±1.2	530.8±6.4	2,129.0±2.8
M±SE	75.7±0.8	627.7±8.4	2,200.6±10.4
Solinst			
1	--	--	--
2	--	--	--
3	--	--	--
4	45.6±0.3	656.1±5.6	2,457.4±55.6
5	52.7±1.0	0.3±.01	3,618.9±47.2
6	62.0±0.8	644.9±1.6	2,492.5±36.6
7	--	552.6±5.8	2,817.0±63.7
M±SE	54.4±0.5	629.9±2.8	2,814.1±30.5

Table 3.5 (continued).

Sensor[1]	Location		
	LMS	GC01	GC03
Aqua TROLL			
1	--	--	--
2	--	--	--
3	--	--	--
4	61.1±0.6	539.3±4.4	2,261.1±34.8
5	77.5±1.0	462.1±2.2	2,264.3±3.3
6	70.8±0.4	668.8±1.5	2,245.2±10.6
7	80.3±1.8	665.7±1.7	2,101.2±28.3
M±SE	72.6±0.6	594.8±3.5	2,215.6±11.3

[1]Deployment periods: 1=March 16, 2011 to April 1, 2011 (16 days); 2=April 14, 2011 to May 5, 2011 (20 days); 3=May 19, 2011 to May 29, 2011 (10 days); 4=June 23, 2011 to July 13, 2011 (20 days); 5=July 28, 2011 to August 17, 2011 (20 days); 6=September 8, 2011 to October 6, 2011 (28 days); and 7-October 28, 2011 to November 20, 2011 (23 days).

Table 3.6. Mean (M) and Standard Errors (SE) of Non-detrended and Non-transformed Discharge (m^3 s^{-1}).

Deployment[1]	Location		
	LMS	GC01	GC03
1	0.6±0.1	0.1±0.0	0.1±0.0
2	3.2±5.0	0.1±0.1	0.6±0.6
3	2.7±3.9	0.0±0.0	0.2±0.1
4	0.4±1.3	0.1±0.0	0.1±0.1
5	0.9±1.9	0.1±0.0	0.1±0.0
6	0.1±0.3	0.0±0.0	0.1±0.0
7	0.3±0.5	0.0±0.0	0.1±0.0
M±SE	1.0±2.6	0.1±0.0	0.2±0.3

[1]Deployment periods: 1=March 16, 2011 to April 1, 2011 (16 days); 2=April 14, 2011 to May 5, 2011 (20 days); 3=May 19, 2011 to May 29, 2011 (10 days); 4=June 23, 2011 to July 13, 2011 (20 days); 5=July 28, 2011 to August 17, 2011 (20 days); 6=September 8, 2011 to October 6, 2011 (28 days); and 7-October 28, 2011 to November 20, 2011 (23 days).

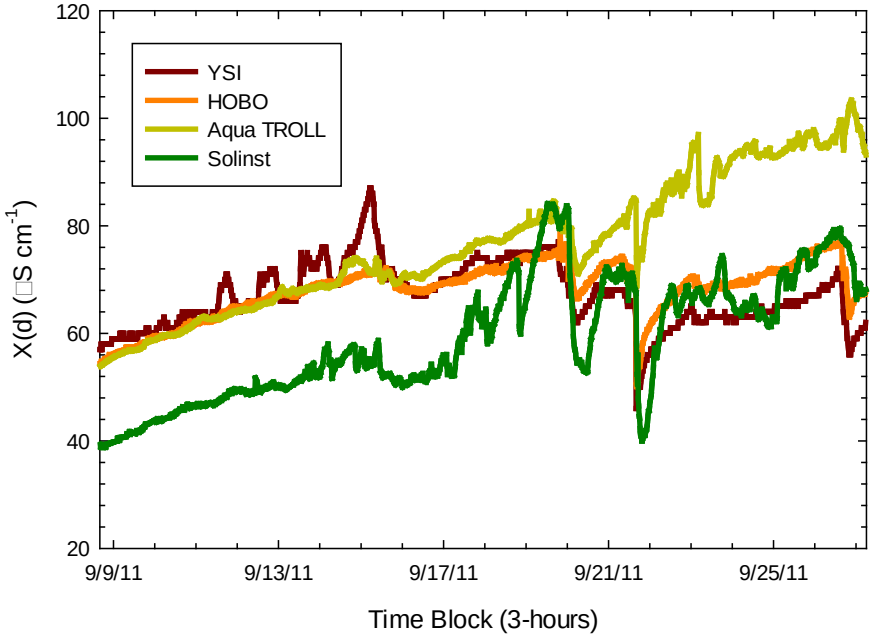

Figure 3.4 Specific Conductance Readings at LMS during Deployment 6.

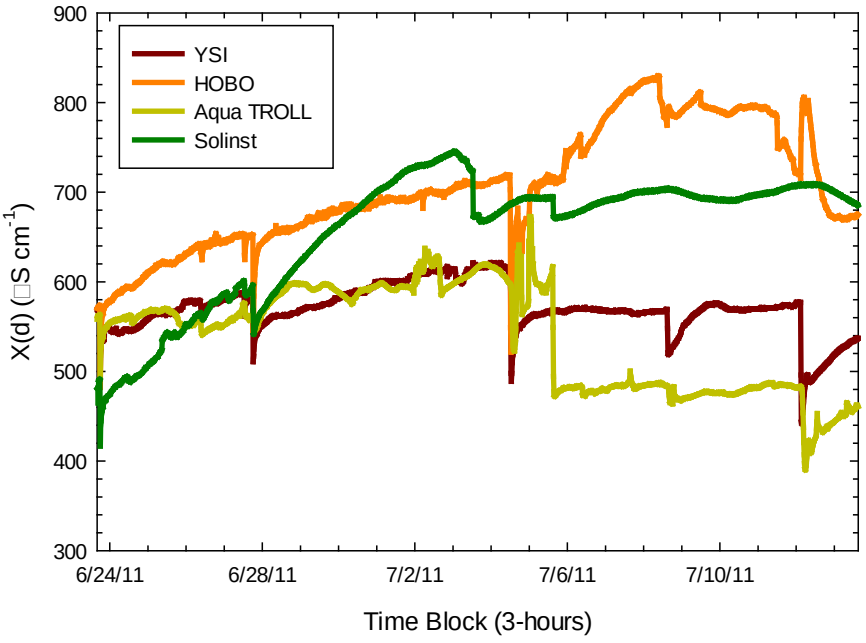

Figure 3.5 Specific Conductance Readings at GC01 during Deployment 4

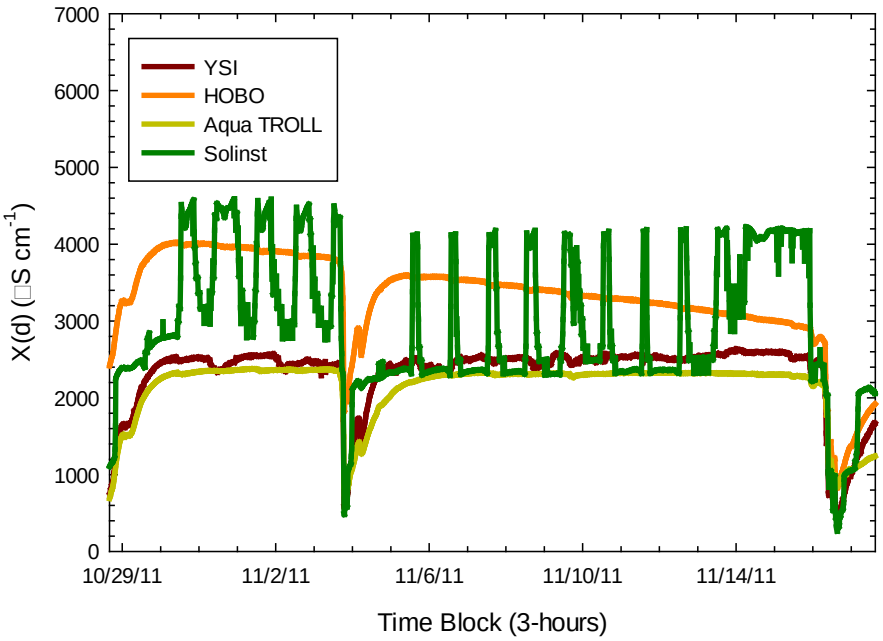

Figure 3.6 Specific Conductance Readings at GC03 during Deployment 7.

known. No appreciable rainfall events, those greater than 12.5 mm, occurred during this deployment period.

At GC01, where $EC_{25°C}$ is higher as compared to LMS, the pattern is different. While the HOBO consistently records higher $EC_{25°C}$ values than the other sensors, the Aqua TROLL largely records lower $EC_{25°C}$ values. The Solinst has a large jump around June 28, 2011 although no rain events, and hence no change in discharge, were recorded at that time. $EC_{25°C}$ readings from the YSI were fairly constant across the period. Table 3 shows that the white noise variance for the sensors at GC01 was comparable to LMS with the exception of the HOBO sensor which recorded the highest variances in addition to the highest $EC_{25°C}$ values. Two rain events greater than 12.5 mm occurred during this deployment period: 19.3 mm on July 11, 2011 and 14.2 mm on July 14, 2011. However, none occurred between July 4, 2011 and July 6, 2011 when the Aqua TROLL $EC_{25°C}$ readings fluctuated largely. The reason for this fluctuation is not known, but the YSI and HOBO sensors also dipped at this time while the Solinst did not.

The $EC_{25°C}$ readings at GC03 were unexpected, particularly with regards to the Solinst sensor. This sensor displayed large fluctuations that resembled a diurnal pattern. This cyclic

pattern was not seen in any of the other sensors. Even those temperature corrected conductivity values are used, a check of the temperature data from all sensors at this site did not reveal any notable temperature fluctuations that would have accounted for the cyclical pattern with the Solinst. As with GC01, the HOBO sensor recorded the highest EC_{25^oC} values. HOBO EC_{25^oC} values at GC03 were about 250 μS cm^{-1} to 1,000 μS cm^{-1} higher than those recorded by the YSI and Aqua TROLL sensors. Two rain events occurred during this period: 15.5 mm on November 2, 2011 and 29.2 mm on November 5, 2011. All four sensors noted the drop in EC_{25^oC} values associated with the dilution effect of the runoff.

As seen in Table 3, white noise variance was highest at GC03 with white noise variances in the 1,000s or even 10,000s with the Solinst sensor. Based on work by Maupin et al. (2012), it was expected that the sensors would display temporal stability at the expected EC_{25^oC} values at GC03. These EC_{25^oC} values were much less than the maximum of 9,986 μS cm^{-1} used in the study. And even at that level, all sensors displayed temporal stability, in the laboratory study by Maupin et al. (2012) at water temperatures encountered at the sites (10-15ºC) with the exception of the HOBO sensors.

The temporal variability seen at GC03, in light of the results from the laboratory experiments carried out by Maupin et al. (2012), suggests that a constituent or combination of constituents in the water was negatively affecting the performance of the sensors, particularly the Solinst sensor. Mastin et al. (2011) noted that the mixed chemistry of the mine drainage emitted from the toe of the valley fill was impacting to a bioreactor treatment system installed at the site. The authors measured low iron levels (<4 mg L^{-1}) in the mine drainage emitted from the toe of the valley fill at Guy Cove, which is in close proximity to GC03. However, these levels were sufficient to precipitate in surface waters due to oxygen exposure thus clogging plumbing to passive treatment bioreactors. The GC03 site is the only one of the three studied with an orange, iron precipitate laden biofilm present on the streambed. Whelan and Regan (2006) noted a biofilm can begin to form on sensors quite quickly (e.g. minutes) after immersion in water, and that this biofilm negatively affects sensor performance. To minimize the impacts of fouling, each sensor was cleaned at the end of all deployment periods. Regardless, some discoloration did occur on the sensor housings.

WHITE NOISE VARIANCE EVALUATION

Results from the multiple-linear regression analyses show that white noise variance was significantly related to $EC_{25°C}$ and discharge for all of the sensors (Table 7). For the YSI sensors, results of the regression analysis indicated that the model was able to explain 47 percent of the white noise variance (R^2=0.47). For the HOBO sensors, the R^2 was 0.39; R^2=0.65 for the Solinst; and R^2=0.35 for the Aqua TROLL. An increase in $EC_{25°C}$ and discharge resulted in an increase in the white noise variance for all sensor types. Increases in $EC_{25°C}$ had the largest influence on the Solinst sensors followed by the YSI, Aqua TROLL, and HOBO. A 1 percent increase in $EC_{25°C}$ produces a 1.7 percent increase in white noise variance for the Solinst sensors. For the YSI, Aqua TROLL, and HOBO sensors, a 1 percent increase in $EC_{25°C}$ results in a 1.3, 1.2, and 1 percent increase, respectively, in white noise variance.

Increases in discharge had a much smaller effect on white noise variance. A 1 percent increase in discharge produced a 0.1 percent or less increase in white noise variance for all sensors. While significant, these results indicate that discharge has little effect on white noise variance. This result was somewhat expected as the conductivity sensors are not measuring discharge. Rather, changes in discharge affect $EC_{25°C}$ values. As discharge increases, as seen in Figures 4-6, $EC_{25°C}$ values tend to decrease due to the diluting effect of the runoff. These results indicate that shifts in discharge, such as with storm events, have minimal impacts on white noise variance.

SIGNAL INTERFERENCE

Based on unexpected cyclic nature of the Solinst $EC_{25°C}$ readings, the possibility of signal interference between the conductivity sensors was investigated using waters collected from GC03 as well as a standard $EC_{25°C}$ solution of 3,860 $\mu S\ cm^{-1}$. Using a hose connected to a PVC pipe with multiple 3.2 mm holes, compressed air was bubbled through both solutions to prevent settling and to simulate water movement in a stream riffle as all sensors were placed in riffles in the field. In the first trial, one sensor each from all four sensor types was simultaneously placed into the GC03 collected waters. These sensors were the same four sensors deployed at GC03. Data were collected at 15-minute intervals, as was done in the field, for over a 24-hour period. The trial was repeated for a YIS supplied standard

calibration solution ($EC_{25°C}$=3,860 μS cm^{-1}). A second trial was also conducted in the same manner using only the Solinst sensor (i.e. only one sensor in the container).

As seen in Figures 3.7 and 3.8, signal interference was not an issue for the Solinst sensor. In the GC03 waters and the standard YSI calibration solution, the Solinst sensor performed in a similar manner whether grouped with the other sensors or alone. No cyclic patterns were observed. Hence, signal interference from other sensors is not an issue. The lack of cyclic patterns in the Solinst sensor output when tested in GC03 waters during this laboratory study suggests that sensor fouling in the field is the likely the cause of the erratic readings. In the field, a thick layer of iron precipitant is present on top of the streambed at GC03. Such precipitants were not present in the laboratory study.

CONCLUSIONS

Four commonly used $EC_{25°C}$ sensors (YSI, HOBO, Solinst and Aqua TROLL) were evaluated at three study sites located on forested and mined lands in eastern Kentucky. Water quality at the sites varied with typical $EC_{25°C}$ values from grab samples of about 40, 450, and 1,700 μS cm^{-1} at LMS, GC01 and GC03, respectively. Seven deployment periods spanning the months of March through November of 2011, for a total of about 135 days, were evaluated. For each sensor at each site, white noise variance was computed and compared to $EC_{25° C}$ and discharge. Multiple linear regression analysis was used to assess the strength of the relationship between $EC_{25° C}$, discharge and white noise variance. Results from the multiple regression analyses indicate that the model explains 65 percent of the white noise variance with the Solinst sensors, 47 percent for YSI sensors, 39 percent for HOBO sensors, and 35 percent for Aqua TROLL sensors.

While both independent variables were significant predictors of white noise variance, increases in $EC_{25° C}$ had a much larger effect than increases in discharge. The small effect of discharge on white noise variance indicates changes in discharge, as in the case of storm events, have minimal impact on sensor performance. As the sensors do not directly measure discharge, this small effect is likely attributable to the dilution effect of increased stream flows resulting from runoff on $EC_{25° C}$ values.

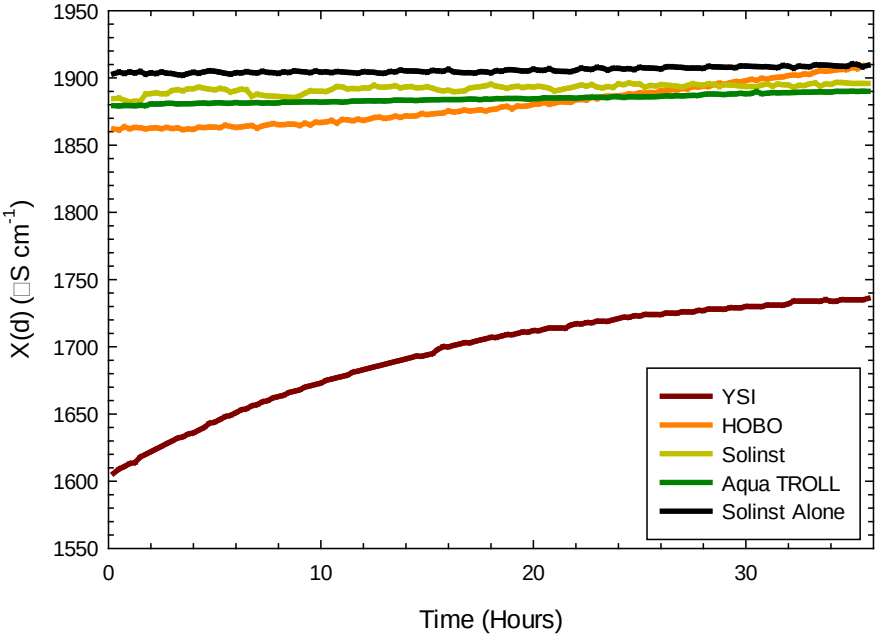

Figure 3.7 Laboratory Signal Interference Testing in GC03 Waters

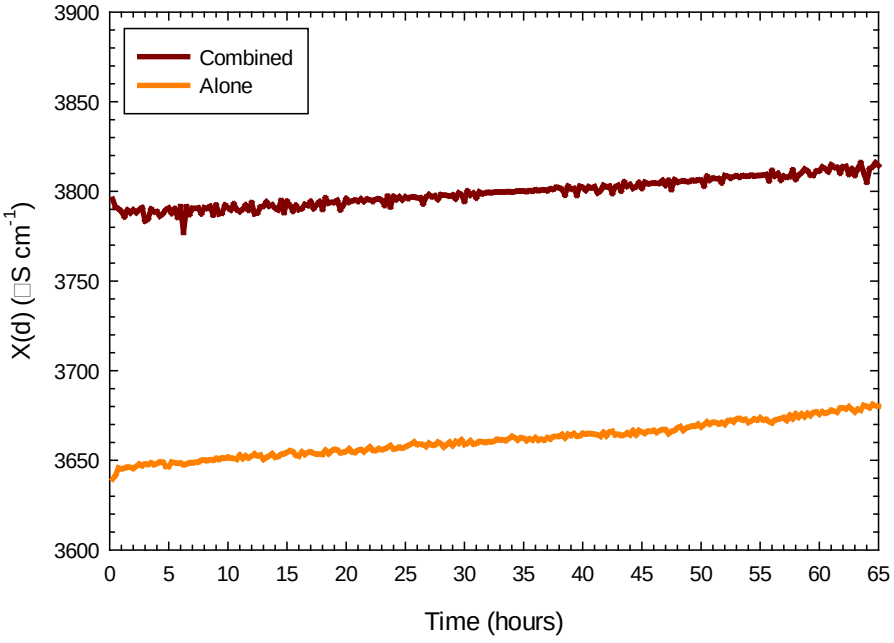

Figure 3.8 Laboratory Signal Interference Testing in $EC_{25°C}$ Standard Waters

Of greater concern is that the Solinst sensors consistently displayed a cyclic pattern at GC03, the site with the highest $EC_{25^{o}C}$ levels. Laboratory tests using waters collected from GC03 as well as a diluted standard $EC_{25^{o}}$ solution eliminated the possibility of signal interference from the other sensors. It is suspected that fouling at GC03 is causing the Solinst sensors to report widely fluctuating $EC_{25^{o}C}$ values. Iron precipitants are prevalent at GC03.

Conductivity sensor selection can be a challenging task, particularly when monitoring waters emanating from mined lands. The mixed chemistry in the waters at these sites means that sensor ruggedness becomes a critical factor. Even with regular cleaning and calibration, sensor fouling can occur rapidly, within hours or days, in locations where precipitants are common such as at the toe of a valley fill. Lastly, consideration should be given to the small sample size. Due to budgetary limitations, only one sensor of each type could be tested at each site. It is possible that a different sensor, of the same sensor type, would perform differently.

CHAPTER 4: HYDROLOGIC ASSESSMENT OF STORM EVENTS AT THE GUY COVE STREAM RESTORATION PROJECT

The surface mining method of mountaintop removal is commonly used to extract coal in the mountainous terrain of the Appalachian Coal Belt Region (Peng, 2000). The excess spoil or overburden that results from this practice is placed in valleys adjacent to the point of extraction. This spoil placement creates valley fills (VFs) that often cover existing streams. Alterations to the hydrologic and water quality characteristics in downstream regions are a result of covering the existing steam systems with overburden (Hartman et al., 2005). Precipitation and groundwater are directed to the underdrain, which is a large rock drain that constructed in the middle of the valley, in addition to permeating through the overburden. As they pass through the underdrain and overburden, these waters pick up contaminates, which are subsequently discharged from the toe of the fill to surface waters (Pond et al., 2008). Research has shown that the water quality downstream of VFs exhibits increased levels of electrical conductivity, suspended sediments, and dissolved minerals (USEPA 2005; Fritz et al., 2008). Valley fills also alter the hydrology of down-gradient streams. These stream, which often times dried up during the summer months, now flow year-round (USEPA, 2010b). Wiley et al. (2001) found the 90 percent flow durations at VFs were 6-7 times greater than those at unmined sites. Baseflow comprised a larger percentage and stormflow a lesser percentage at VFs as compared to unmined sites.

Traditional surface mine reclamation practices, as promulgated by the Surface Mining Control and Reclamation Act (SMCRA), have resulted in high compaction rates with ground cover that is largely composed of grasses (Angel et al., 2005; Taylor et al., 2009). This reclamation practice has resulted in lands with low infiltration rates (Weiss and Razem; Jorgensen and Gardner; 1987), increased discharge (Bonta et al., 1997; Philips, 2004; Ferrari et al., 2009), poor reforestation potential (Angel et al., 2009; Burger et al., 2005), and poor water quality (Pond et al., 2008; Fritz et al., 2010). Over the past 15 years, efforts have been underway to modify surface mine reclamation practices to ameliorate these issues, largely by focusing on improving the reforestation potential of mined lands primarily by alleviating compaction. Through a technique known as the Forestry Reclamation Approach (FRA), mined lands are reclaimed in a way that promotes tree growth and thus the re-establishment of a productive forest (Graves et al., 2000; Burger et al., 2005; Miller et al., 2011). The FRA

consists of five steps: 1) use topsoil, weathered sandstone, or best available material to create suitable rooting medium (1.2-m deep), 2) loosely grade the spoil to create a uncompacted layer, 3) use tree compatible native ground covers, 4) plant both early succession tree species for wildlife and soil stability as well as high-value trees, and 5) use proper tree planting techniques (Burger et al., 2005).

The FRA also has the potential to improve the hydrology and quality of waters discharged from mine lands in addition to re-establishing forests. Taylor et al. (2009) examined the hydrologic characteristics discharge volume, peak discharge, discharge duration, lag time and response time on test cells constructed using the FRA. The authors found the test cells had low discharge volumes, small peak discharges, and long discharge durations. Preliminary results indicated that the FRA produced hydrology similar to a forested watershed even while the trees were seedlings. Agouridis et al. (2012) demonstrated that the specific conductance levels in waters discharged from test cells, constructed in accordance to the FRA, were below 500 $\mu S\ cm^{-1}$ within a two-year period. By the third year, average specific conductivity levels for grab samples from the test cells were 380 $\mu S\ cm^{-1}$ for gray unweathered sandstone and 290 $\mu S\ cm^{-1}$ for a mixture of brown weathered sandstone, gray unweathered sandstone, and shale. These results are encouraging, particularly when considering Fritz et al. (2010) who measured specific conductance levels between 2,000 and 3,000 $\mu S\ cm^{-1}$ in waters discharged from 10+ year old VFs.

Addressing the issues created by VFs (e.g. altered hydrology, poor water quality, and stream habitat loss) requires a paradigm shift in the way coal mining and reclamation is performed in Appalachia (Warner and Agouridis, 2011). It requires modifying the way valley fills are designed and constructed and looking at new ways to create aquatic and terrestrial habitats. By limiting the amount of water allowed to flow through the VF, it is hypothesized that water quality improvements are possible (USEPA, 2010b). Stream restoration, used in conjunction with FRA, holds promise a way to further reduce the impacts of mining on stream habitat loss. The Guy Cove stream restoration project was the first of its kind to demonstrate that a stream could be constructed on a VF. Approximately 1.6 km of stream channel (ephemeral, intermittent and perennial) was created on a retrofitted 10+-year old VF. Results from the third year monitoring period are promising; the stream is stable and salamanders and macroinvertebrates are recolonizing the site (Agouridis et al., 2011).

However, the question remains as to what level of functionality (e.g. hydrology, water quality, and habitat) the restoration site achieving. The focus of this chapter is on the hydrology.

The goal of this study was to evaluate the hydrological characteristics that have resulted from a headwater stream restoration on a retrofitted valley fill (Guy Cove) that incorporates both the FRA and natural channel design components. The objectives of this study were to 1) measure and compare the hydrograph characteristics of the restored stream to a stream from an unmined, forested watershed and a stream from a mined but unrestored, traditionally reclaimed watershed. The **storm event** hydrologic characteristics examined were discharge volume, peak discharge, discharge duration, time to peak, lag time, and response time.

METHODS

SITE LOCATIONS

The study sites are located within the University of Kentucky's 6,100-ha experimental forest, Robinson Forest, which is located on the Cumberland Plateau in southeastern Kentucky. The forest landscape consists of long, steep side slopes cut into layers of sandstone, shale, siltstone and clay. Vegetation ranges from xeric oak-pine dominated stands to rich mesic cove hardwoods; a typical vegetation type for the mixed Mesophytic forest region. The majority of the forest is comprised of 90+ year old second growth. However, portions of Robinson Forest were surface mined during the mid-1990s resulting in the creation of several VFs.

Within Robinson Forest, three separate stream systems were monitored: Little Millseat (LMS), Wharton Branch (WB), and Guy Cove (GC). Little Millseat is an unmined headwater stream with steep side slopes (25-60%) and narrow valleys. Elevation differences between ridge tops and valley bottom is about 150 m. Ridge top and side slope soils are shallow and well-drained; valley bottom soils are deep and well-drained. The drainage area for the LMS watershed is 87.8 ha (Cherry, 2006). Wharton Branch is a mined headwater stream, a portion of which was buried by a VF. The site is within 6 km of LMS. The drainage area for WB is 44.1 ha. The WB watershed is comprised mostly of open hay pasture with a regenerating mixed mesophytic forest at the toe of the VF.

Like WB, GC is a mined headwater stream; it too was buried by a VF. However, the crown (top surface) of the VF was retrofitted and about 1.6 km of stream was created and over 16 ha were reforested using the FRA (Agouridis et al., 2009). The GC watershed is located less than 1 km upstream of WB. At GC, hydrologic monitoring is done in three locations on the created intermittent and perennial stream reaches (Figure 4.1). The first location, GC 01, is located immediately above the start of the restoration project and monitors runoff from a 22.7 acres regenerated forest. While this portion of the GC watershed was not mined, the trees were harvested in preparation for mining. However, mining did not occur here as the coal seam stopped. The closed canopy forest is approximately 15 years in age and is comprised of yellow poplar, white oak, sweet birch (*Betula lenta*), American beech (*Fagus grandifolia*), red maple (*Acer rubrum*), black walnut, and sycamore (*Plantanus occidentalis*) (Mastin, 2010).

The second location at GC, GC02, is located downstream of GC01 and is at the crest or the interface between the crown and the face of the valley fill. This location receives drainage from over 38 ha. The up-gradient watershed is comprised of the regenerated forest and retrofitted portion of the VF (i.e. created streams and reforested area). Land cover includes young trees (3-4 years old) and grasses for ground cover. The riparian area forest is comprised of American sycamore (*Platanus occidentalis*), American beech (*Fagus grandifolia*), green ash (*Fraxinus pennsylvanica var. subintegerrima*), swamp chestnut oak (*Quercus michauxii*), white oak (*Quercus alba*), silver maple (*Acer saccharinum*), river birch (*Betula nigra*), dogwood (*Cornus sp.*), and black willow (*Salix nigra*). The uplands consist of Yellow poplar (*Liriodendron tulipifera*), white oak (*Quercus alba*), northern red oak (*Quercus rubra*), chestnut oak (*Quercus prinus*), white ash (*Fraxinus americana*), sugar maple (*Acer saccharum*), eastern white pine (*Pinus strobus*), black locust (*Robinia pseudoacacia*), dogwood and redbud (*Cercis Canadensis*). The portion of land that was retrofitted to FRA standards is minimal compared to the entire drainage area at GC 02. A large amount of the land along the hillside above the restored stream section is still highly compacted and has minimal tree growth.

The third site at GC, GC 03, is located at the toe of the VF and collects both discharged waters from the underdrain and created stream system atop the VF. In addition to these

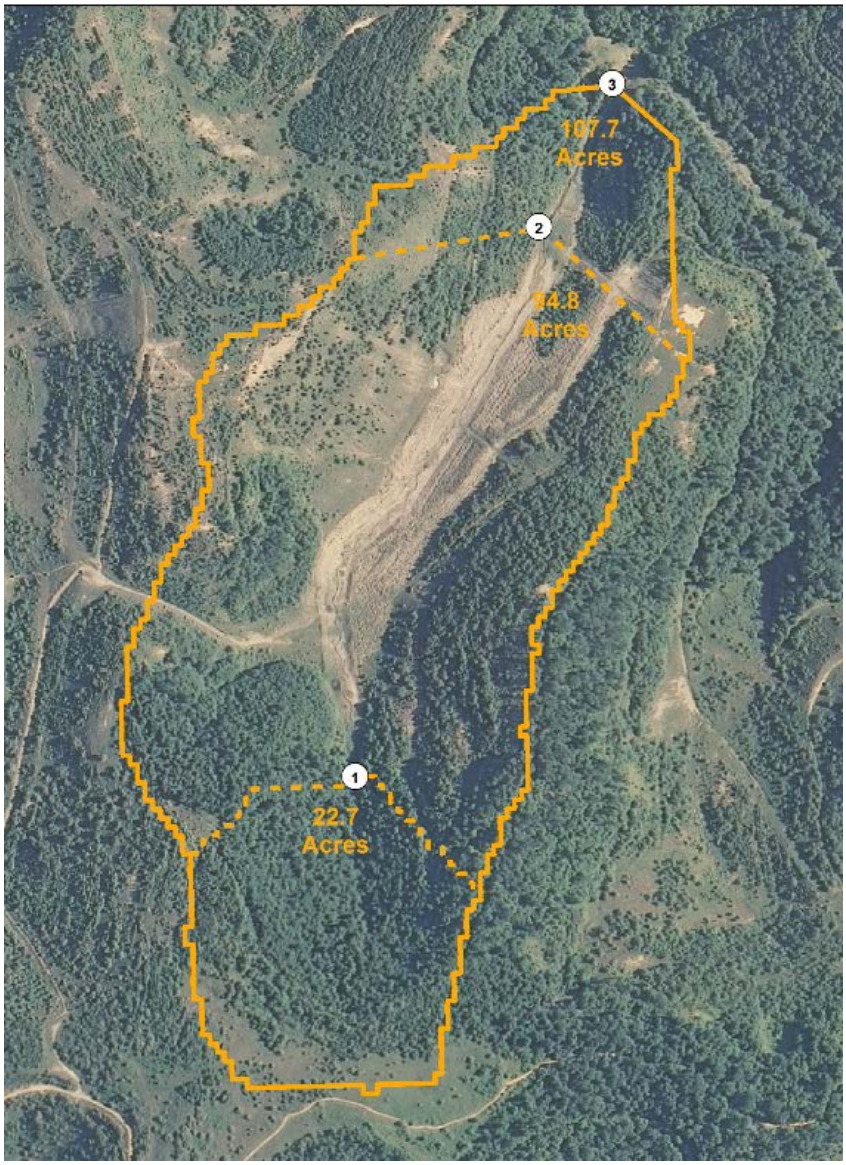

Figure 4.1 Guy Cove Hydrologic Monitoring Locations.

waters GC 03 collects surface runoff from the compacted, non retrofitted area, up gradient from GC 02. This runoff tends to reach GC 03 prior to that from the underdrain and stream system, often times causing two peaks in the hydrograph. The drainage area for GC 03 is about 44 ha.

HYDROLOGIC DATA

Rainfall data were collect with tipping bucket gages that recorded the period rainfall every 15 minutes. The minimum rainfall event used in this analysis was 12.4 mm; the maximum rainfall event was 42.2 mm (Table 4.1). The mean rainfall for the 34 events was 21.9 mm.

At GC01, GC02, and GC03, streamflow was measured using trapezoidal flumes (Grant, 1992), stilling wells, and In-Situ Level TROLL® 500 (5 psig) pressure transducers (Fort Collins, CO). At WB, an H-flume was used to accommodate the size of the unrestored channel and adjacent floodplain. At LMS, streamflow was measured using a 3:1 side-sloped broad-crested combination weir and an In-Situ Level TROLL® 500 (5 psig) pressure transducer (Cherry, 2006). Data were continuously recorded using 15-minute intervals from mid-March to mid-November for both years 2010 and 2011. For GC02, data were recorded from mid-March to July in 2011 due to equipment failure. Streamflow data were not recorded during the winter months due to freezing conditions.

For each site, the baseflow from each hydrograph was separated using the concave method as outlined by McCuen (2004). This method is described as being a more realistic representation of the flow separation during storm events when compared to other baseflow equations. For each hydrograph at each site, the following parameters were calculated for the storm events: discharge volume, peak discharge, discharge duration, time to peak, lag time, and response time (Table 4.2). Time to peak is defined as time between the centroid of the hydrograph and the time of peak discharge. Response time is defined as the start of precipitation to the start of discharge. Lag time is defined as the start of precipitation to the time of peak discharge (Taylor et al., 2009).

STATISTICAL ANALYSIS

To account for the linear connection and the potential to share flow between GC01, GC02, and GC03, a second-order autoregressive model was used (PROC AUTOREG). The autoregressive model is useful in instances where the present value depends on preceding

Table 4.1. Rainfall Events for the 2-year Study Period (n=34).

Event Date	Rainfall (mm)	Duration (hr)	Total 5-day Antecedent Rainfall (mm)
12 March 2010	14.0	3.8	3.0
8 April 2010	23.1	5.3	1.0
27 April 2010	14.5	7.8	31.2
1 May 2010	24.6	5.5	14.5
2 May 2010	31.0	10.5	24.6
14 May 2010	14.5	5.8	5.1
4 June 2010	22.1	3.5	3.8
28 June 2010	29.2	5.3	8.9
11 August 2010	34.8	1.5	0.8
18 August 2010	34.0	9.5	7.9
11 September 2010	17.3	3.3	0.0
25 October 2010	17.8	4.8	0.0
26 October 2010	13.2	5.8	17.8
2 April 2011	33.0	11.8	25.4
8 April 2011	17.8	2.5	0.0
8 April 2011	16.0	1.3	17.8
10 April 2011	35.3	22.5	33.8
14 April 2011	42.2	14.5	35.3
23 April 2011	14.2	4.5	16.8
26 April 2011	41.1	11.3	25.2
2 May 2011	23.4	8.5	43.4
12 May 2011	17.3	1.8	2.5
16 May 2011	11.7	15.0	20.1
22 May 2011	16.8	2.0	13.2
25 May 2011	15.5	17.5	39.1
17 June 2011	13.0	3.5	4.1
18 June 2011	12.4	6.3	29.5

Table 4.1 (continued)

Event Date	Rainfall (mm)	Duration (hr)	Total 5-day Antecedent Rainfall (mm)
14 July 2011	14.2	14.8	23.9
3 September 2011	14.2	8.3	0.0
20 September 2011	16.0	7.8	6.6
18 October 2011	37.1	15.0	0.0
2 November 2011	15.5	5.0	10.9
15 November 2011	29.2	15.3	2.3

Table 4.2. Mean and Standard Errors of the Hydrograph Parameter Monitored during the Study Period.

Site	Hydrograph Parameter					
	Response Time (hr)	Lag Time (hr)	Time to Peak (hr)	Peak Flow (m^3 s^{-1})	Flow Duration (hr)	Total Flow (m^3)
	2010 Rainfall Events					
LMS	19.9±2.3	24.8±0.4	33.0±2.5	0.152±0.079	41.6±4.7	13,041.0±4,270.6
GC01	32.5±12.7	51.2±12.5	24.3±7.7	0.008±0.004	47.6±13.1	317.2±164.9
GC02	24.8±6.5	38.1±7.7	15.2±9.2	0.037±0.010	30.0±19.6	600.3±272.9
GC03	21.8±0.5	27.9±0.8	10.5±2.6	0.077±0.020	18.2±3.1	690.8±295.3
WB	21.8±0.4	28.1±1.0	6.5±1.0	0.101±0.044	15.0±2.6	1,252.4±805.7
	2011 Rainfall Events					
LMS	20.1±2.6	44.8±4.4	26.4±4.7	0.722±0.405	38.6±4.7	22,646.8±12,758.5
GC01	23.2±2.3	54.6±4.8	30.9±5.8	0.002±0.001	59.3±3.6	422.9±133.1
GC02[1]	19.4±1.5	30.5±1.5	11.1±1.6	0.021±0.007	22.9±3.2	610.2±242.0
GC03	19.3±2.5	31.2±2.0	12.0±2.4	0.052±0.015	24.1±3.3	924.8±265.8
WB	24.8±2.2	34.1±2.8	9.2±2.0	0.127±0.036	22.5±3.2	2,254.5±668.4
	2 Year Combined Rainfall Events					
LMS	20.1±1.8	37.3±3.4	28.9±3.1	0.509±0.229	39.7±3.4	19,044.6±8,079.5
GC01	27.3±5.7	53.1±6.0	28.0±4.6	0.006±0.002	54.1±6.1	375.9±101.8
GC02[1]	20.9±2.0	32.5±2.3	12.2±2.5	0.028±0.006	24.8±5.3	766.0±312.8
GC03	20.3±1.5	29.9±1.3	11.1±1.8	0.063±0.012	21.7±2.4	832.0±196.3
WB	23.8±1.5	32.0±1.9	8.3±1.4	0.118±0.028	19.9±2.4	1,907.6±517.6

[1]Data were not recorded from mid-June to mid-November 2011 due to equipment failure.

values, such as the case of accumulating streamflow (Hann, 1977). The independent regressors for the model included drainage area, site, and rainfall event. Since the drainage area of each site differs, it was important to incorporate drainage area into the independent variables as a covariate to allow for normalization between the sites. This resulted in a standardized comparison between the dependent variables. Each hydrograph parameter was evaluated individually, as a dependent variable within the model, to test the null hypothesis of no difference in hydrograph parameter between the sites using the t-test. Significance indicates that, for the given hydrograph parameter, at least one of the five sites differed.

Significantly different hydrograph parameters were further evaluated using a linear mixed model (PROC MIXED). The dependent variable is hydrograph parameter and the independent variable is rainfall event. Contrasts between the sites were used to determine if the recreated stream reaches are significantly different from LMS or WB based on the F test. A significant level of $p=0.05$ was used for all statistical analyses. All statistical calculations were performed using SAS version 9.2 (SAS Institute, Inc., 2008).

Statistically significant site differences were determined for the number of days of streamflow using a one-way ANOVA on ranks in SigmaPlot® (

Table 4.3 2010 and 2011 Monthly Precipitation Totals for Jackson, Kentucky and Robinson Forest.

Month	Monthly Precipitation (mm)				
	Normal	Jackson	Robinson Forest	Jackson Departure from Normal	Robinson Forest Departure from Normal
	2010				
January	90.4	108.2	--	+17.8	--
February	93.5	75.2	51.8[1]	-18.3	--
March	111.3	60.5	44.7	-50.8	-66.6
April	96.3	66.3	75.4	-30.0	-20.9
May	131.1	201.2	107.7	+70.1	-23.4
June	118.6	141.7	98.6	+23.1	-20.0
July	116.6	66.8	78.0	-49.8	-38.6
August	104.9	89.2	86.9	-15.7	-18.0
September	95.8	52.1	56.9	-43.7	-38.9
October	80.8	42.7	38.1	-38.1	-42.7
November	106.7	139.7	49.0[1]	-33.0	--
December	108.5	81.5	--	-26.9	--
Total for 2010 Period	*1,254.3*	*1,125.0*	--	*-129.3*	--
	2011				
January	90.4	68.6	--	-21.8	
February	93.5	101.3	--	+7.9	--
March	111.3	120.1	32.0[1]	+8.9	--
April	96.3	259.8	229.1	+163.6	+132.8
May	131.1	169.2	120.1	+38.1	-11.0
June	118.6	139.4	72.1	+20.8	-46.5
July	116.6	152.9	65.0	+36.3	-51.6
August	104.9	78.0	--	-26.9	--
September	95.8	81.3	2.3	-14.5	-36.6
October	80.8	108.0	3.8	+27.2	+15.7
November	106.7	139.2	2.8[1]	+32.5	--
December	108.5	106.2	--	-2.3	--
Total for Period	*1,254.3*	*1,524.0*	--	*+269.7*	--

[1]Partial month.

STUDY SITE COMPARISON

A comparison of the storm event hydrograph characteristics discharge volume, peak discharge, discharge duration, time to peak, lag time, and response time showed significant differences among the sites. Significant differences were found for time to peak (2010, 2010, combined 2010 and 2011 rainfall events) and flow duration (2011 and combined 2010 and 2011 rainfall events) among the sites (Tables 4.4 and 4.5). With regards to the parameter time to peak, GC01 and LMS had significantly higher values than GC03 and WB. On average, 1.2 days were required for peak discharge to occur at GC01 and LMS whereas about half the time was needed at GC03 and WB. It was somewhat surprising that GC03 and WB behaved similarly with regards to time to peak as the entrance to the underdrain, on the crown of the VF, was sealed at GC and about 4 ha of the watershed was reclaimed using FRA. The FRA was expected to increase time to peak and reduce peak discharge at the site (Taylor et al., 2009). This does not appear to be the case for GC03 where the efficiency, at which the underdrain moves storm waters and ground waters away from the VF, is high. Storm flows quickly passed through the underdrain to the stream. It also appears that a large amount of overland flow is still occurring from the non-retrofitted land areas up gradient of GC 03. This flow is reaching the stream system rather quickly and causing a quicker time to peak value and a much steeper hydrograph at GC 03. However, at GC02, the similarity between this site and GC01 and LMS indicates that the FRA and stream creation efforts are having some mitigation effect.

For flow duration, GC01 had the largest values with an average of over 2-days. It is surprising that a reach of stream so high in the headwaters would have such long storm flow durations; however, this result is likely because the origin of this stream is a small headwater spring located near the ridge top. Next were LMS and GC02 which averaged 1 to 1.8 days. This result is promising in that the created stream reach on top of the crown of the VF is exhibiting storm flow durations that are equivalent to the unmined, forested watershed of LMS. This result also suggests that the FRA and stream creation efforts are having a mitigating effect. The sites at the toes of the VFs, GC03 and WB, had the shortest storm flow durations averaging less than 1 day. Reclamation efforts only on the crown of the VF did little to modify flow duration at the toe of the VF.

Table 4.4 Summary of Second-order Auto Regression Results.

Hydrograph Parameter	p-value	t-statistic	Reject
	2010 Rainfall Events		
Response Time (hr)	0.93	-0.09	No
Lag Time (hr)	0.20	-1.29	No
Time to Peak (hr)	0.03	-2.32	Yes
Peak Flow ($m^3 s^{-1}$)	0.40	-0.85	No
Flow Duration (hr)	0.07	-1.88	No
Total Flow (m^3)	0.56	-0.59	No
	2011 Rainfall Events		
Response Time (hr)	0.07	1.85	No
Lag Time (hr)	0.31	-1.02	No
Time to Peak (hr)	0.03	-2.21	Yes
Peak Flow ($m^3 s^{-1}$)	0.78	-0.28	No
Flow Duration (hr)	0.05	-2.00	Yes
Total Flow (m^3)	0.56	-0.59	No
	2 Year Combined Events		
Response Time (hr)	0.57	0.57	No
Lag Time (hr)	0.11	-1.63	No
Time to Peak (hr)	0.01	-2.82	Yes
Peak Flow ($m^3 s^{-1}$)	0.88	-0.15	No
Flow Duration (hr)	0.01	-2.57	Yes
Total Flow (m^3)	0.54	-0.62	No

Table 4.5 Time to Peak and Flow Duration for 2 Year Combined Rainfall Events.

Hydrograph Parameter	Site				
	LMS	GC01	GC02	GC03	WB
Time to Peak (hr)	28.9 ± 3.1^{a}	28.0 ± 4.6^{a}	12.2 ± 2.5^{ab}	11.1 ± 1.8^{b}	8.3 ± 1.4^{b}
Flow Duration (hr)	39.7 ± 3.4^{b}	54.1 ± 6.1^{a}	24.8 ± 5.3^{b}	21.7 ± 2.4^{c}	19.9 ± 2.4^{c}

Within row values followed by the same letter are not significantly different (

Figure 4.2 illustrates the difference in flow duration, as well as time to peak, between the sites for a representative storm event (42.2 mm depth; 14.5 hour duration). The hydrographs shapes between LMS, GC01, GC02, GC03 and WB were quite varied. An important point to note in Figure 4.2 is the large peak discharge and runoff volume at WB. The drainage area at WB is 44.1 ha, which is equivalent to GC03's drainage area of 44 ha. However, the hydrograph response between the two, although statistically similar for all examined variables, has important differences. In Figure 4.2, the peak discharge at GC03 is about 3 times less than that of WB. The reason for the difference between the two sites, whether inherent or treatment related, is unknown as pre-restoration flow data are not available.

Also of equal interest are the variables where a significant difference (

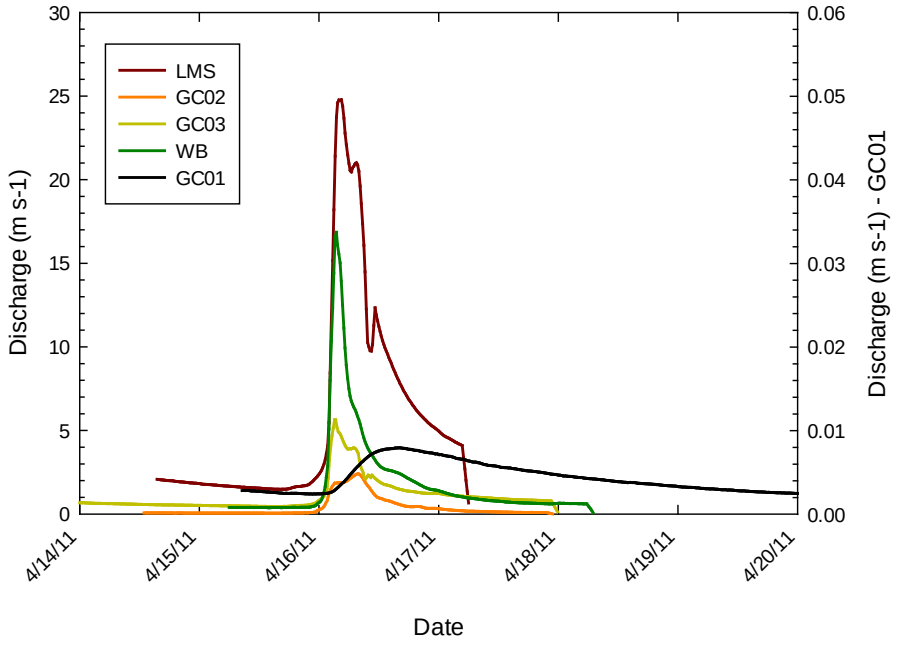

Figure 4.2. Representative Hydrologic Response for LMS, GC01, GC02, GC03 and WB for a storm event on April 14, 2011 with a rainfall depth of 42.2 mm and a duration of 14.5 hours. *GC01 is on the secondary axis.*

Table 4.6. Number of Days of Flow at Main Channel Monitoring Stations.[1]

Month	Number of Days of Flow				
	LMS	GC01	GC02	GC03	WB
	2010				
February	28	28	28	28	--
March	27	31	31	31	--
April	26	30	30	30	--
May	31	31	28	31	31
June	30	30	0	30	30
July	31	24	0	30	31
August	29	13	0	31	31
September	26	0	0	30	30
October	31	0	0	31	31
November	19	0	0	19	19
	2011[2]				
March	15	15	15	15	15
April	30	30	30	30	30
May	31	31	31	31	31
June	30	30	7	30	30
July	31	31	23	31	31
August	31	30	3	31	31
September	30	20	10	30	30
October	31	31	14	31	31
November	19	18	14	19	19

[1]Monitoring started on February 1, 2010 and ended on November 19, 2010.
[2]Monitoring started on March 17, 2011 and ended on November 19, 2011.

Table 4.7. Mean and Standard Error of Number of Days of Flow for 2010 and 2011.

Parameter	Site				
	LMS	GC01	GC02	GC03	WB
Days of flow	27.7±1.1[a]	22.6±2.6[a]	13.9±2.9[b]	28.4±1.1[a]	28.4±1.1[a]

CONCLUSIONS

Hydrologic parameters at five sites located in three watersheds within the University of Kentucky Robinson Forest were monitored in 2010 and 2011. One study site was located in an unmined, forested watershed (LMS) and four were located on mined lands. Three of the four sites were located in Guy Cove, which is the site of a VF retrofit using FRA and natural channel design principles to recreated about 1.6 km of stream. One of these monitoring points was immediately up-gradient of the recreated stream reach (GC01); one at the interface of the crown and the face of the VF (GC02); and one down-gradient of the toe of the VF (GC03). A fourth site was located down-gradient of the toe of a non-retrofitted VF (WB). Results of this study indicate that the hydrologic parameters time to peak and flow duration significantly differed between the sites when examining only storm flows. For time to peak, the stream reach located on the crown of the VF (GC01 and GC02) was similar to the unmined, forested reference watershed. The sites below the VF had much shorter time to peaks. For flow duration, GC01 had much larger values and GC02 was similar to the reference watershed. Flow duration was much shorter for the sites below the VF. Sites below the VF exhibited a flashy hydrology, partially due to the large amount of highly compacted land area that drains into these locations. No significant differences were noted between any of the sites and the hydrologic parameters response time, lag time, peak flow, and total flow. When considering a base flow condition such as the number of days of flow at each reach, significant differences emerge between GC02 and the other sites. GC02 is the only site without a baseflow contribution, and as such, it had the least number of days with flow, particularly during the summer and fall months.

The results from this study indicate the created stream reach, on the crown of the VF (GC01 and GC02), is performing similarly to an unmined, forested watershed (LMS) with regards to the hydrograph parameters evaluated for storm events. However, lack of a groundwater contribution at GC02 is affecting baseflow. Results also indicate that the FRA and stream restoration work did little to modify the hydrologic characteristics of the stream down-gradient of the toe of the VF.

CHAPTER 5: SUMMARY OF CONCLUSIONS

The objectives of this study were to evaluate specific conductivity sensor performance and the hydrologic characteristics of the Guy Cove stream restoration project. Sensor evaluation of four continuously recording specific conductivity sensors was completed both in a controlled lab setting (i.e. known temperature and EC_{25^oC} standards) and in the field. Conclusions were made based on the accuracy and temporal consistency of recordings for each sensor in the lab research. Since there was no specific conductivity standard for comparison, only temporal consistency was analyzed in the field setting. Characterization of the hydrologic properties of the Guy Cove stream restoration project was completed by comparing the storm event hydrologic characteristics to reference locations that were located below an unrestored valley fill and within an unmined watershed. Recent USEPA guidance pertaining to water quality thresholds for Appalachian streams within mined watersheds make it particularly important that sensor output are consistent and accurately represent the true water quality of the stream systems. Combining these results with anticipated hydrologic characteristics of discharge from mined areas could give insight to reclamation practices and monitoring methods that properly improve and monitor water quality.

Background information about surface mining techniques and previous reclamation practices are introduced in Chapter 1. The reclamation methods used to design the Guy Cove stream restoration project are also described. Threshold water quality levels defined by recent USEPA guidance can be found in Chapter 1.

Specific conductivity sensor performance was compared in Chapter 2 and Chapter 3. The controlled lab study (Chapter 2) revealed that both the YSI and Aqua Troll sensors were temporally consistent over all temperature and EC_{25^oC} combinations. The results also indicated that temporal inconsistencies in the HOBO and Solinst sensors were due to the highest tested EC_{25^oC} standard, 9,986 $\mu S\ cm^{-1}$, and were consistent over all other temperature and EC_{25^oC} combinations. In regards to accuracy, all four the sensors tested had slopes that significantly differed from one and intercept values that were not significantly different from zero. In the lab analysis multiple sensors of each type were tested and in several instances at least one sensor of the same type performed quite differently than the others. Therefore, sensors should be regularly tested against NIST EC_{25^oC} standards and careful attention should be paid to individual sensor performance; particularly when the sensor is used for regulatory

enforcement. The white noise variance of field recordings for each sensor type was evaluated in Chapter 3. It was found that white noise variance for each sensor is positively correlated with $EC_{25°}$ levels and discharge. Results indicated that $EC_{25°C}$ and discharge explain 65 percent of the white noise variance with the Solinst sensors, 35 percent for Aqua TROLL sensors, 47 percent for YSI sensors, and 39 percent for HOBO sensors. In addition to performance, the selection of which $EC_{25°C}$ sensor to purchase requires consideration of costs, additional parameters that a particular sensor can monitor, calibration needs of the sensor, and ruggedness of the sensor depending on deployment conditions.

In Chapter 4 the hydrologic characteristics of five study locations were compared. Results from the study indicated that there were no significant differences between the sites for the hydrologic parameters response time, lag time, peak flow, and total flow when examining only storm events. However, significant differences were noted for the parameters of time to peak and flow duration for storm events. Sites below the valley fill, GC03 and GC04, had much shorter time to peaks and exhibited flashy hydrology with smaller flow durations in comparison to the unmined, forested watershed (LMS). The restored stream reach located atop the VF (GC01 and GC02) had time to peak values that were similar to LMS. The flow duration at GC01 was much longer than either of the reference locations but GC02 resembled that of LMS. Overall results from this study demonstrate that the restored stream reach on the crown of the VF (GC01 and GC02) is hydrologically performing similar to the unmined, forested watershed (LMS) for storm events. Results also indicate that the FRA and stream restoration work did little to modify the hydrologic characteristics of the stream down-gradient of the toe of the VF.

CHAPTER 6: FUTURE WORK

To fully understand the effects of the Guy Cove stream restoration and retrofitted valley fill design, further analysis of not only the hydrology but water quality needs to be performed. The hydrologic characteristics of the site need to be continually monitored to highlight the effect of increased tree and vegetation growth.

The water quality of discharge from the Guy Cove site also needs to be compared to the mined (GC04) and unmined watersheds (LMS). This comparison will indicate if restoration efforts are effectively creating water quality that is trending towards USEPA designated thresholds for the Appalachian region. In addition to the elemental water quality parameters currently being analyzed in the University of Kentucky laboratories, further analysis of the electrical conductivity, total dissolved solids (TDS), and total suspended solids (TSS) associated with discharge from the Guy Cove project and reference streams needs to be compared. TDS and TSS values could give information pertaining to the stream and VF stability. It is also of interest to compare the differences in the electrical conductivity levels and temporal fluctuations that may occur in mined and unminded watersheds. Continuous and in-situ monitoring of $EC_{25^{o}C}$ and the associated temporal fluctuations will give added insight to monitoring methods that could be implemented for regulatory practices.

APPENDICES

APPENDIX A: $EC_{25^{o}C}$ DEPLOYMENT READINGS FOR EACH SENSOR

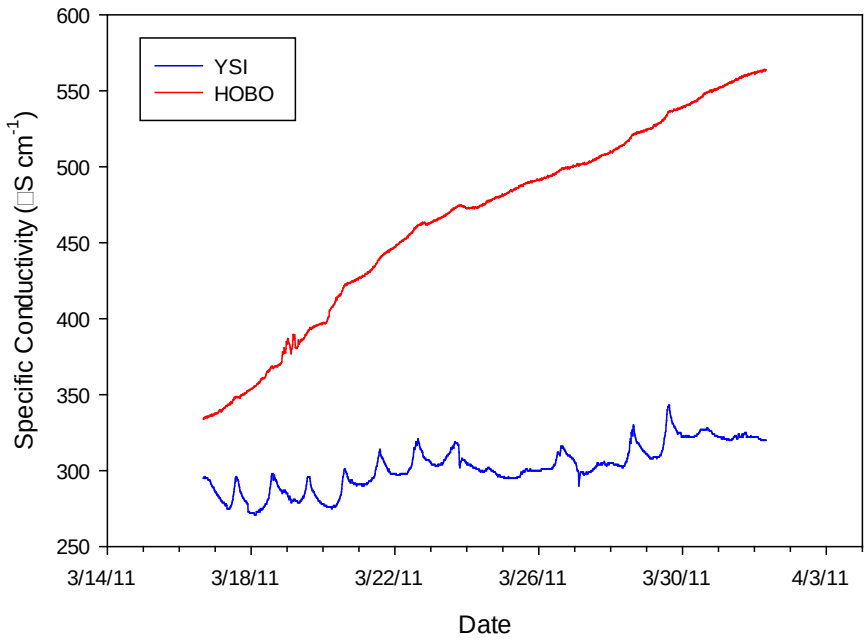

Figure A.1. Specific Conductivity (

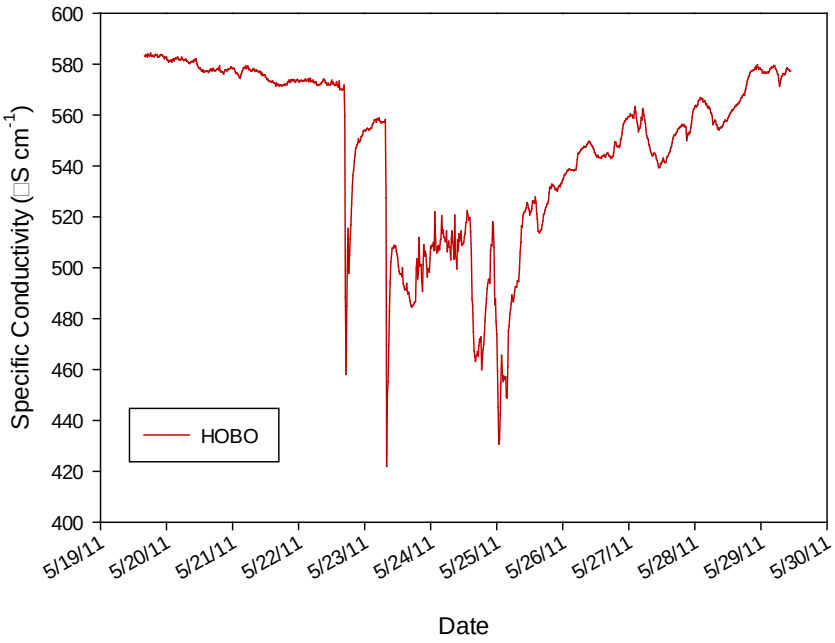

Figure A.3. Specific Conductivity (

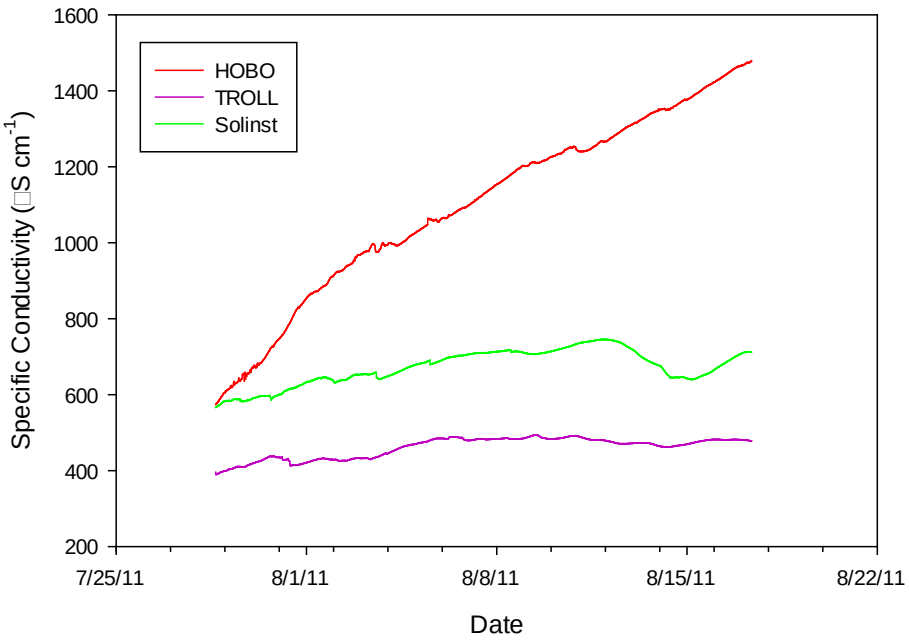

Figure A.5. Specific Conductivity (

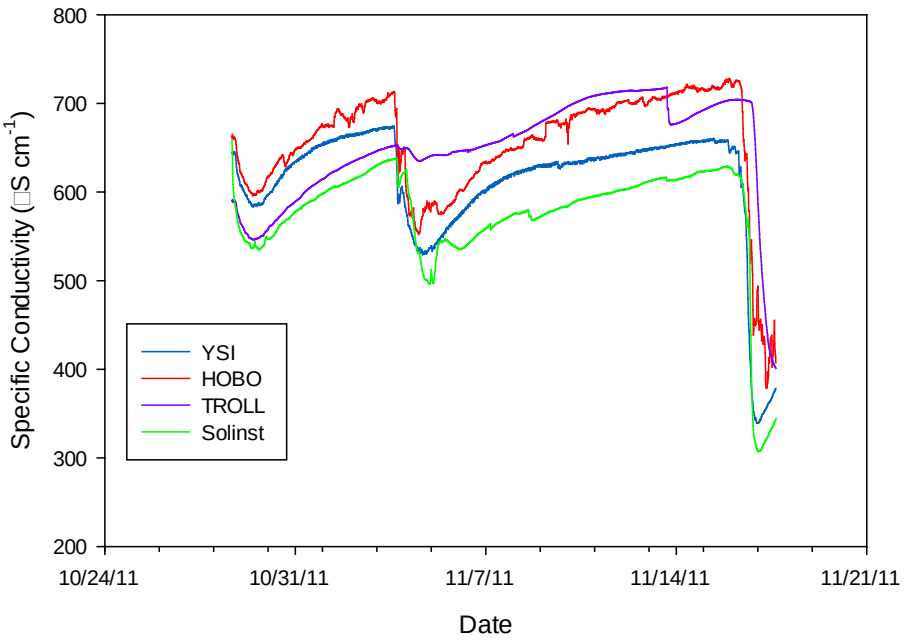

Figure A.7. Specific Conductivity (

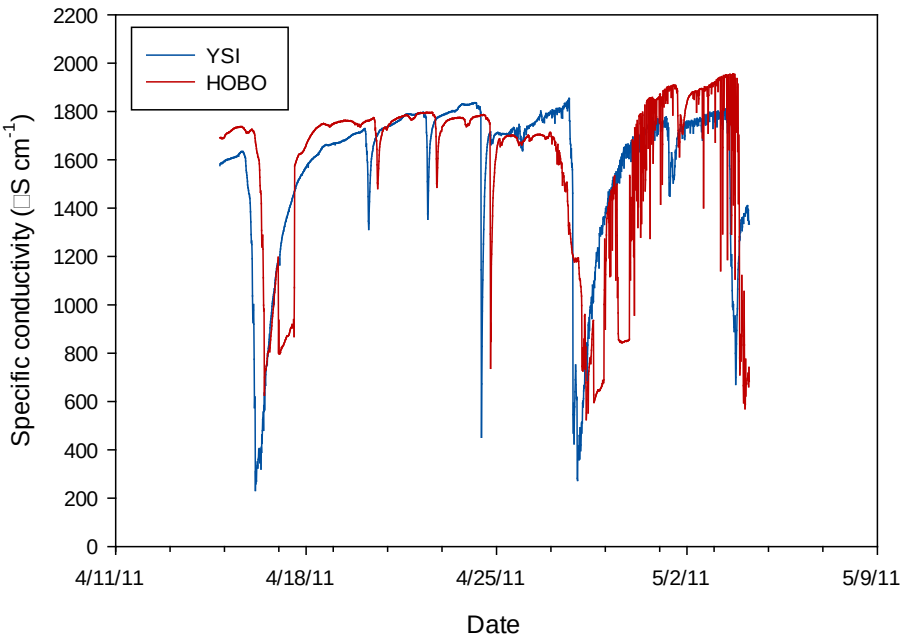

Figure A.9. Specific Conductivity (

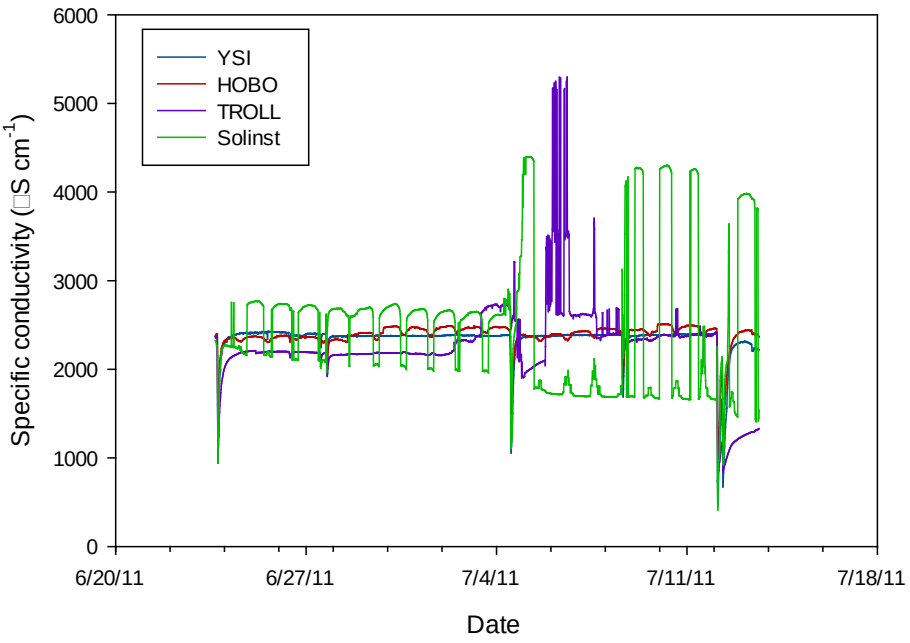

Figure A.11. Specific Conductivity (

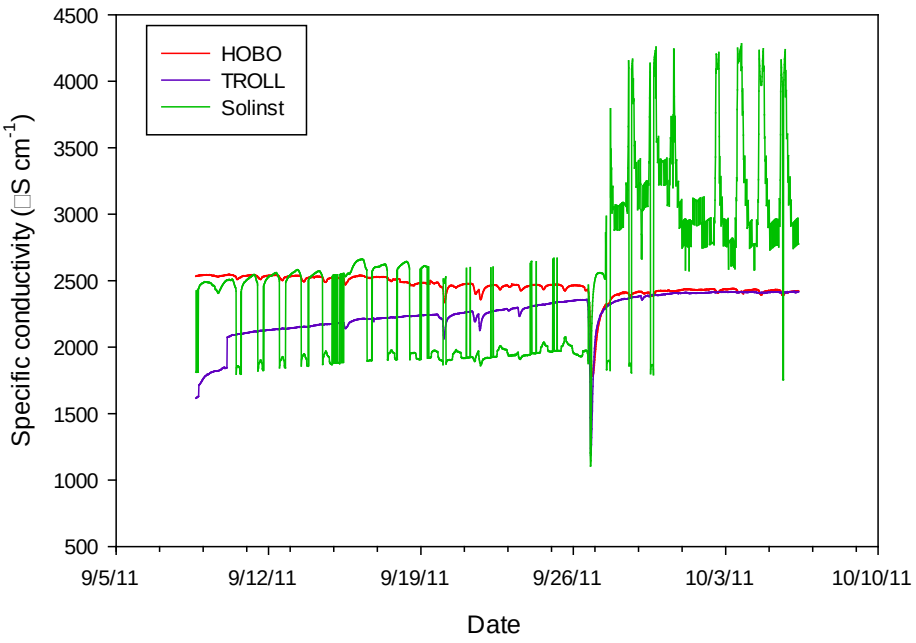

Figure A.13. Specific Conductivity (

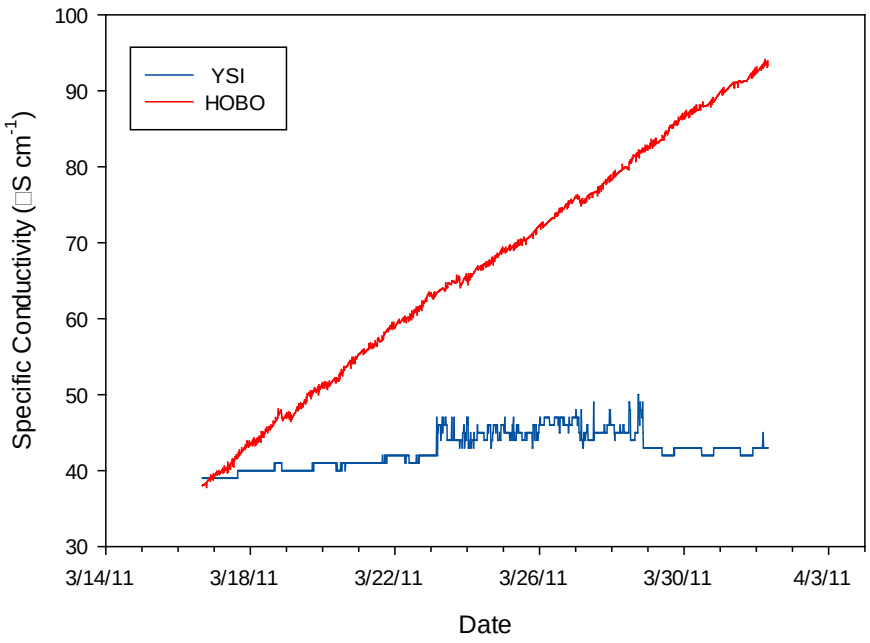

Figure A.15. Specific Conductivity (

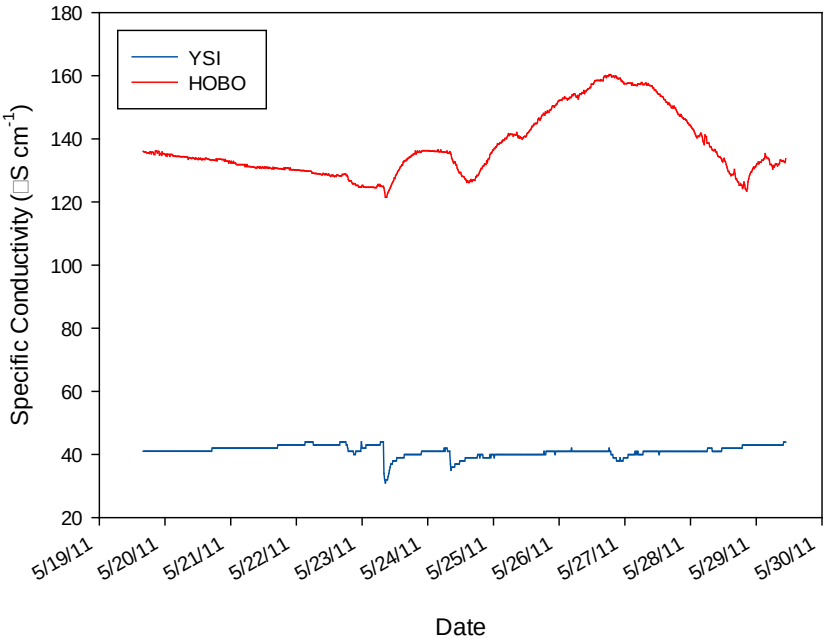

Figure A.17. Specific Conductivity (

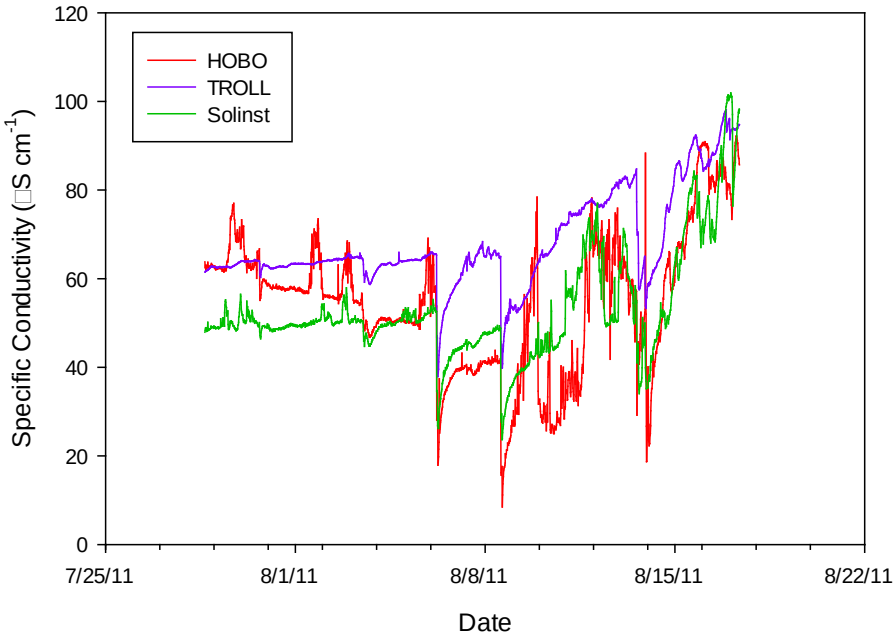

Figure A.19. Specific Conductivity (

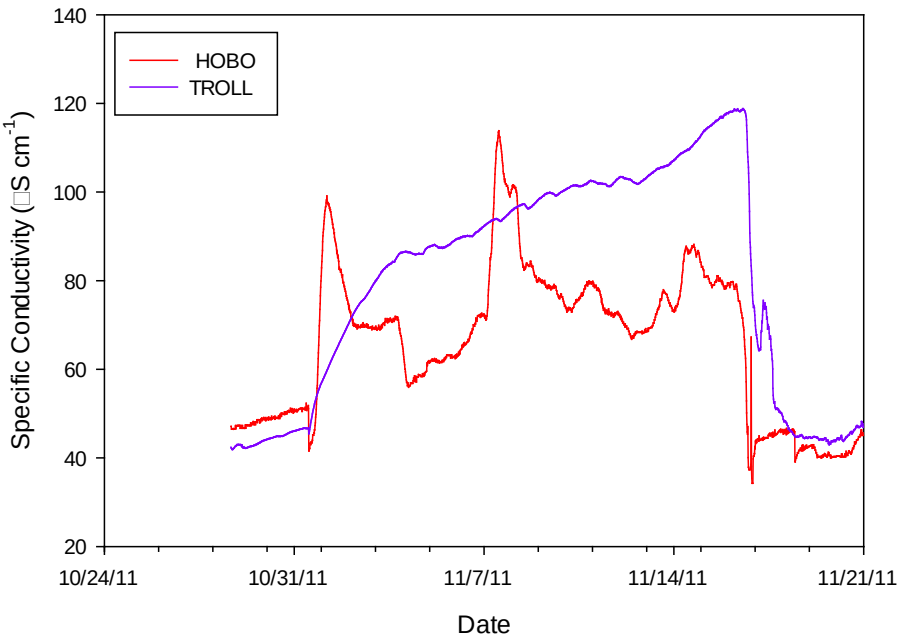

Figure A.21. Specific Conductivity (

APPENDIX B: HYETOGRAPHS

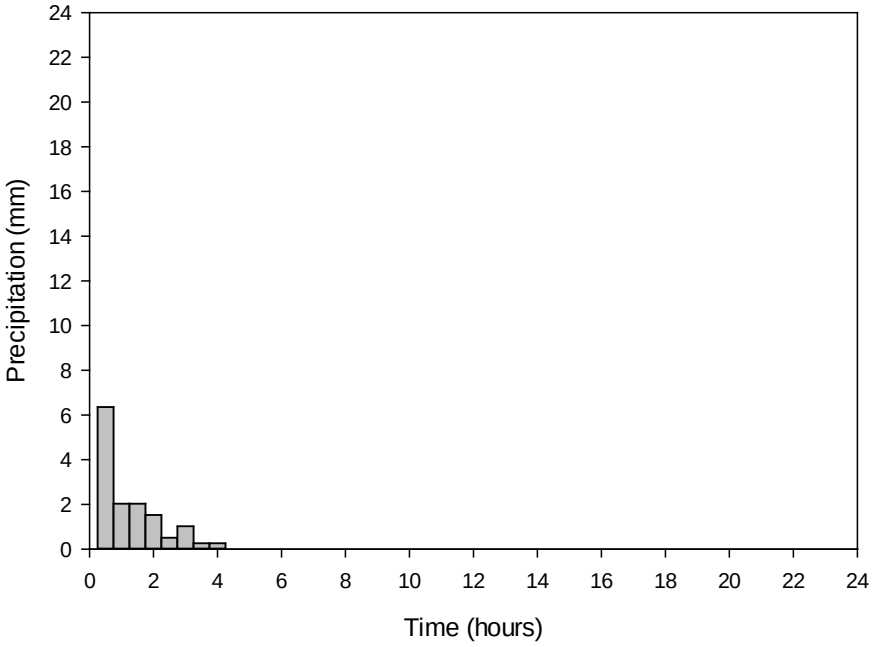

Figure B.1. Rainfall Event on March 12, 2010.

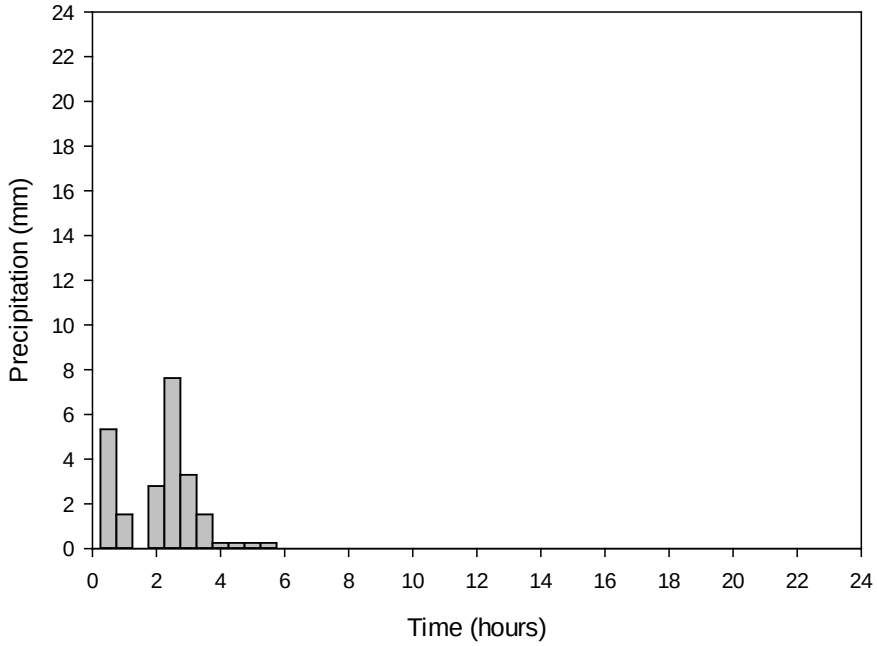

Figure B.2. Rainfall Event on April 8, 2010.

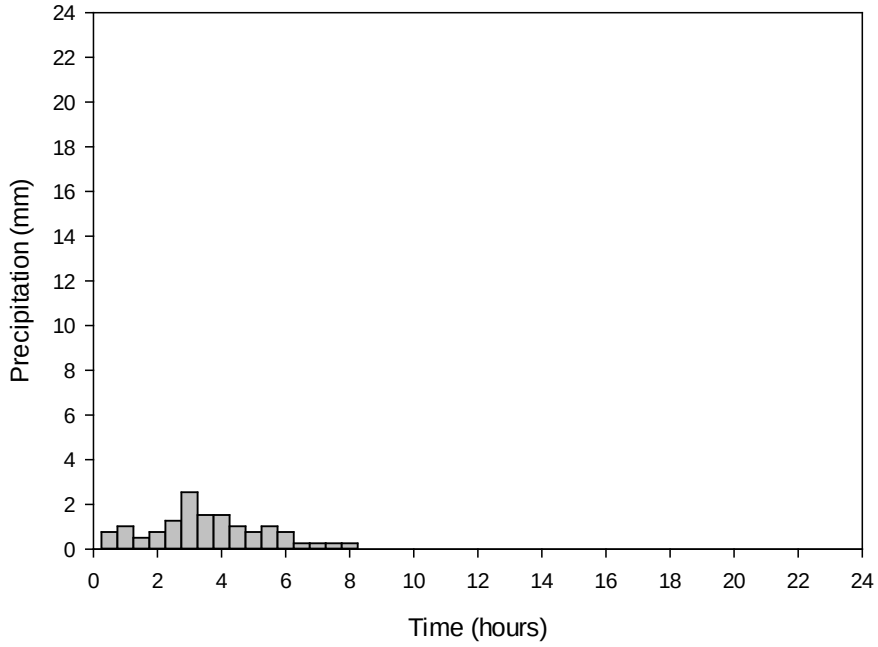

Figure B.3. Rainfall Event on April 27, 2010.

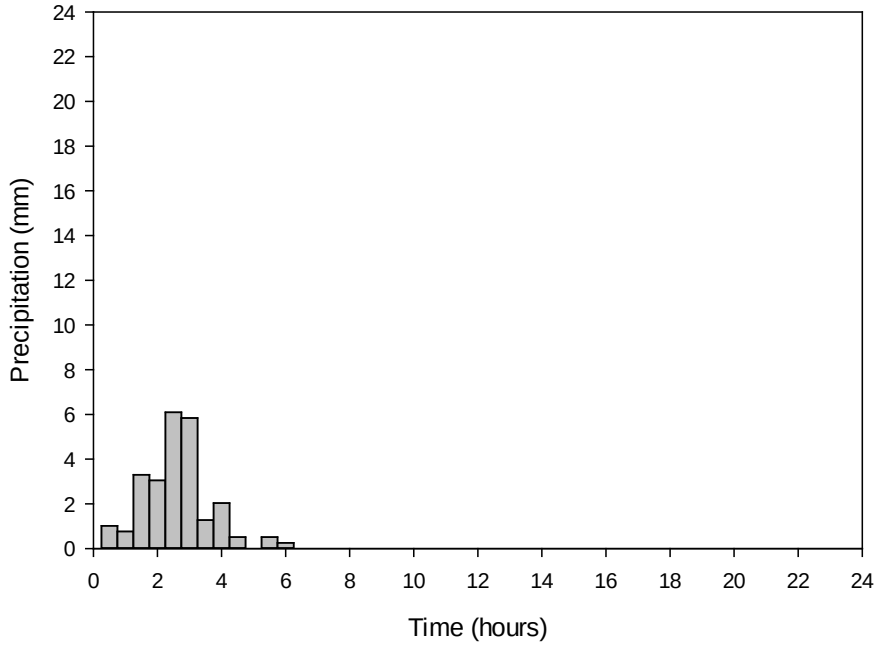

Figure B.4. Rainfall Event on May 1, 2010.

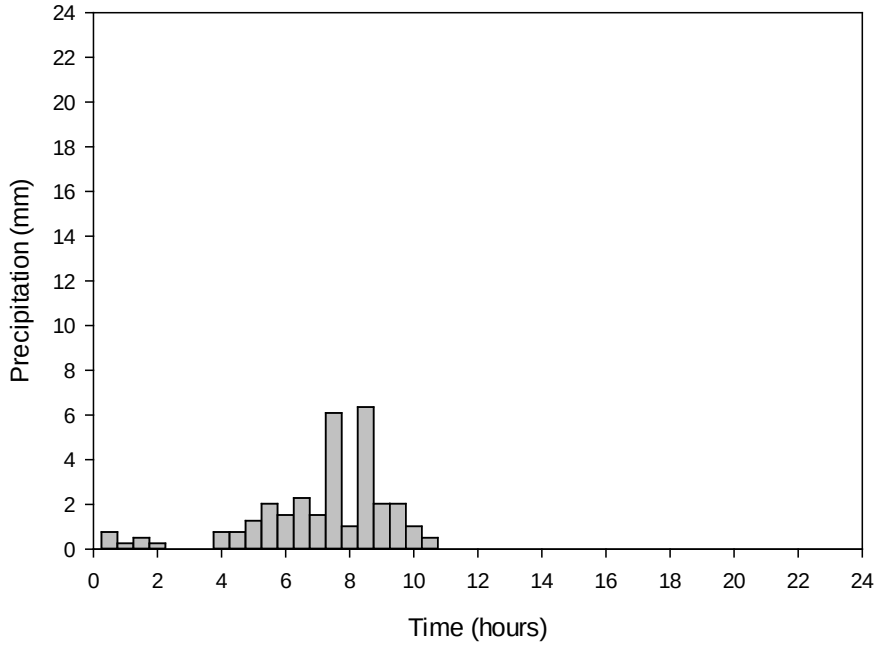

Figure B.5. Rainfall Event on May 2, 2010.

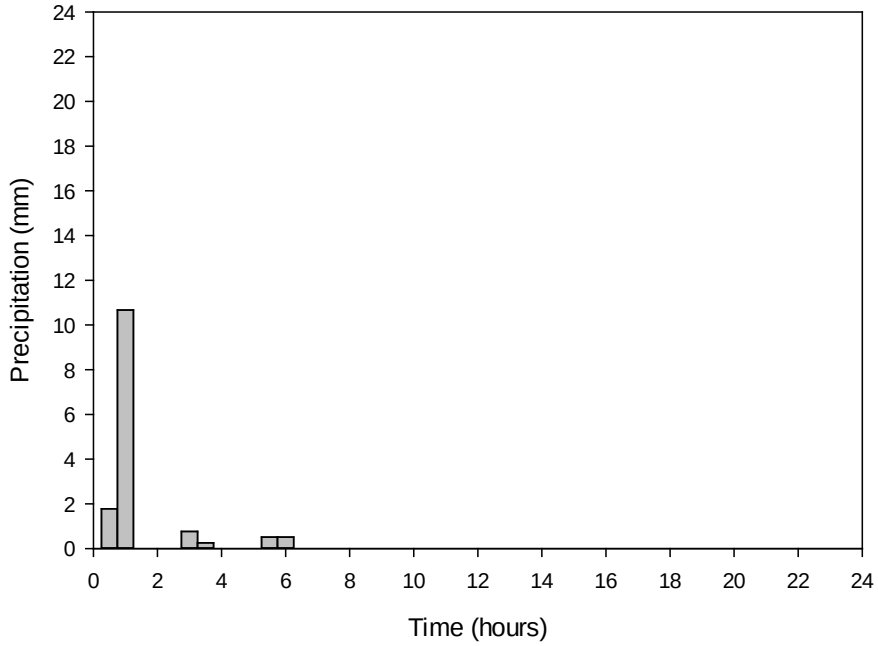

Figure B.6. Rainfall Event on May 14, 2010.

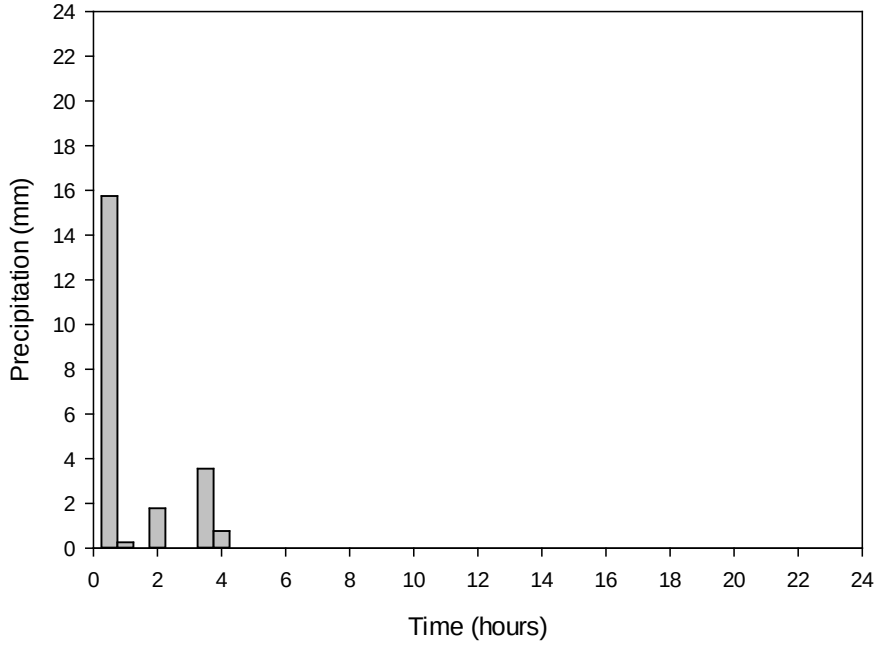

Figure B.7. Rainfall Event on June 4, 2010.

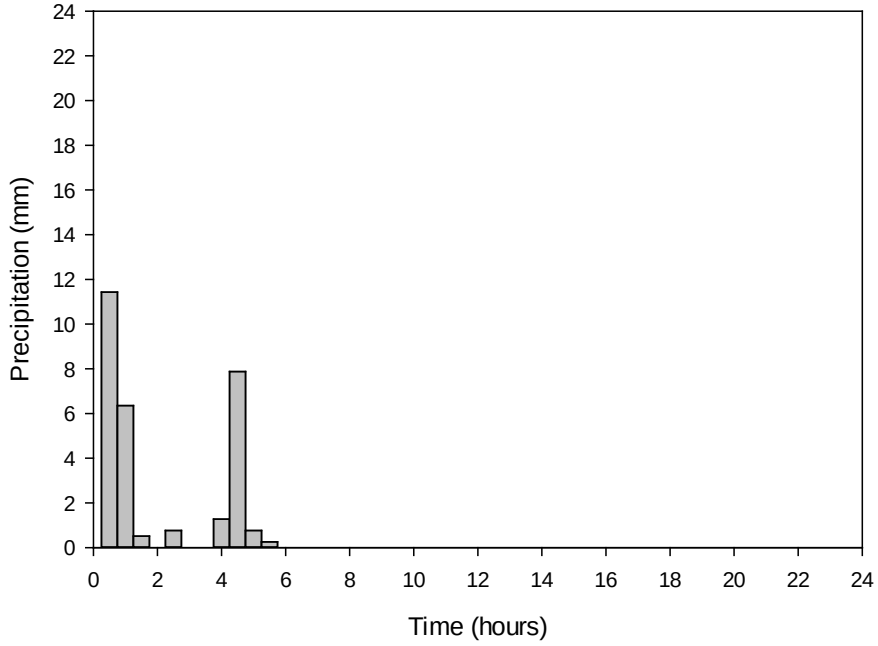

Figure B.8. Rainfall Event on June 28, 2010.

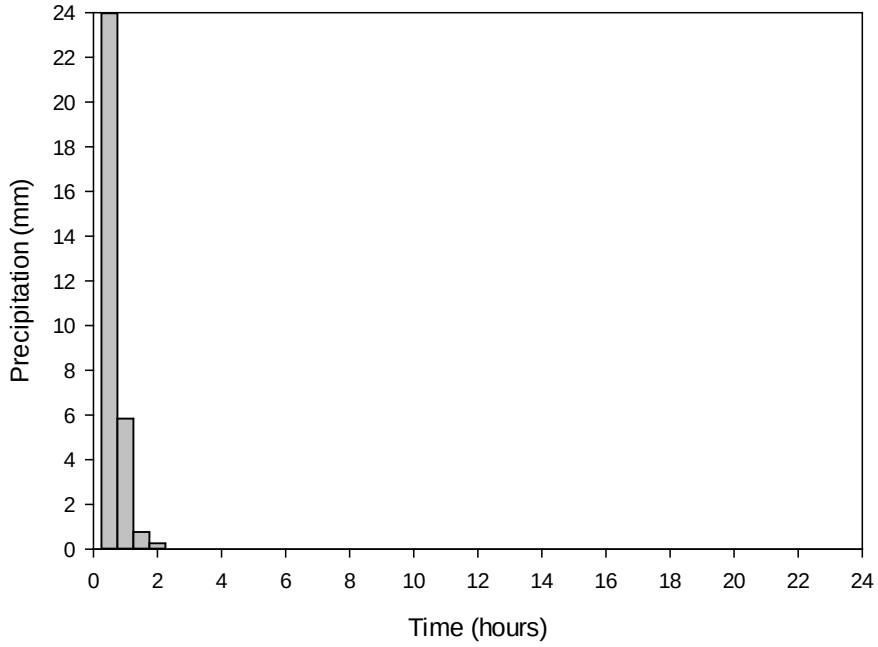

Figure B.9. Rainfall Event on August 11, 2010.

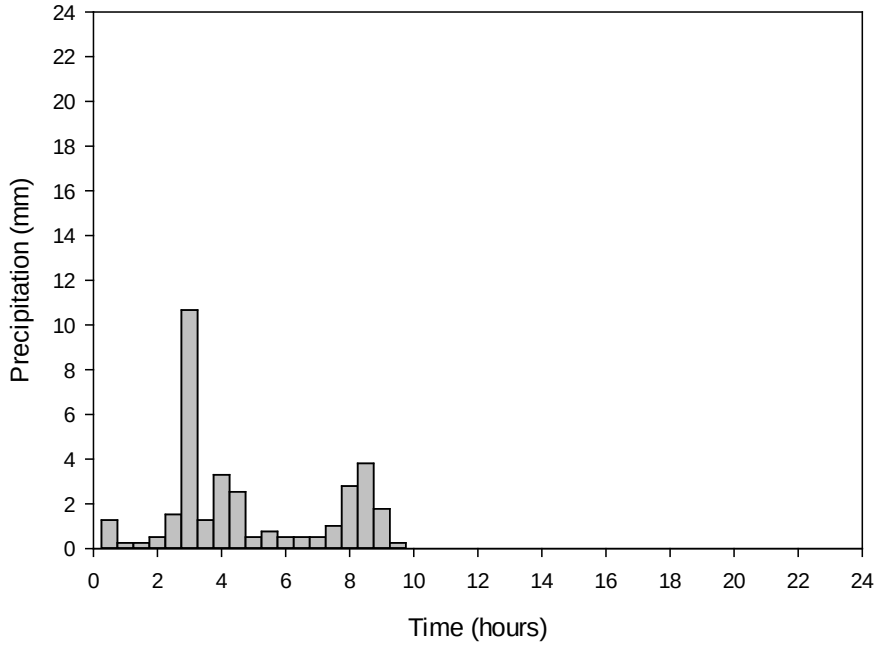

Figure B.10. Rainfall Event on August 18, 2010.

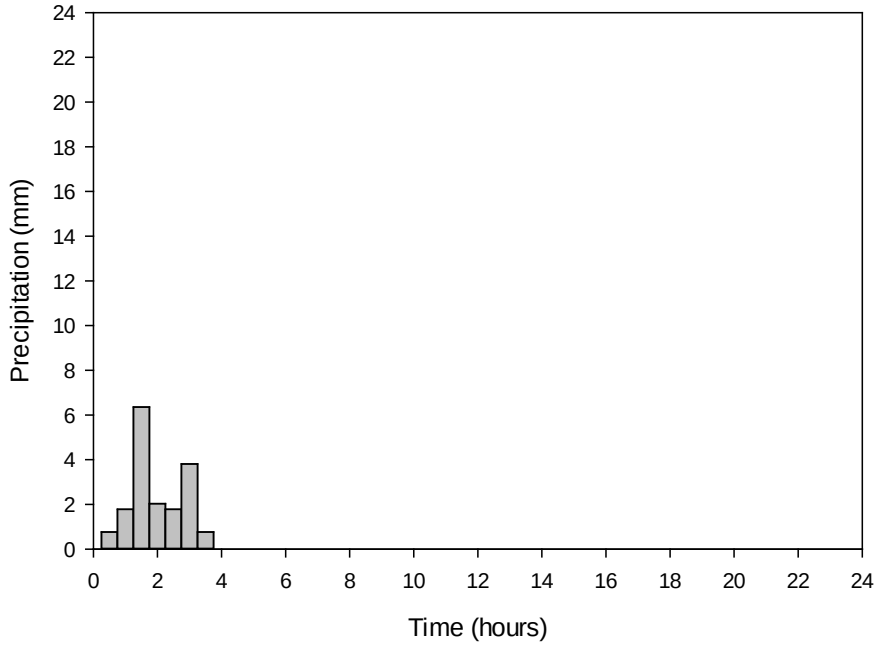

Figure B.11. Rainfall Event on September 11, 2010.

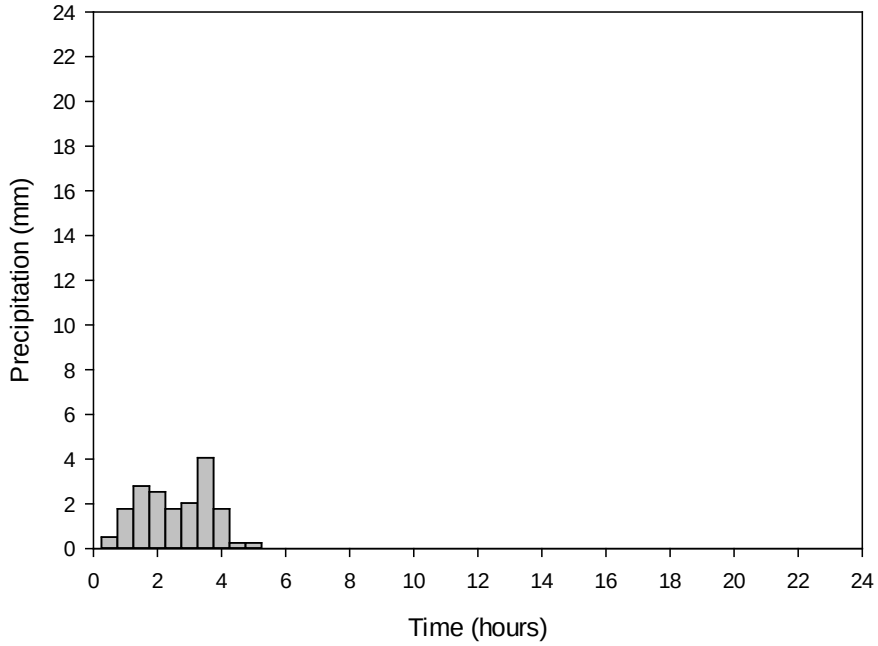

Figure B.12. Rainfall Event on October 25, 2010.

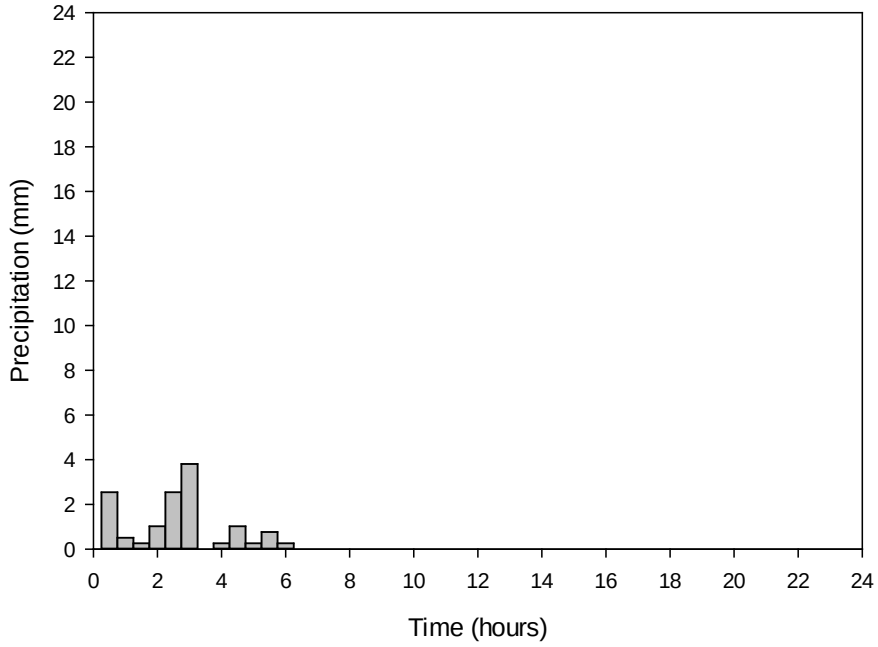

Figure B.13. Rainfall Event on October 26, 2010.

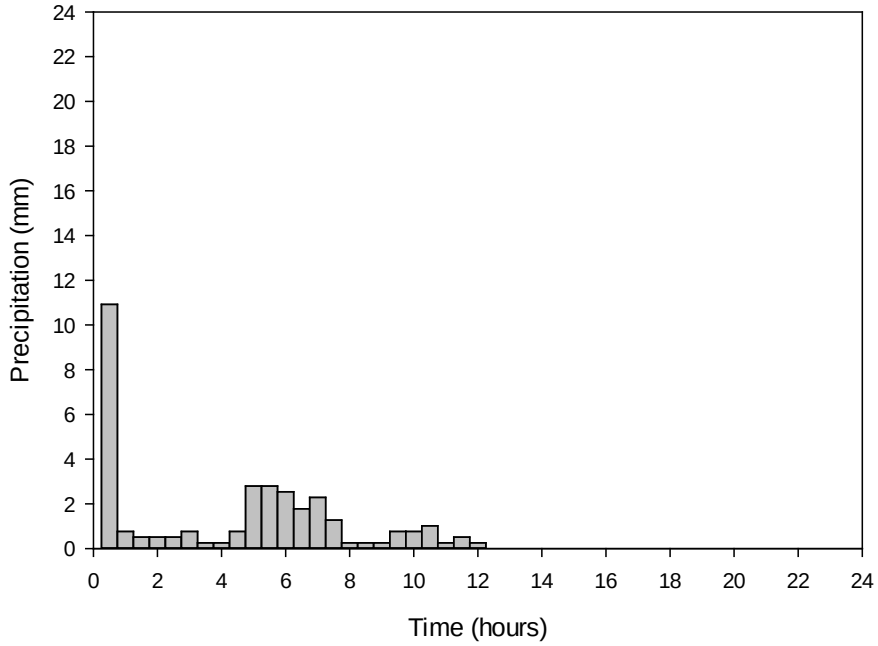

Figure B.14. Rainfall Event on April 2, 2011.

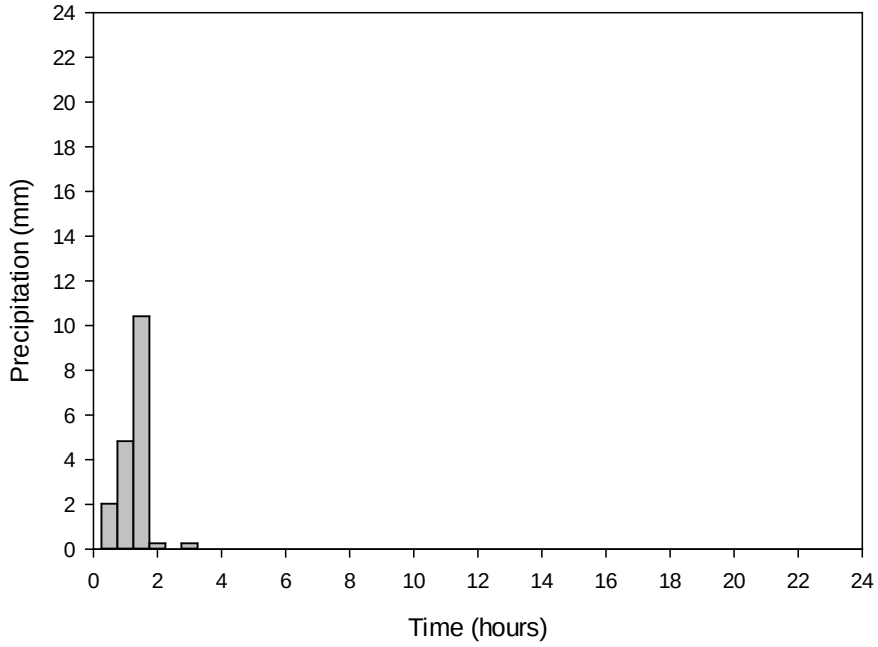

Figure B.15. Rainfall Event on April 8, 2011.

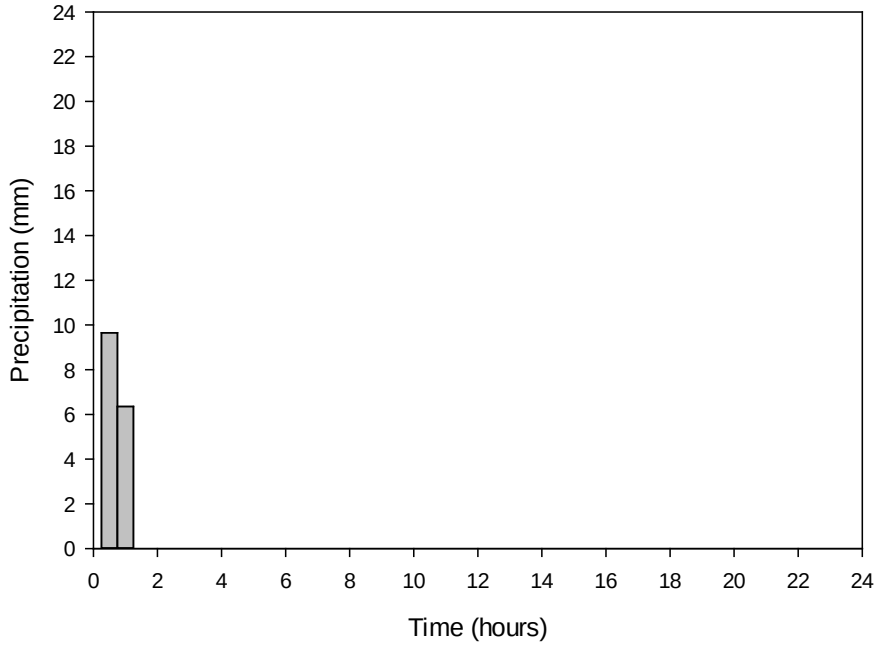

Figure B.16. Rainfall Event on April 8, 2011.

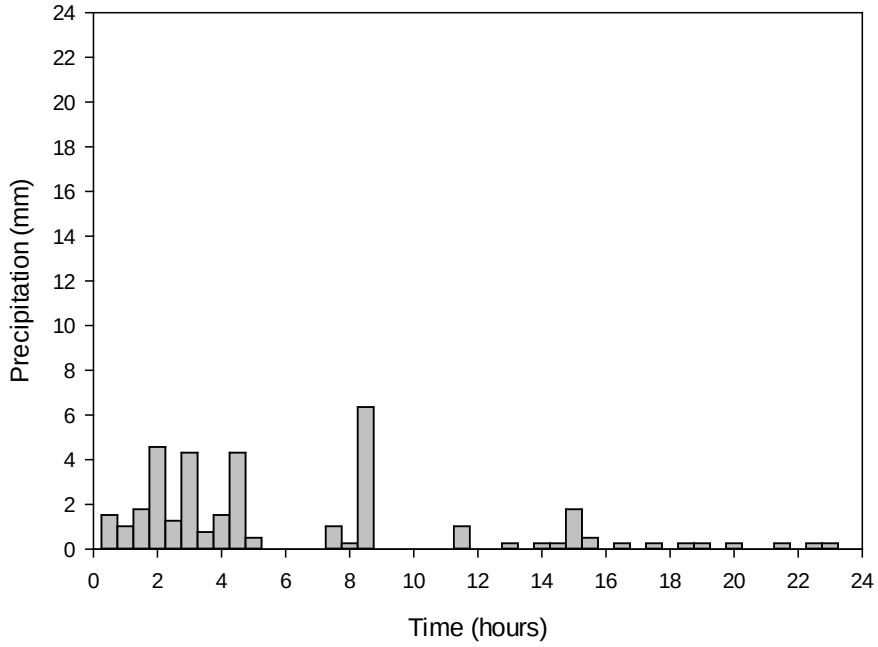

Figure B.17. Rainfall Event on April 10, 2011.

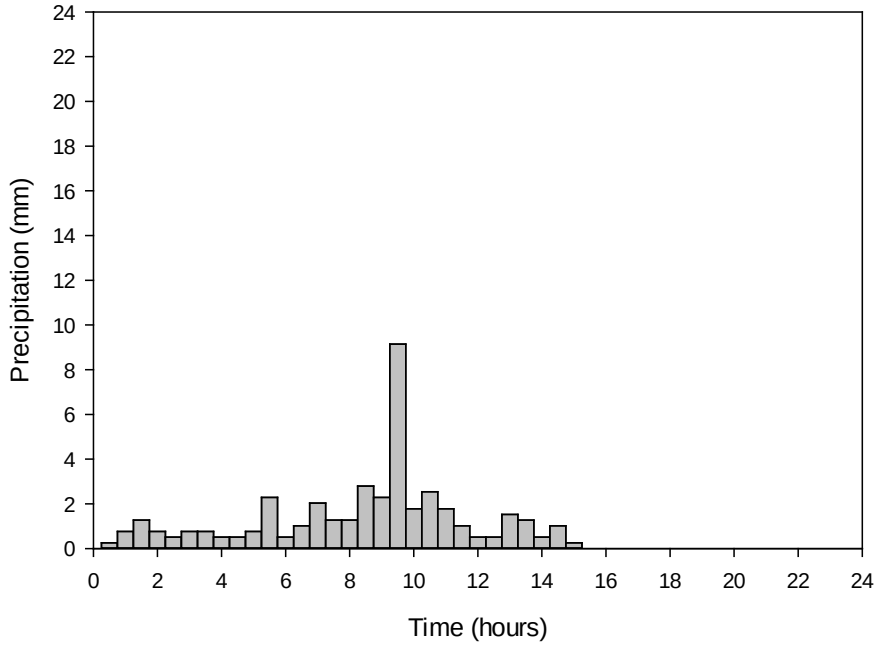

Figure B.18. Rainfall Event on April 14, 2011.

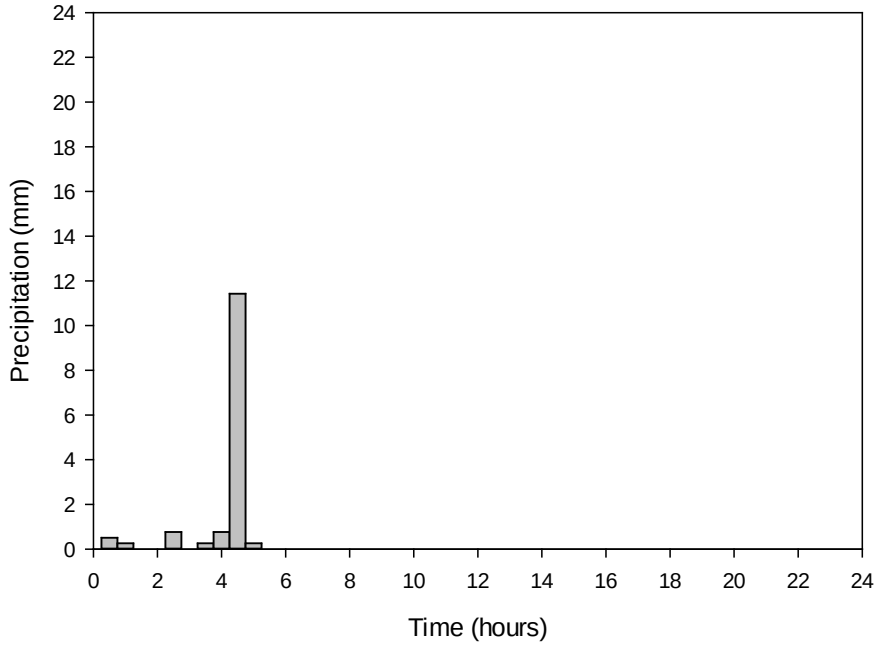

Figure B.19. Rainfall Event on April 23, 2011.

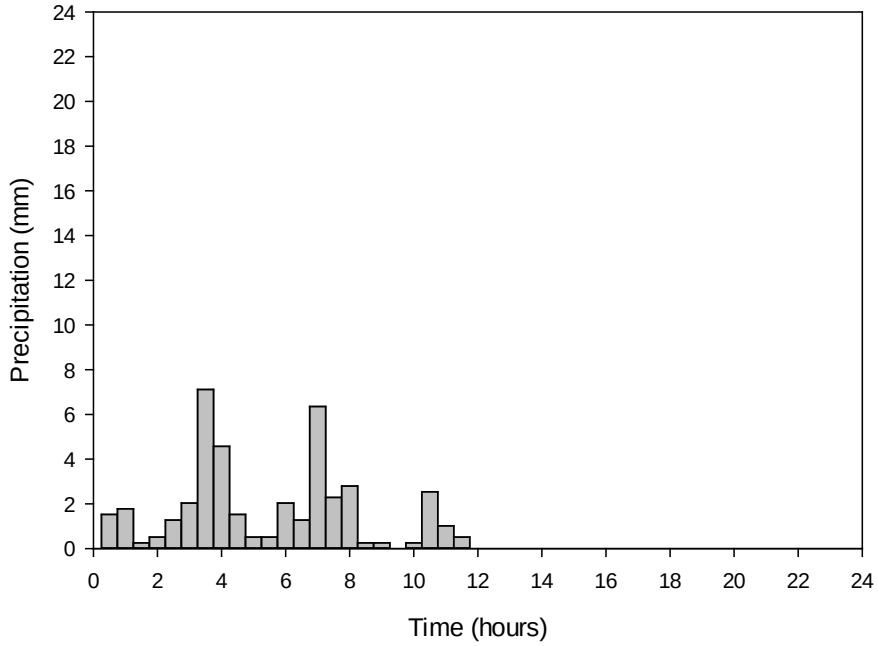

Figure B.20. Rainfall Event on April 26, 2011.

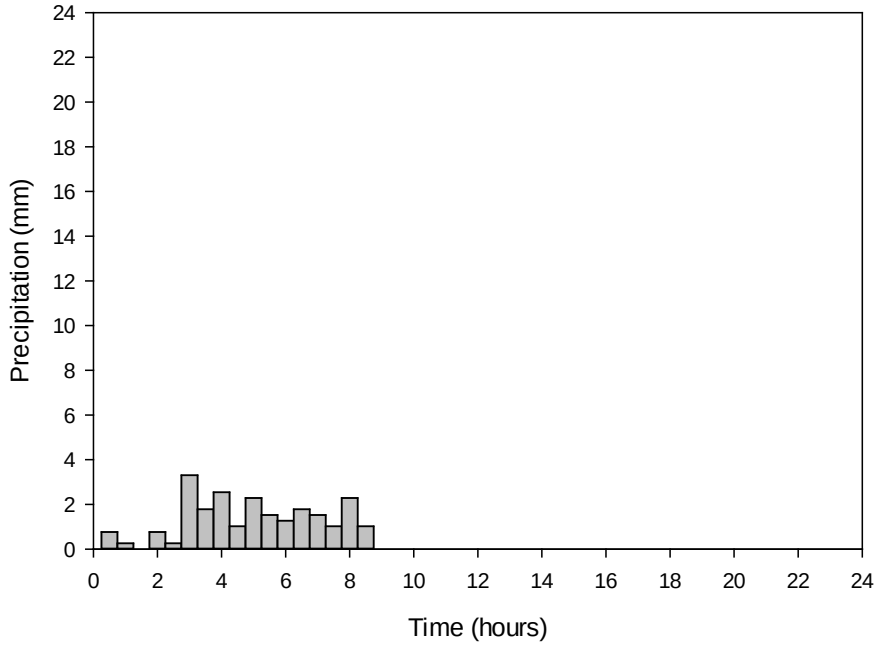

Figure B.21. Rainfall Event on May 2, 2011.

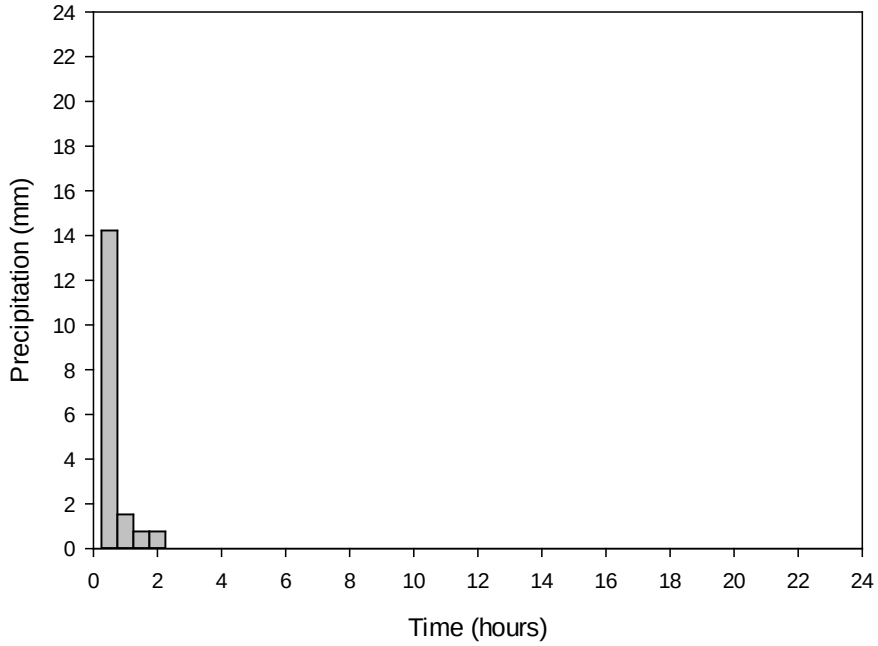

Figure B.22. Rainfall Event on May 12, 2011.

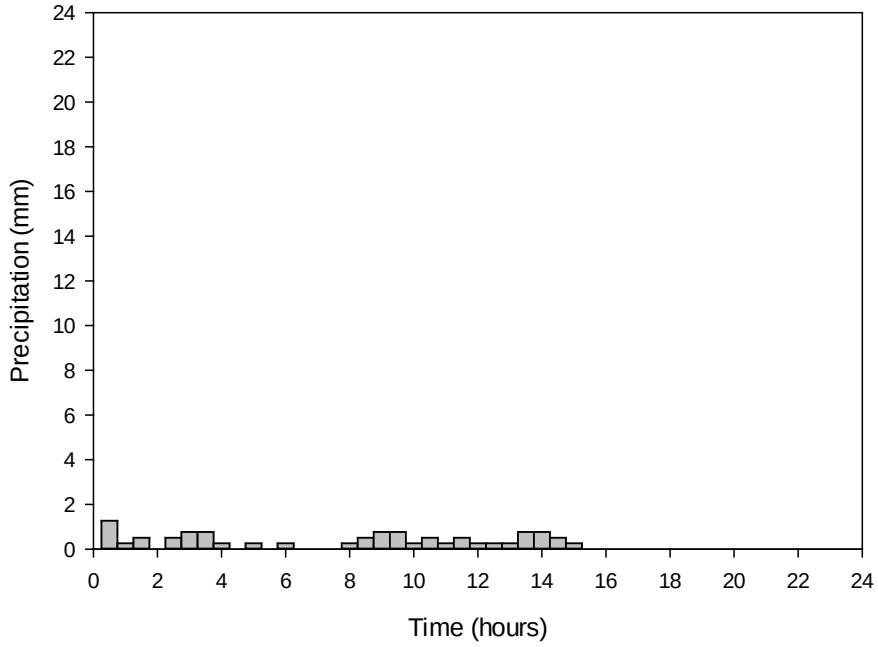

Figure B.23. Rainfall Event on May 16, 2011.

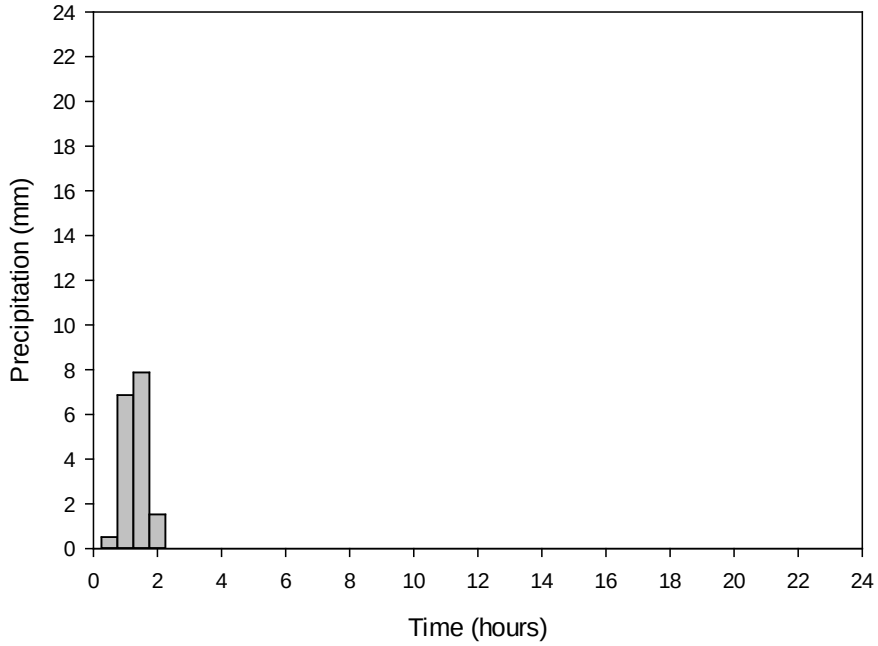

Figure B.24. Rainfall Event on May 22, 2011.

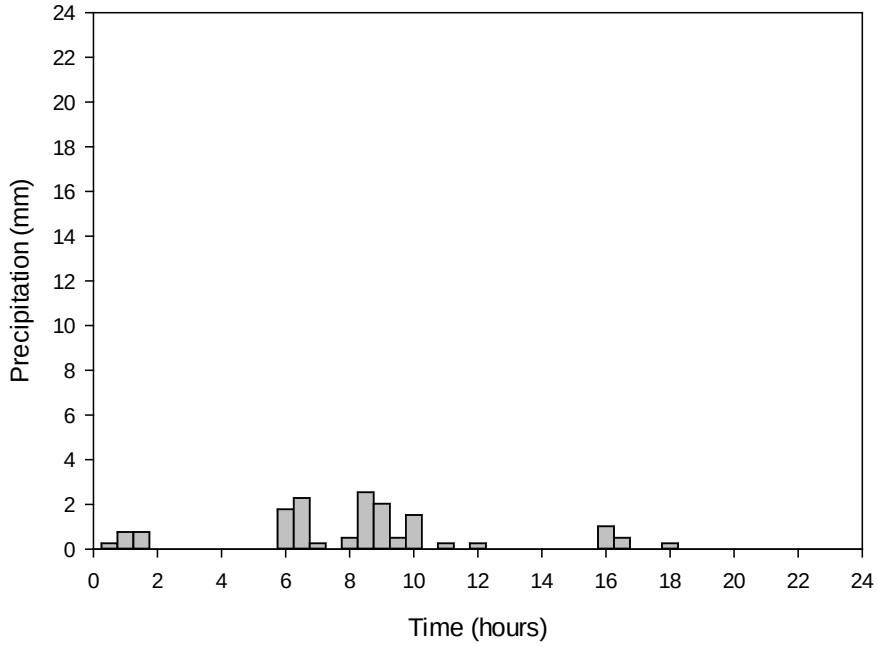

Figure B.25. Rainfall Event on May 25, 2011.

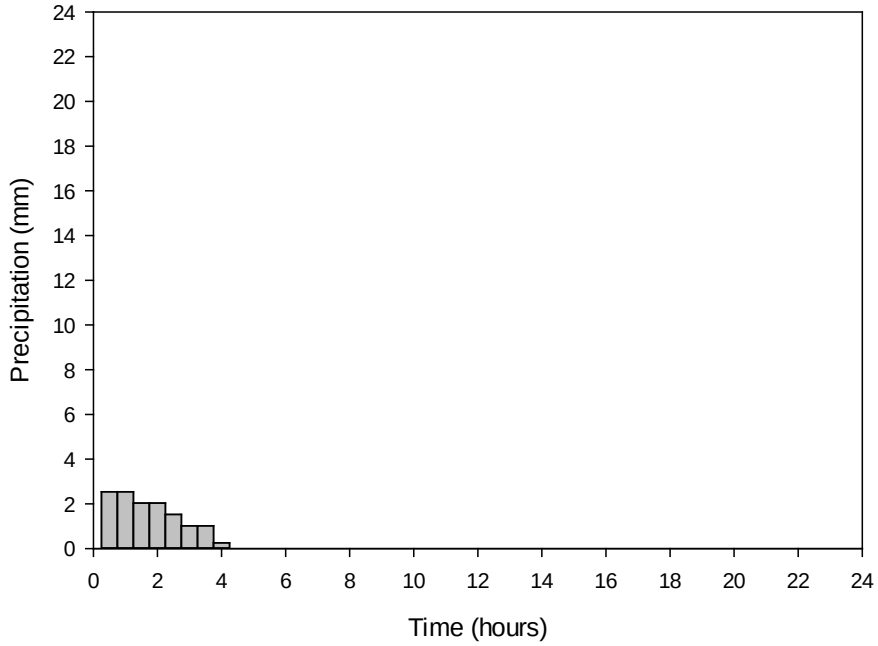

Figure B.26. Rainfall Event on June 17, 2011.

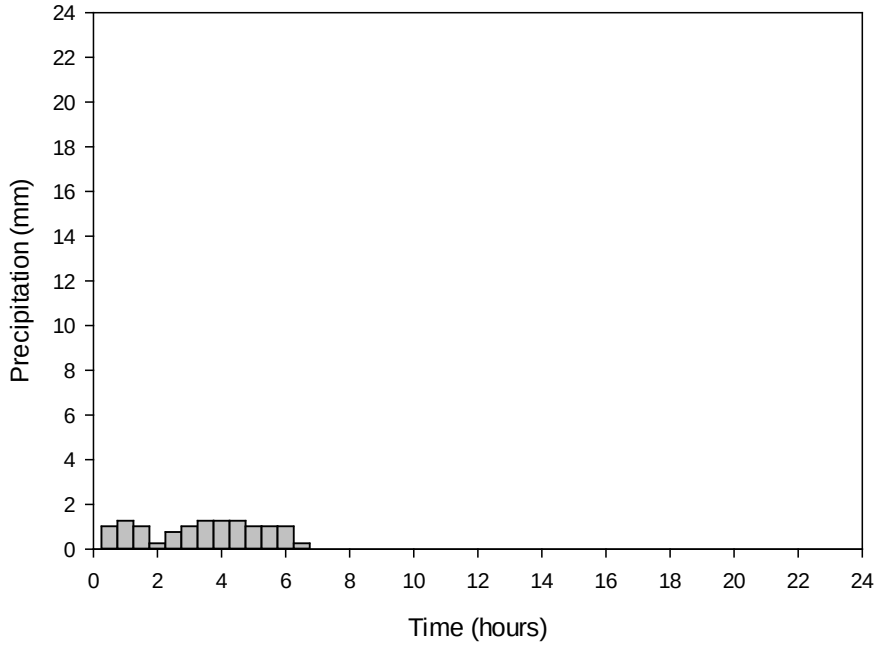

Figure B.27. Rainfall Event on June 18, 2011.

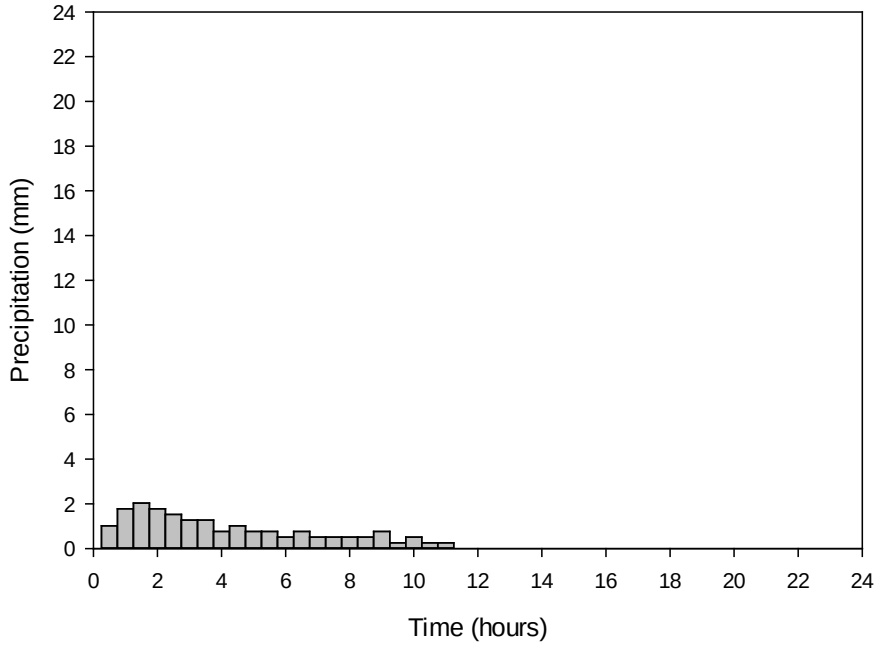

Figure B.28. Rainfall Event on July 11, 2011.

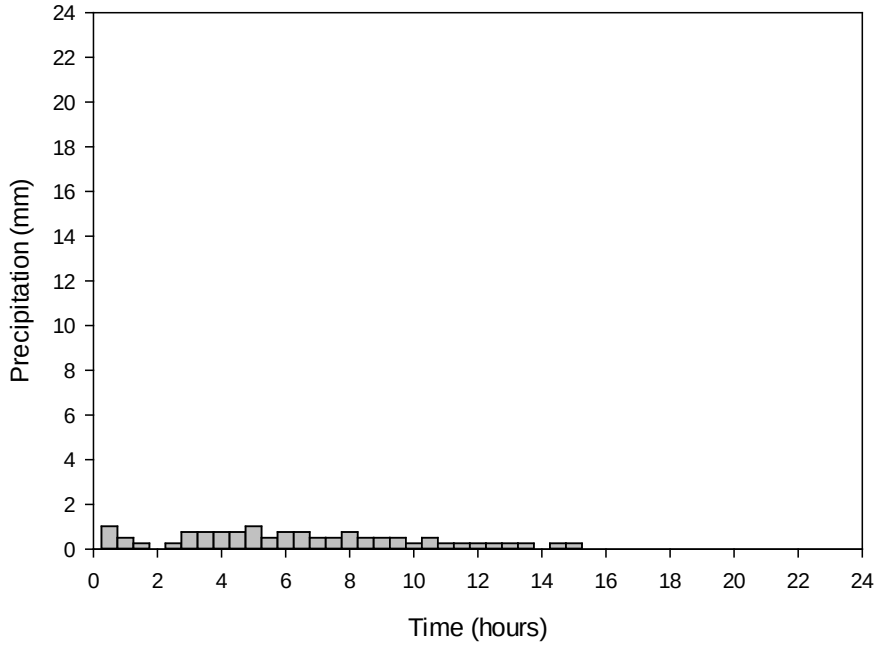

Figure B.29. Rainfall Event on July 14, 2011.

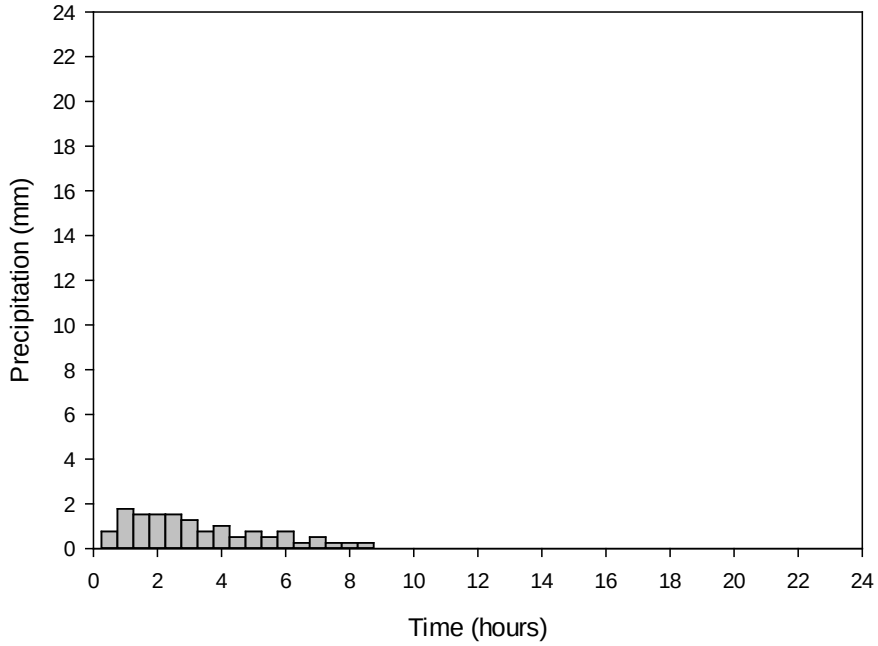

Figure B.30. Rainfall Event on September 3, 2011.

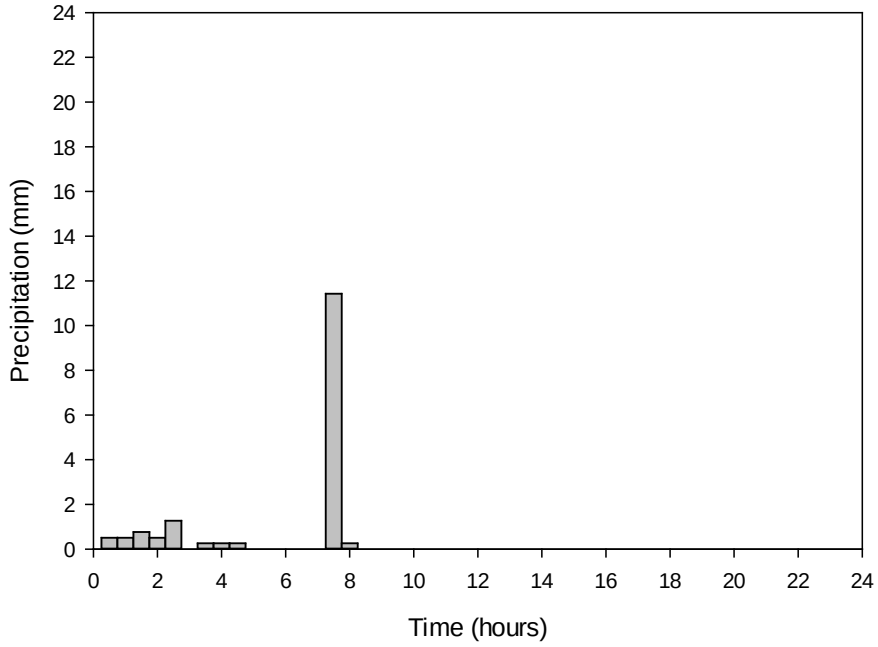

Figure B.31. Rainfall Event on September 20, 2011.

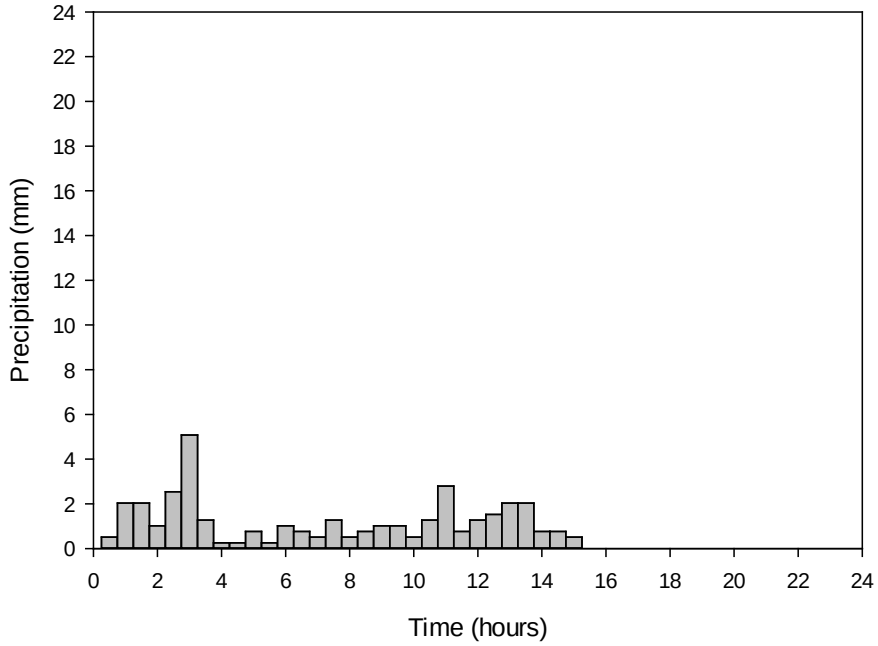

Figure B.32. Rainfall Event on October 18, 2011.

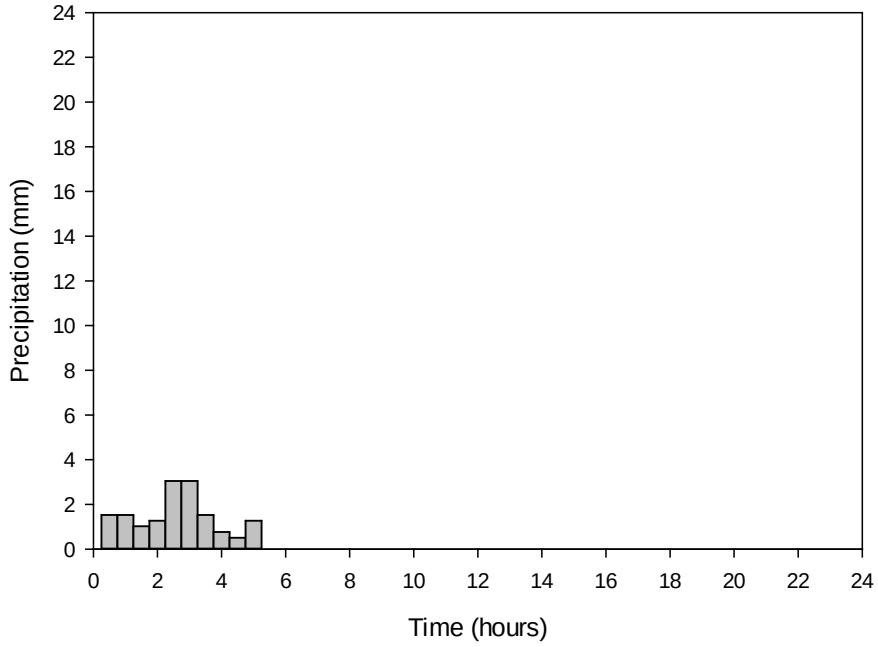

Figure B.33. Rainfall Event on November 2, 2011.

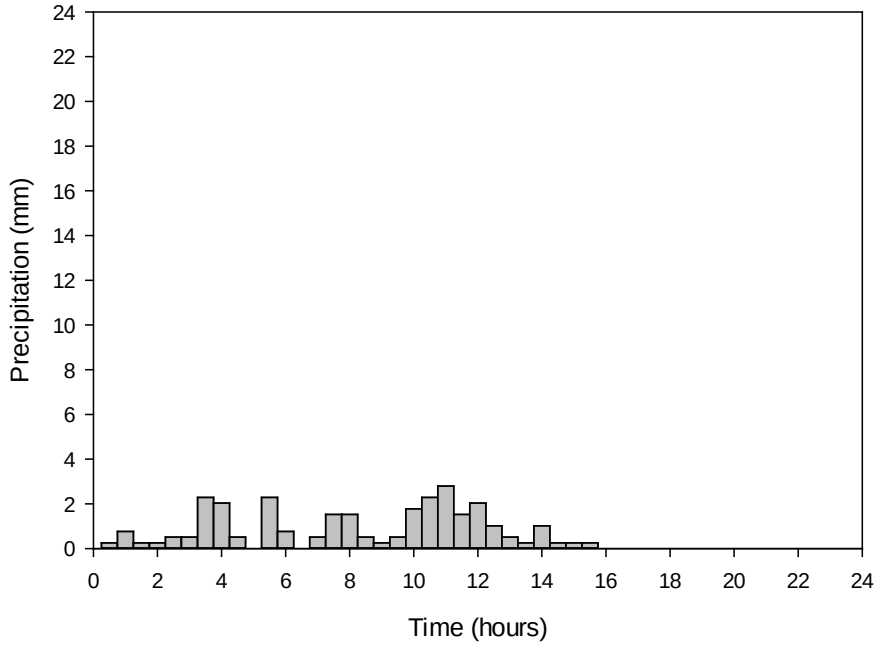

Figure B.34. Rainfall Event on November 15, 2011.

APPENDIX C: GC01 HYDROGRAPHS

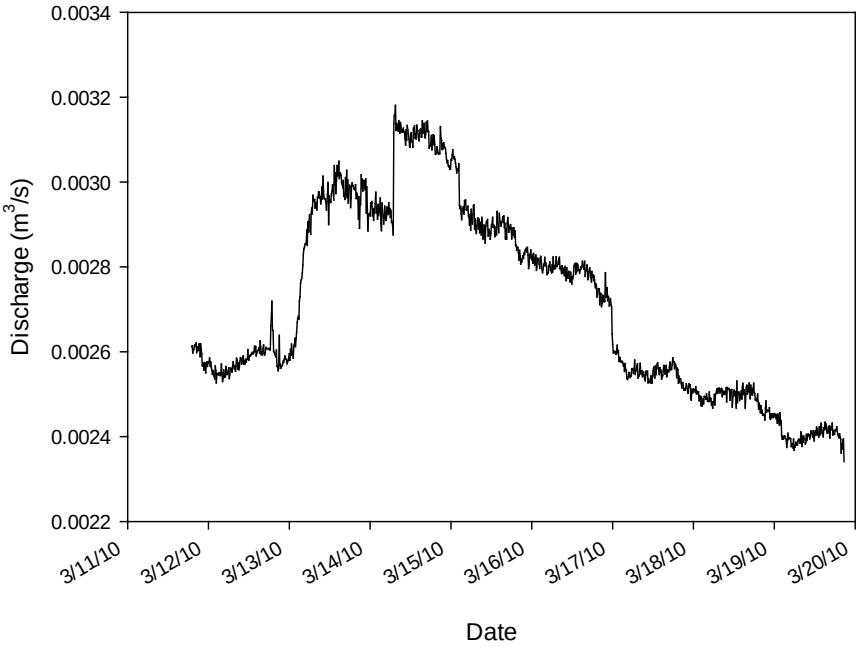

Figure C.1. Discharge from GC01 on March 12, 2010.

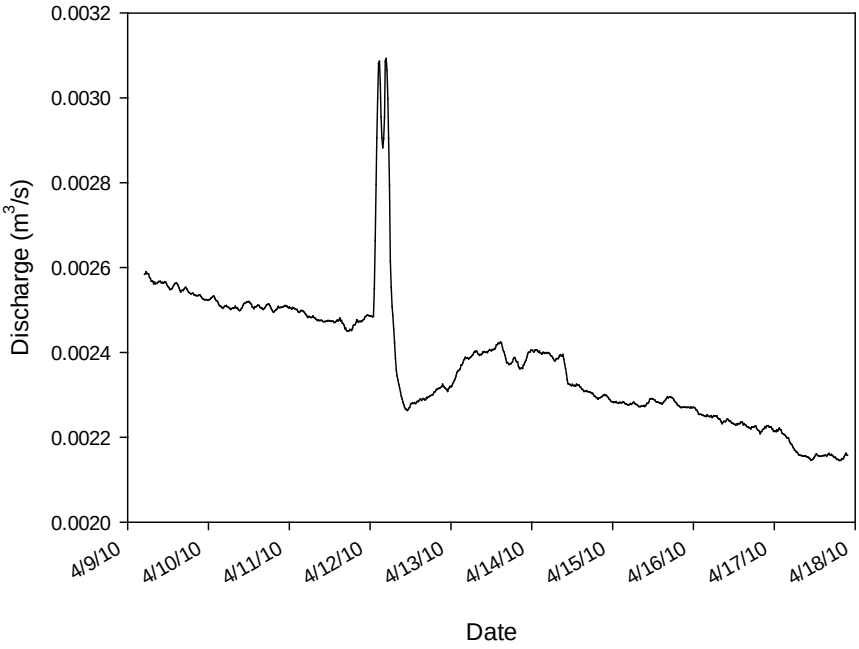

Figure C.2. Discharge from GC01 on April 8, 2010.

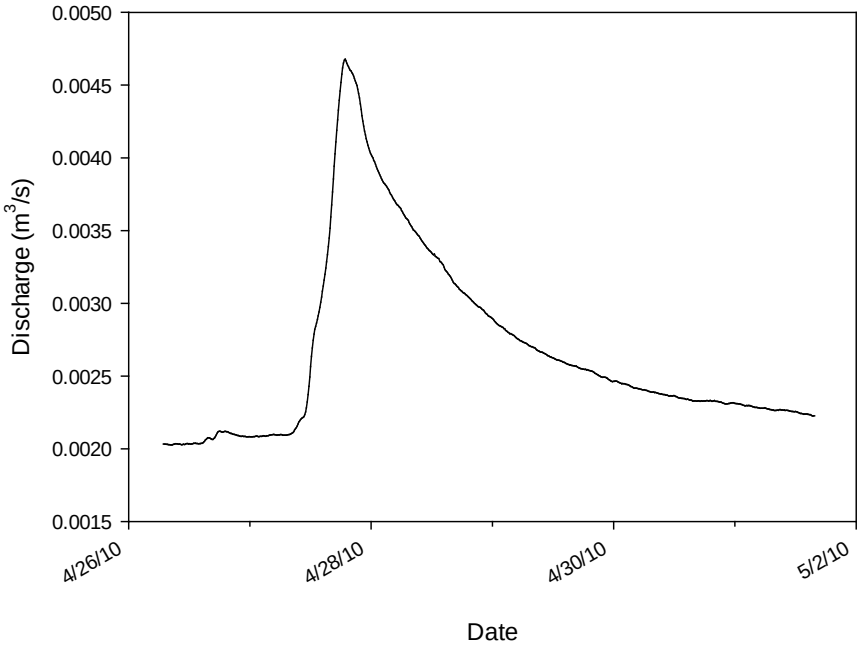

Figure C.3. Discharge from GC01 on April 27, 2010.

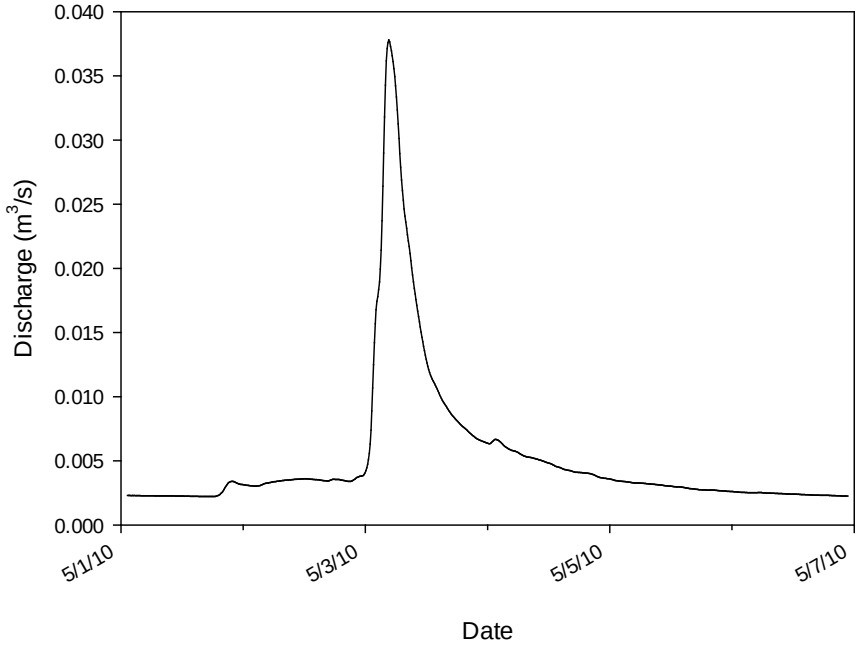

Figure C.4. Discharge from GC01 on May 1, 2010.

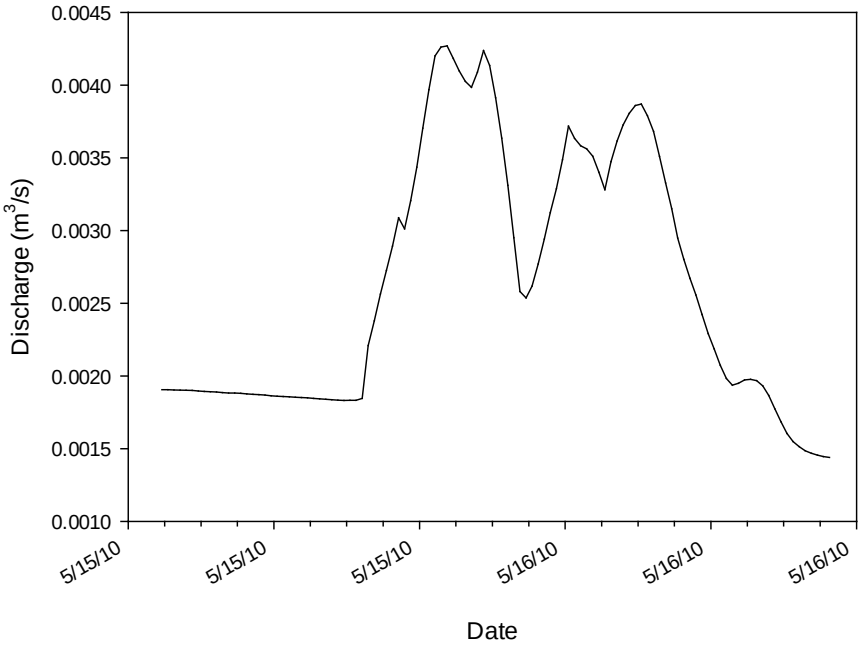

Figure C.5. Discharge from GC01 on May 14, 2010.

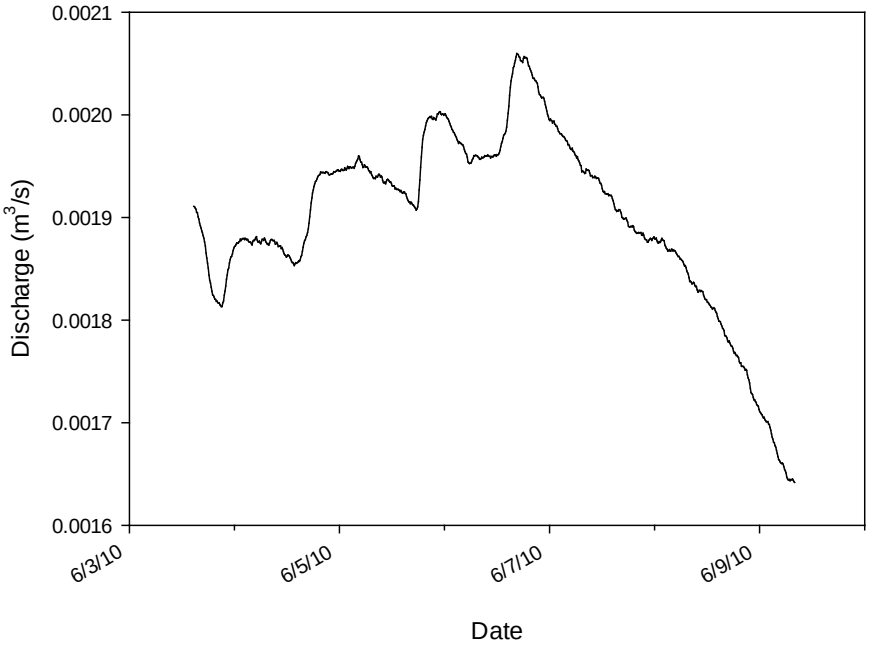

Figure C.6. Discharge from GC01 on June 4, 2010.

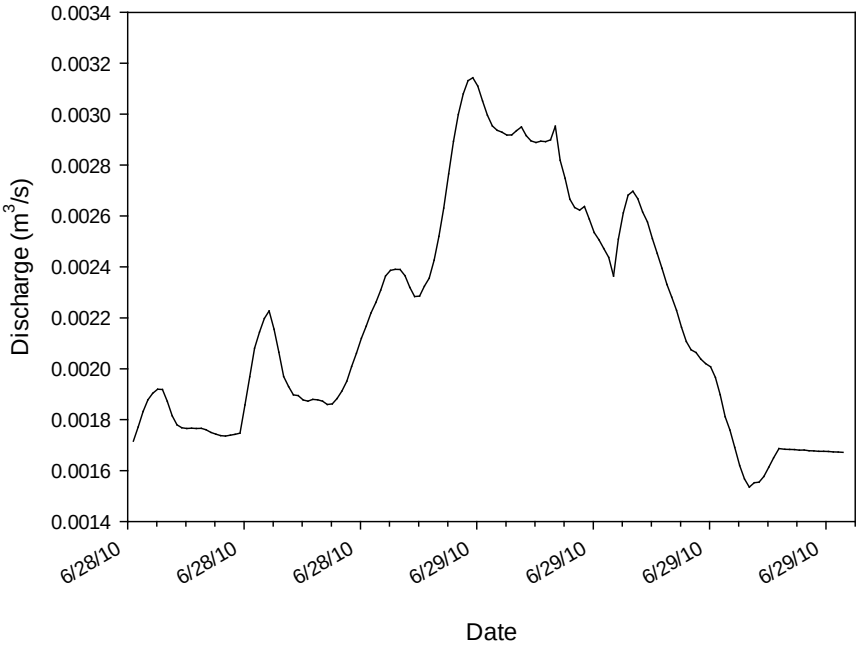

Figure C.7. Discharge from GC01 on June 28, 2010.

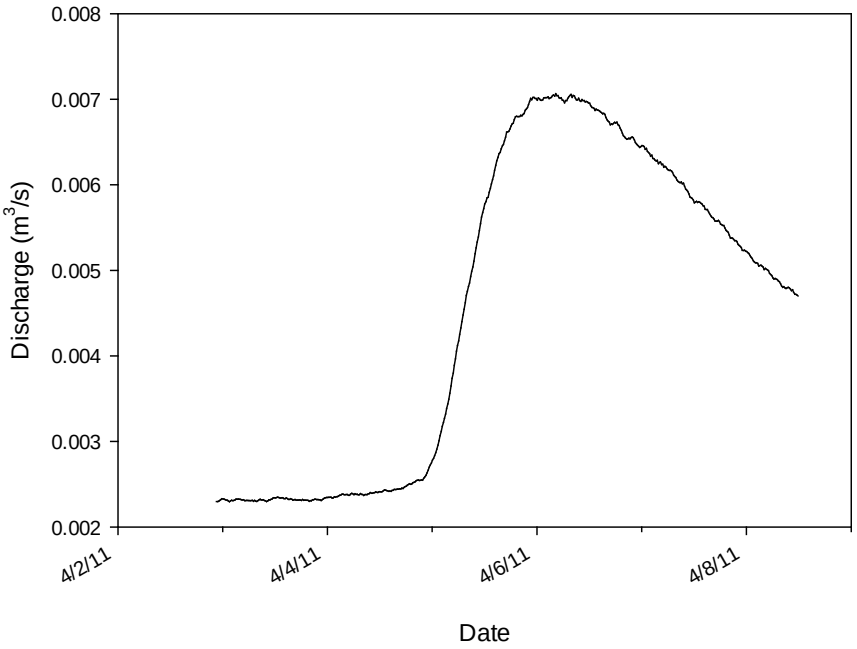

Figure C.8. Discharge from GC01 on April 2, 2011.

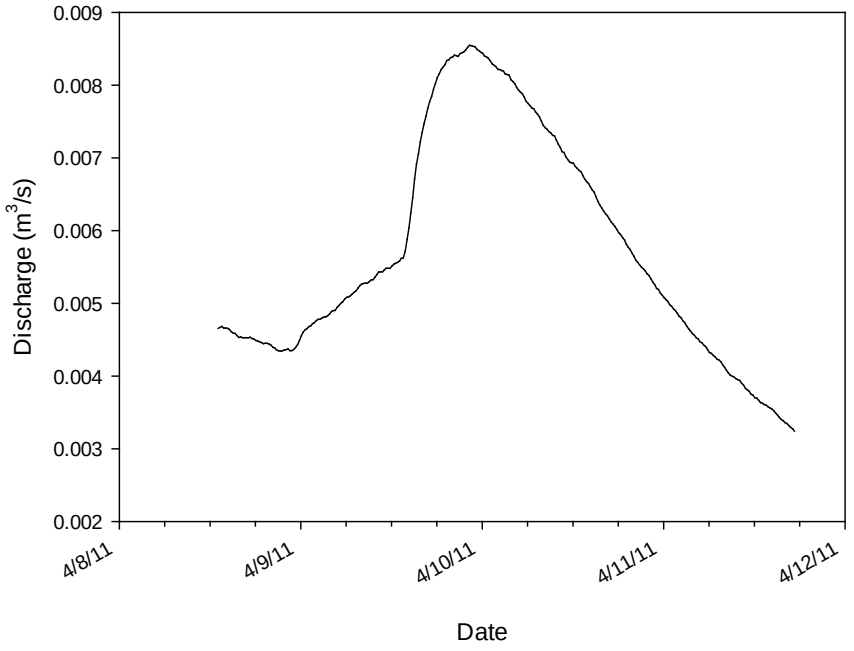

Figure C.9. Discharge from GC01 on April 8, 2011.

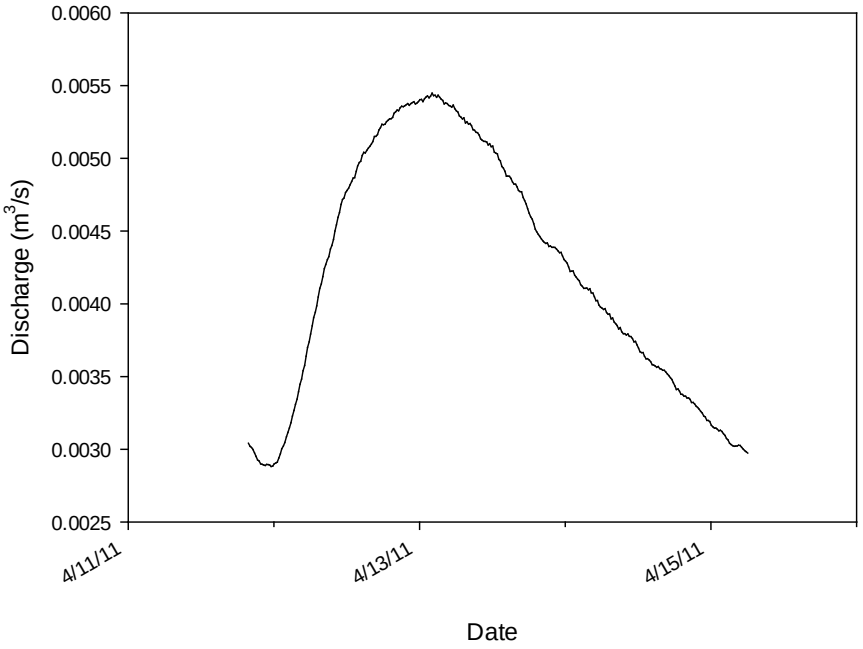

Figure C.10. Discharge from GC01 on April 10, 2011.

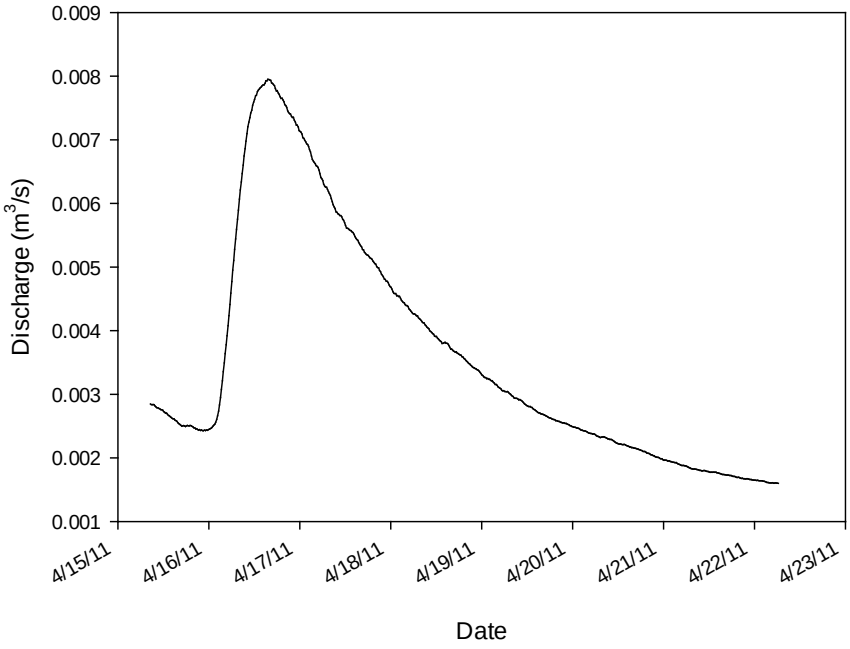

Figure C.11. Discharge from GC01 on April 14, 2010.

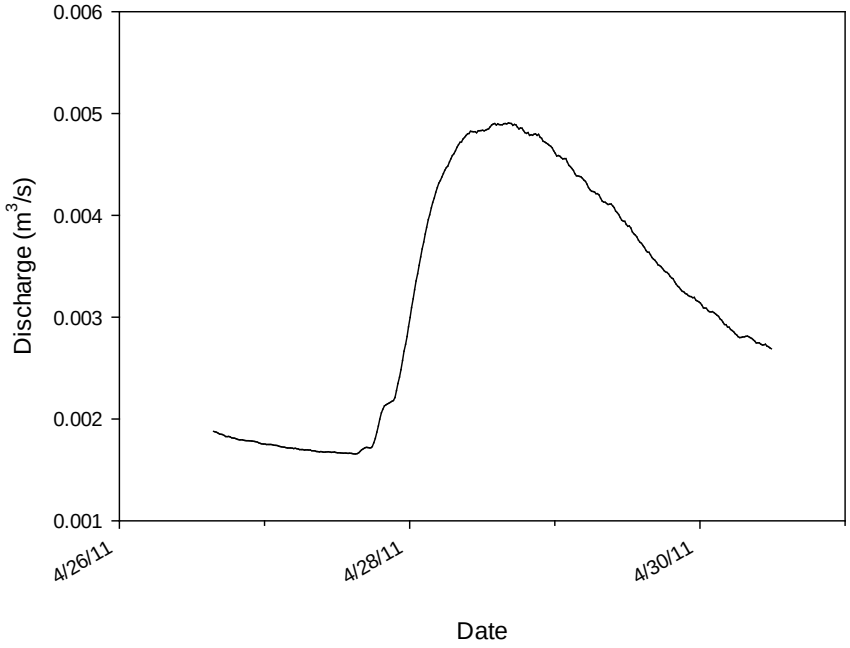

Figure C.12. Discharge from GC01 on April 26, 2011.

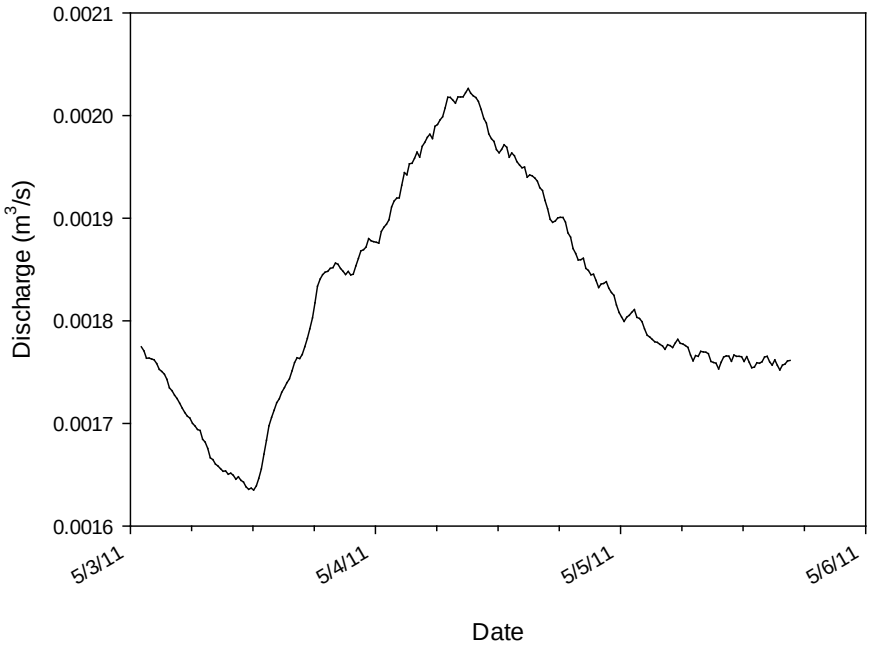

Figure C.13. Discharge from GC01 on May 2, 2011.

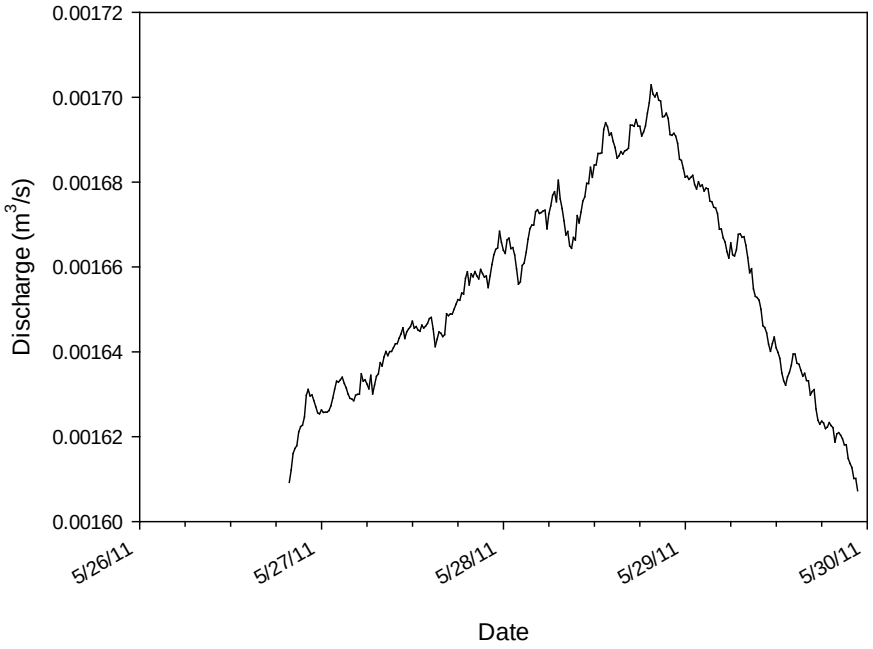

Figure C.14. Discharge from GC01 on May 25, 2011.

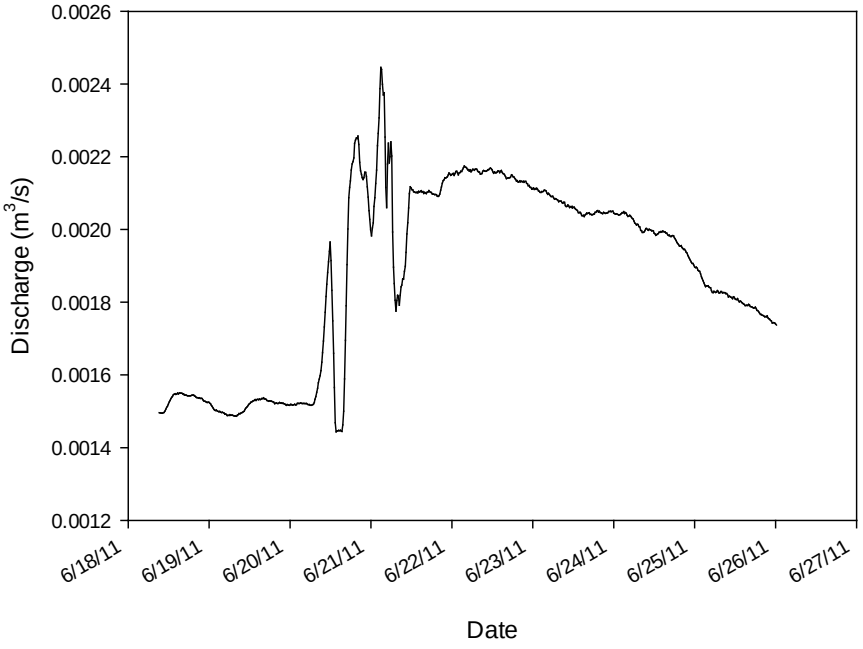

Figure C.15. Discharge from GC01 on June 18, 2011.

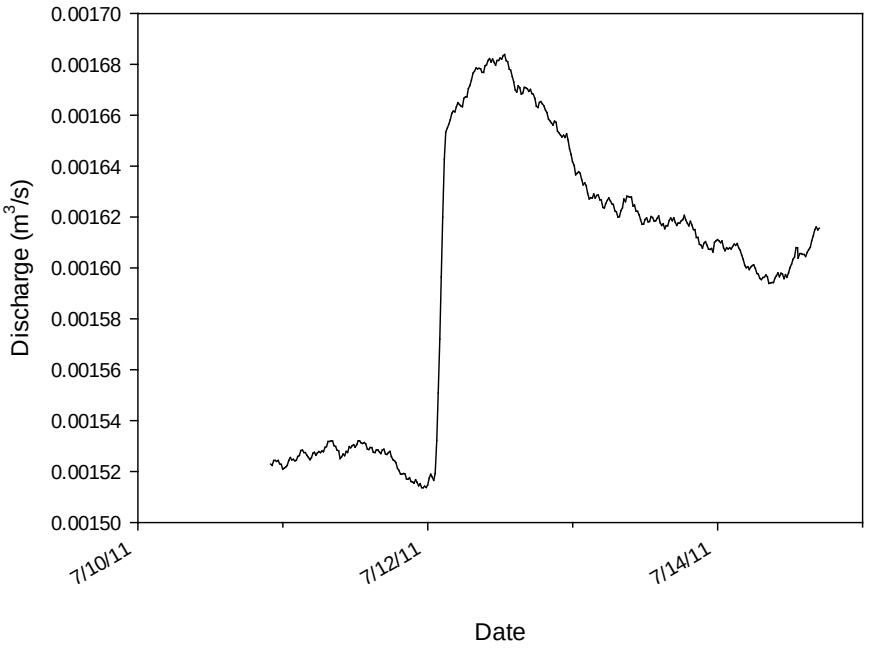

Figure C.16. Discharge from GC01 on July 11, 2011.

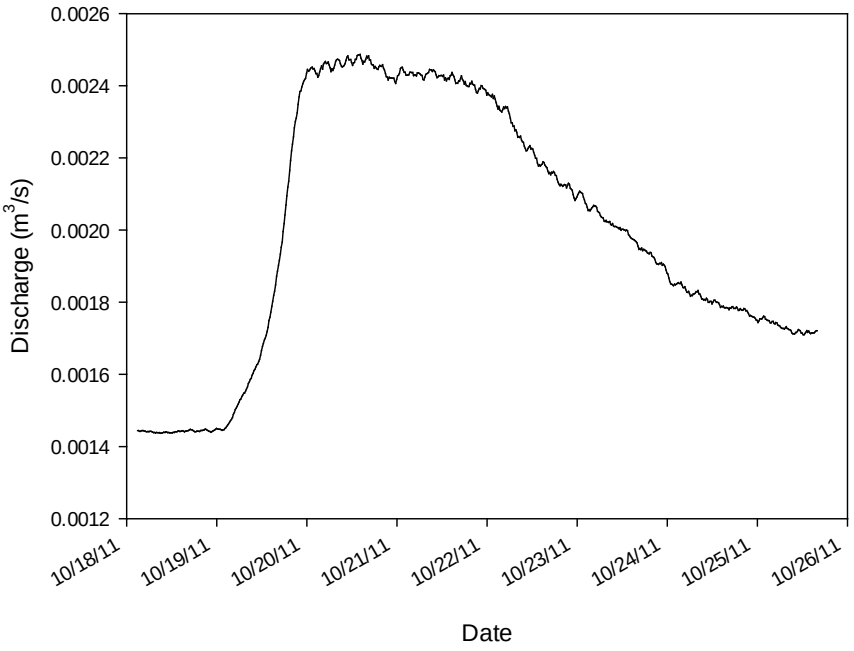

Figure C.17. Discharge from GC01 on October 18, 2011.

APPENDIX D: GC02 HYDROGRAPHS

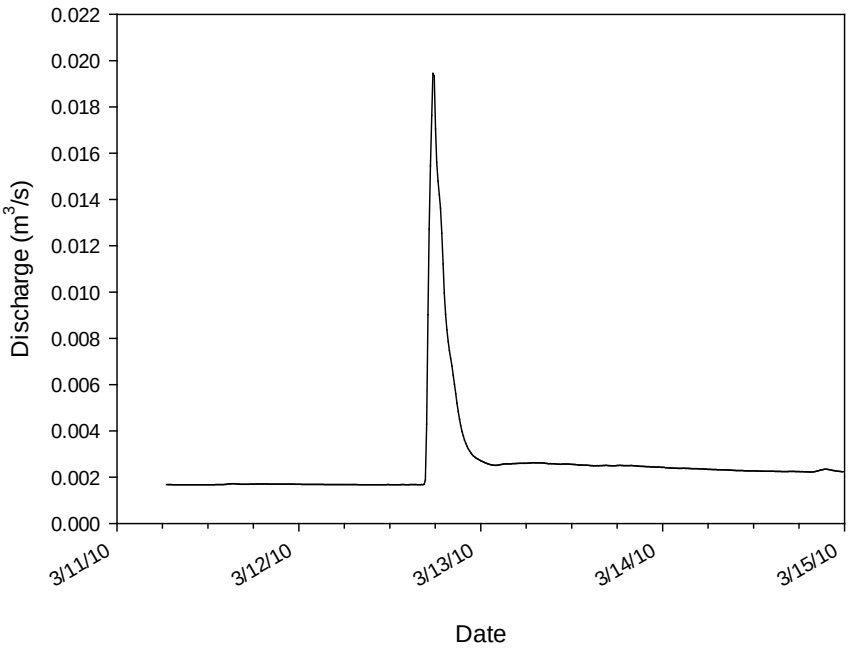

Figure D.1. Discharge from GC02 on March 12, 2010.

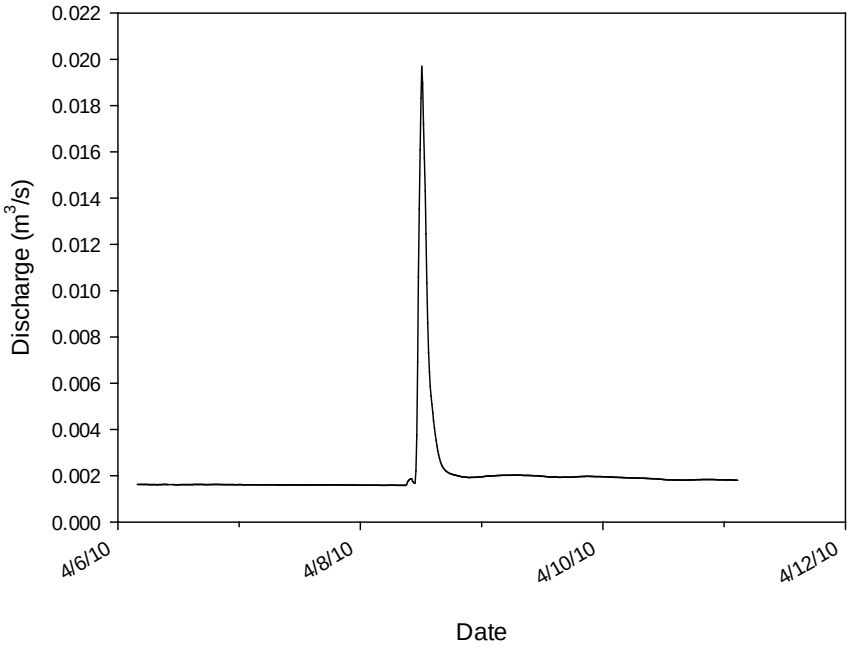

Figure D.2. Discharge from GC02 on April 8, 2010.

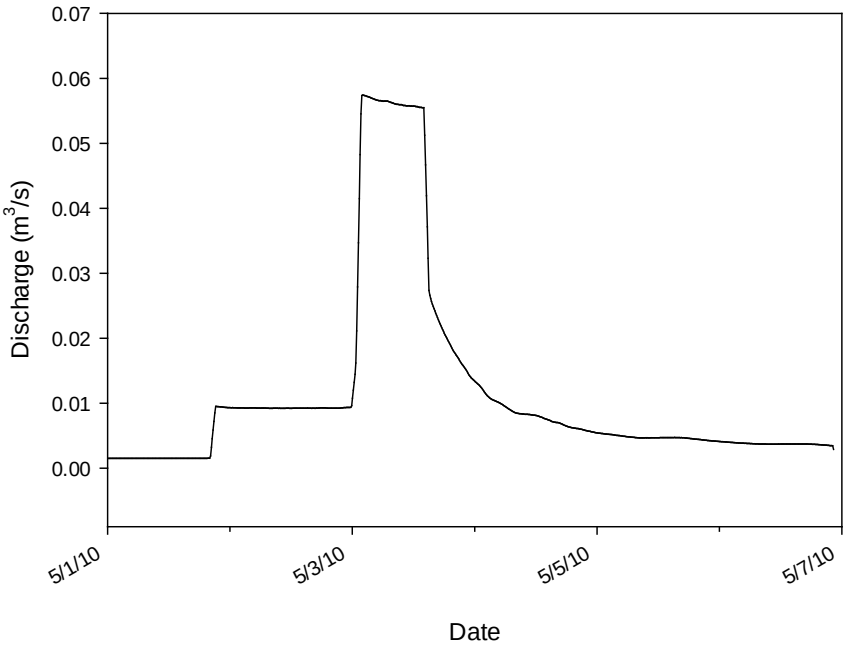

Figure D.3. Discharge from GC02 on May 1, 2010.

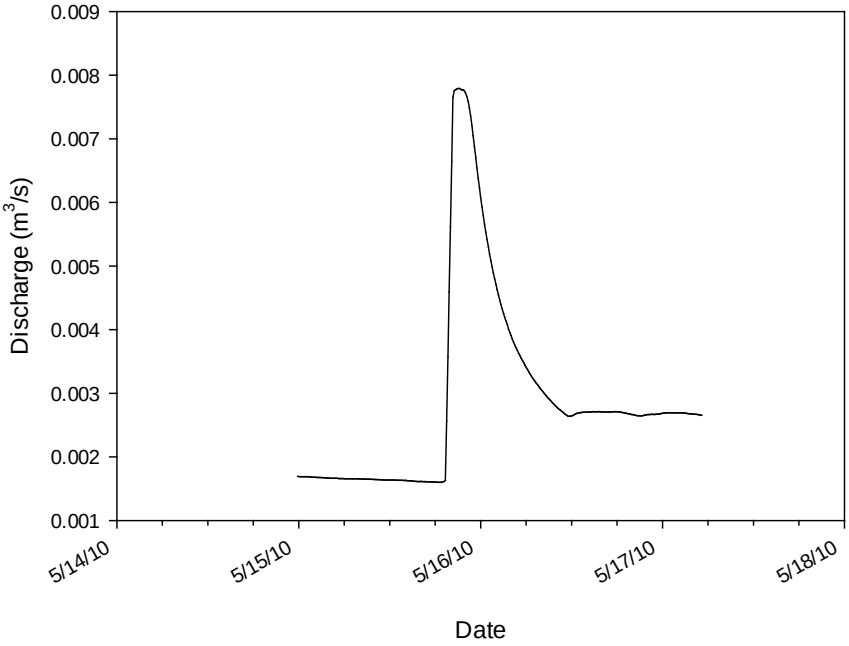

Figure D.4. Discharge from GC02 on May 14, 2010.

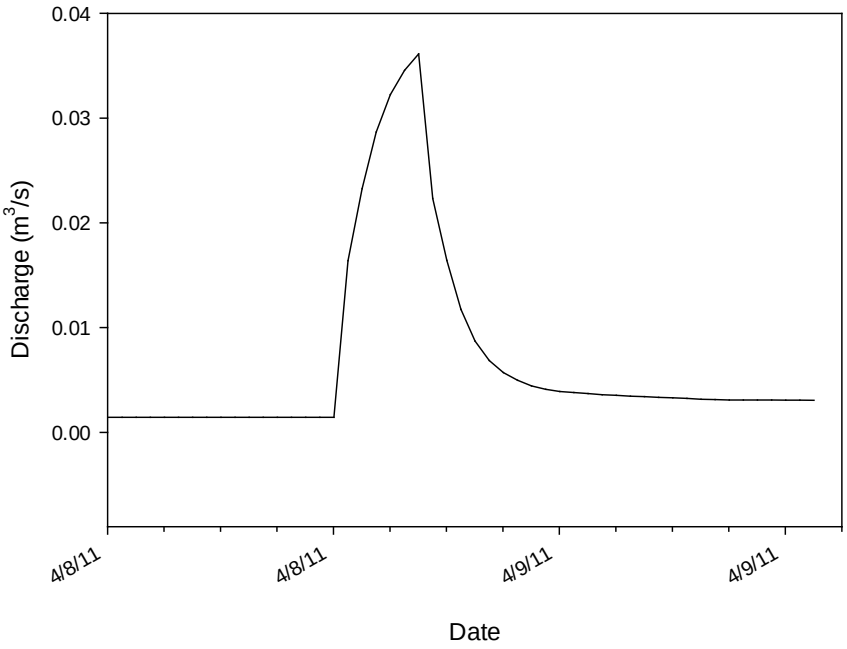

Figure D.5. Discharge from GC02 on April 8, 2011.

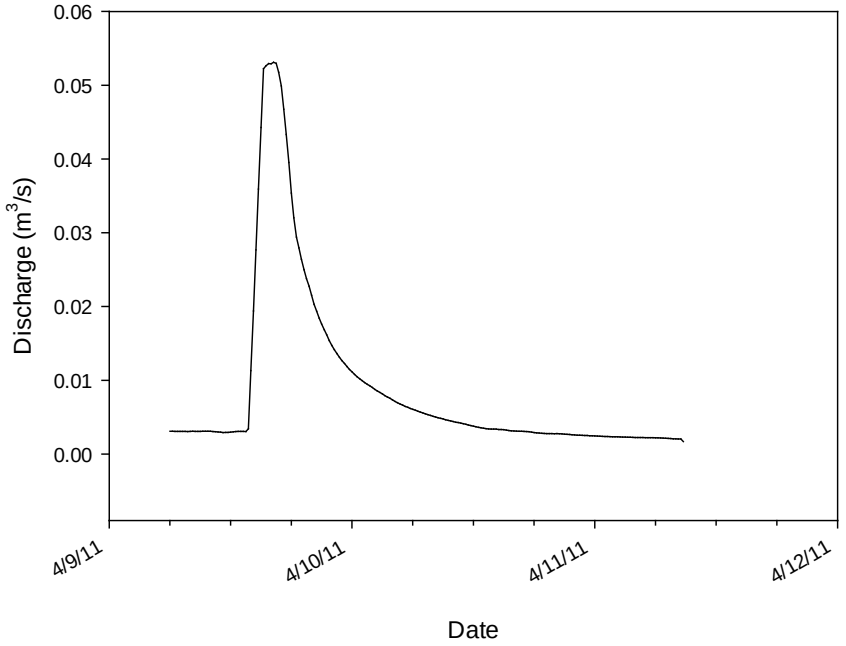

Figure D.6. Discharge from GC02 on April 8, 2011.

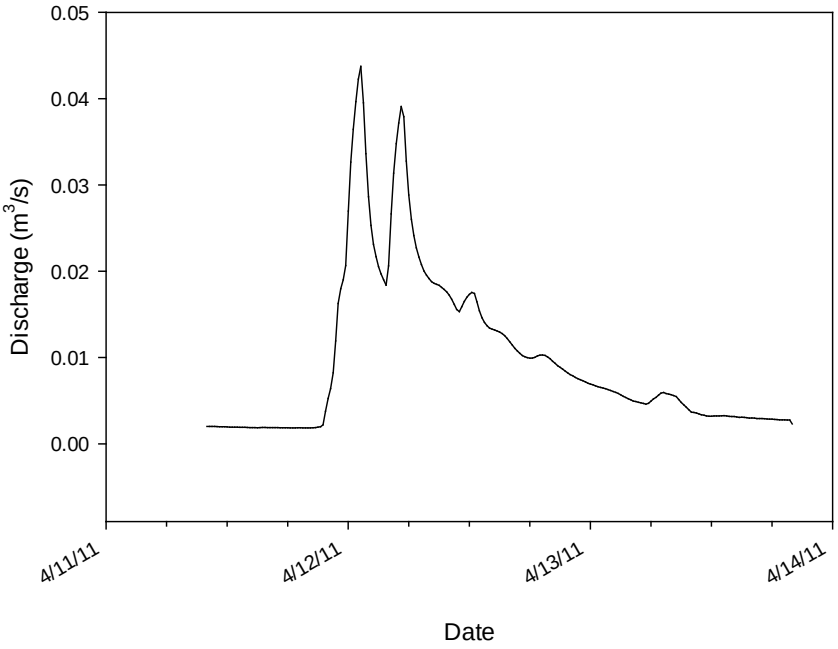

Figure D.7. Discharge from GC02 on April 10, 2011.

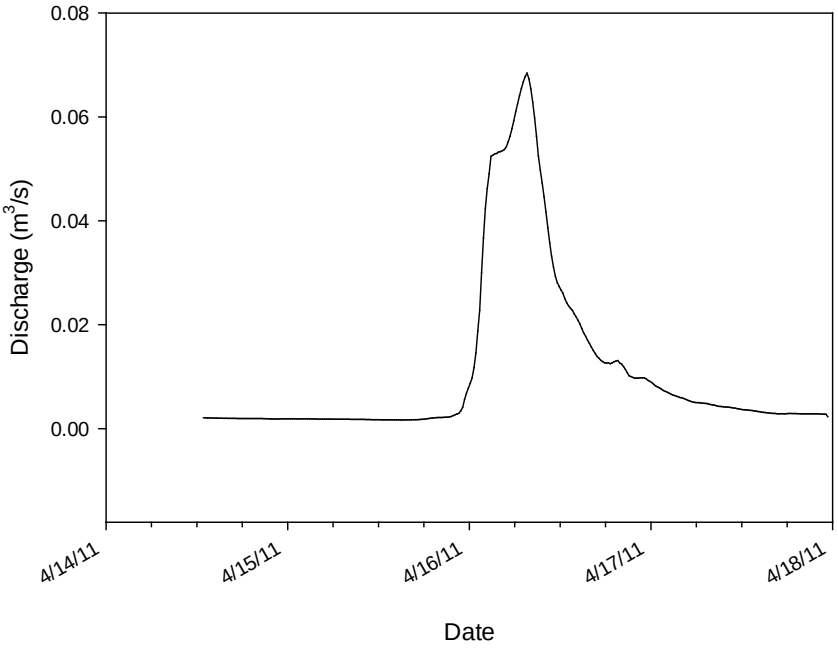

Figure D.8. Discharge from GC02 on April 14, 2011.

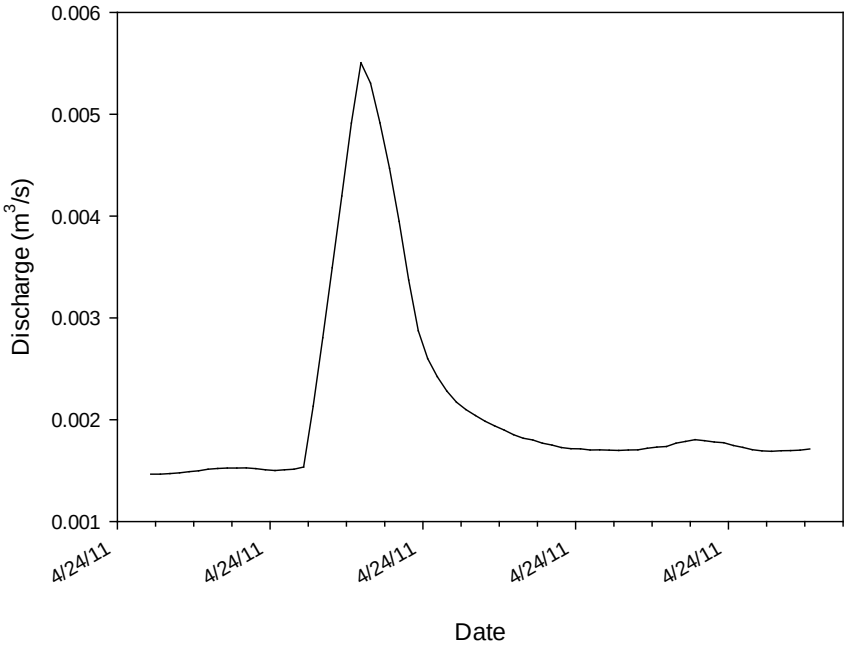

Figure D.9. Discharge from GC02 on April 23, 2011.

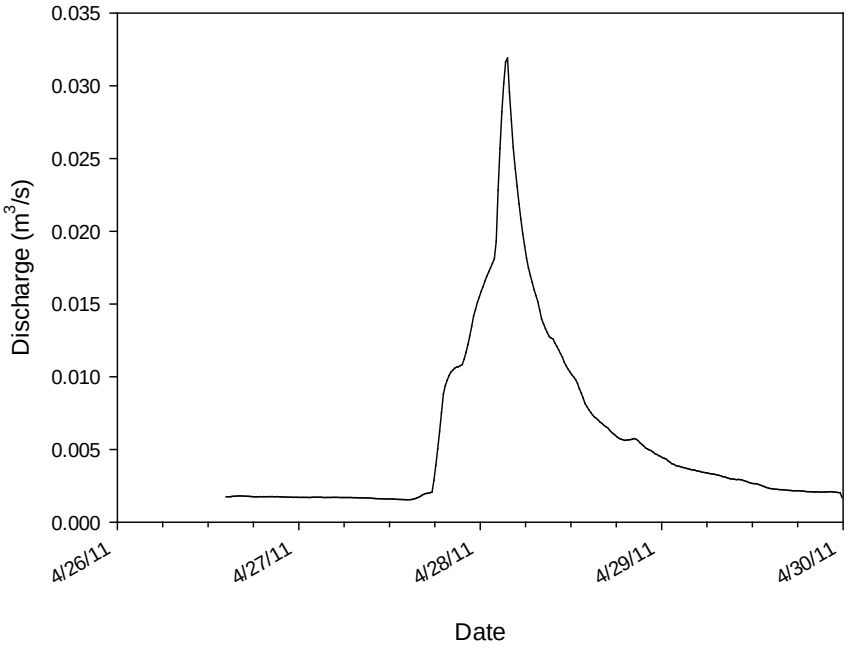

Figure D.10. Discharge from GC02 on April 26, 2011.

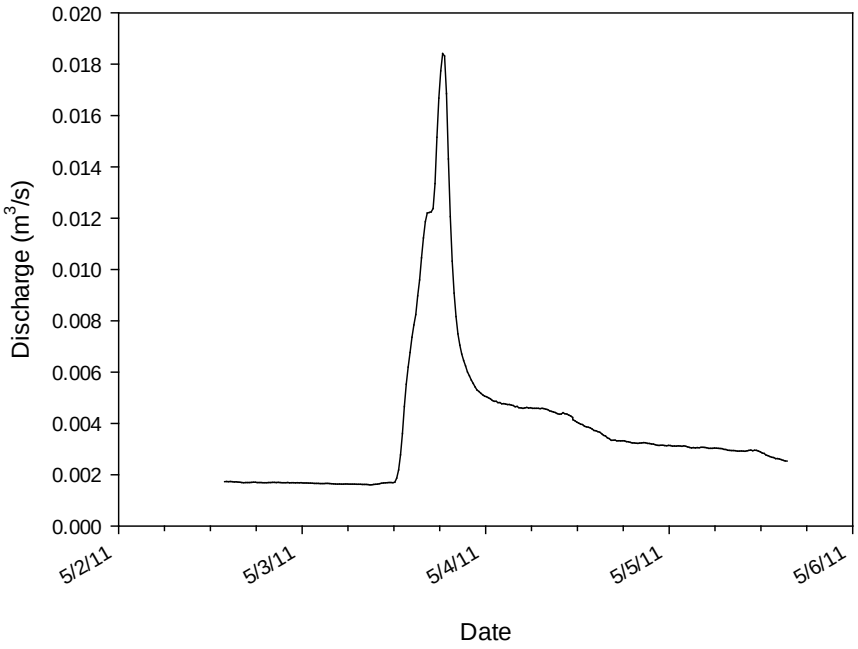

Figure D.11. Discharge from GC02 on May 2, 2011.

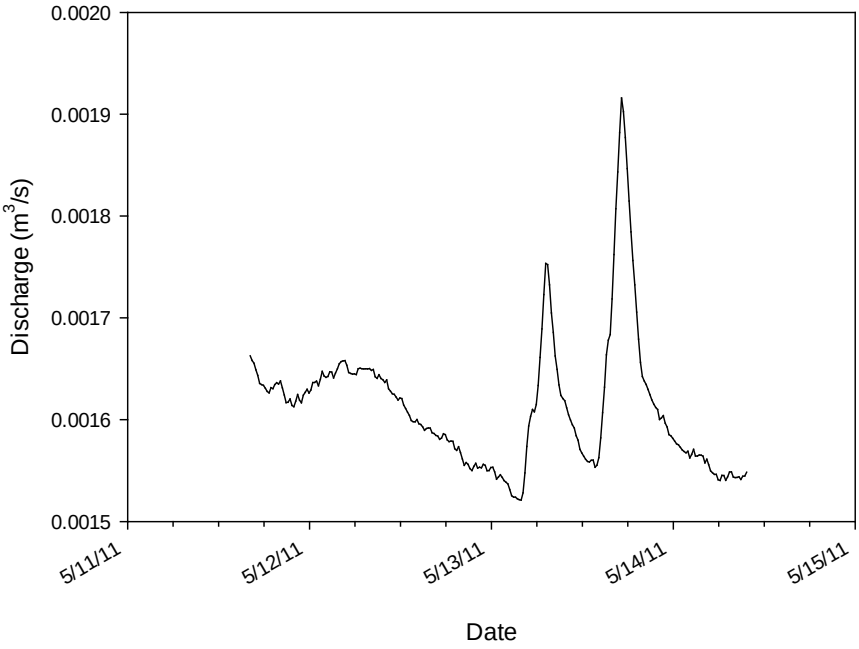

Figure D.12. Discharge from GC02 on May 12, 2011.

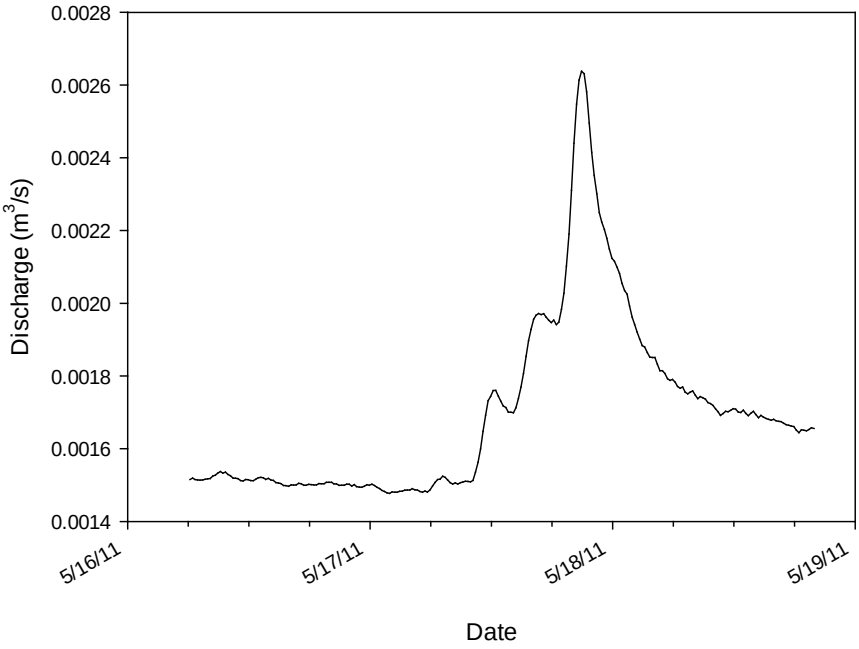

Figure D.13. Discharge from GC02 on May 16, 2011.

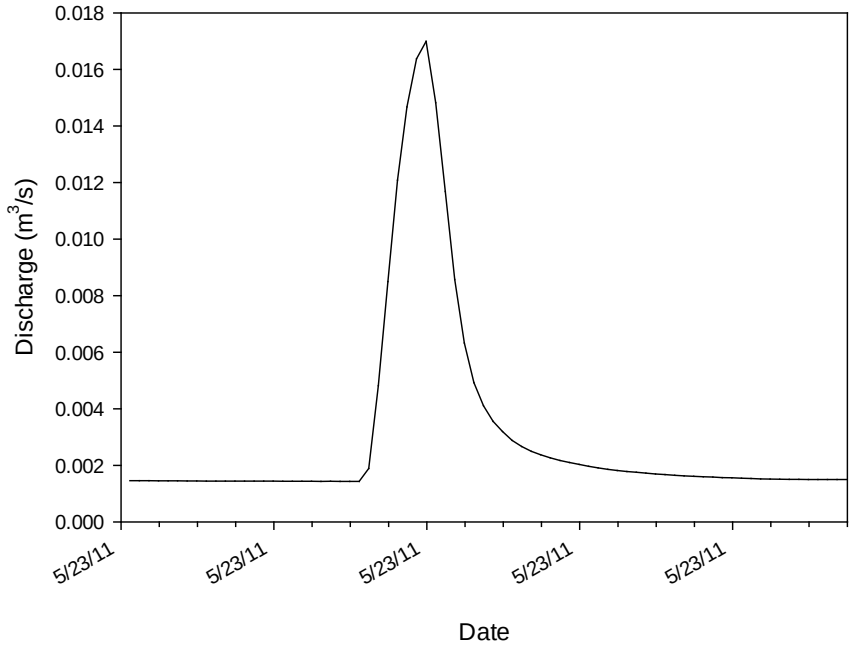

Figure D.14. Discharge from GC02 on May 22, 2011.

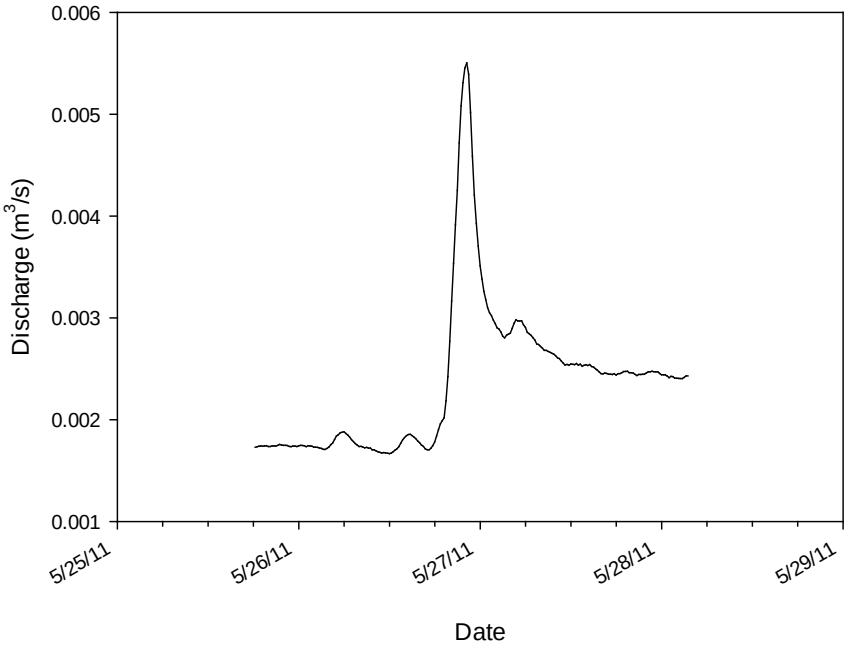

Figure D.15. Discharge from GC02 on May 25, 2011.

APPENDIX E: GC03 HYDROGRAPHS

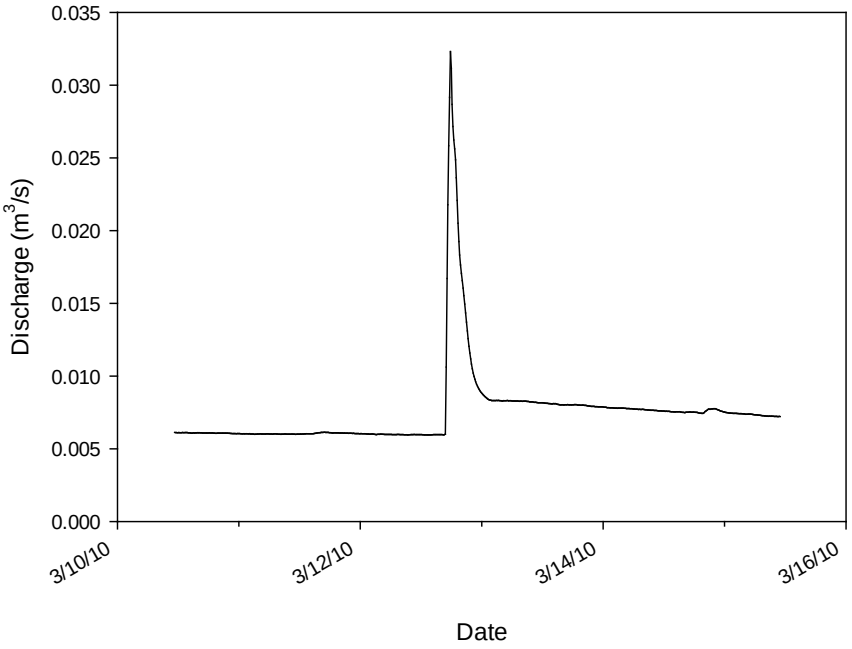

Figure E.1. Discharge from GC03 on March 12, 2010.

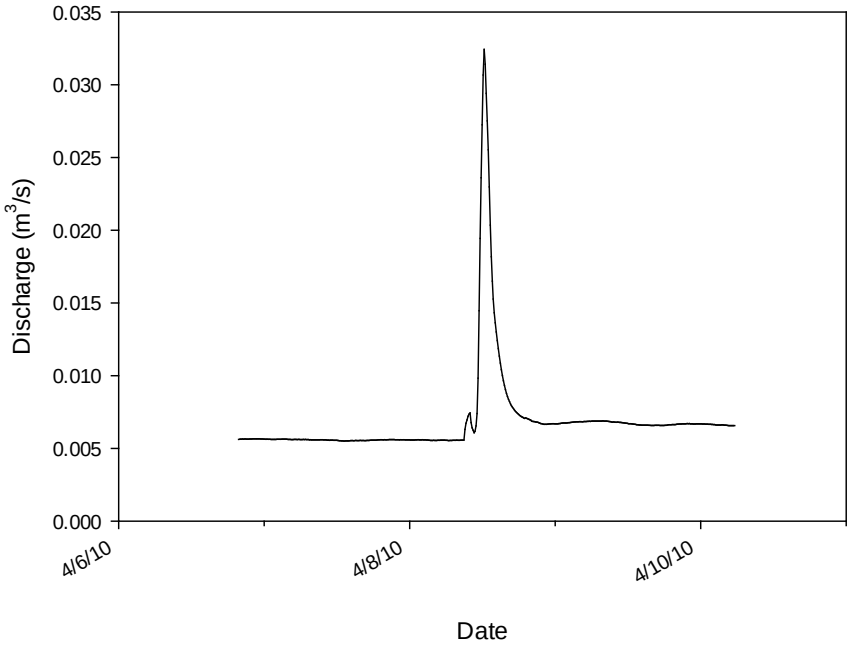

Figure E.2. Discharge from GC03 on April 8, 2010.

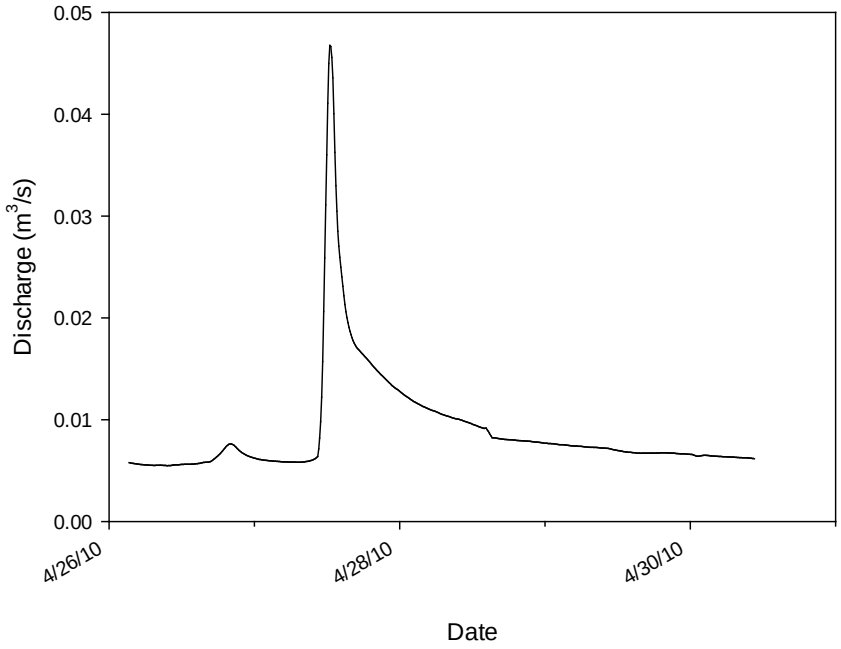

Figure E.3. Discharge from GC03 on April 27, 2010.

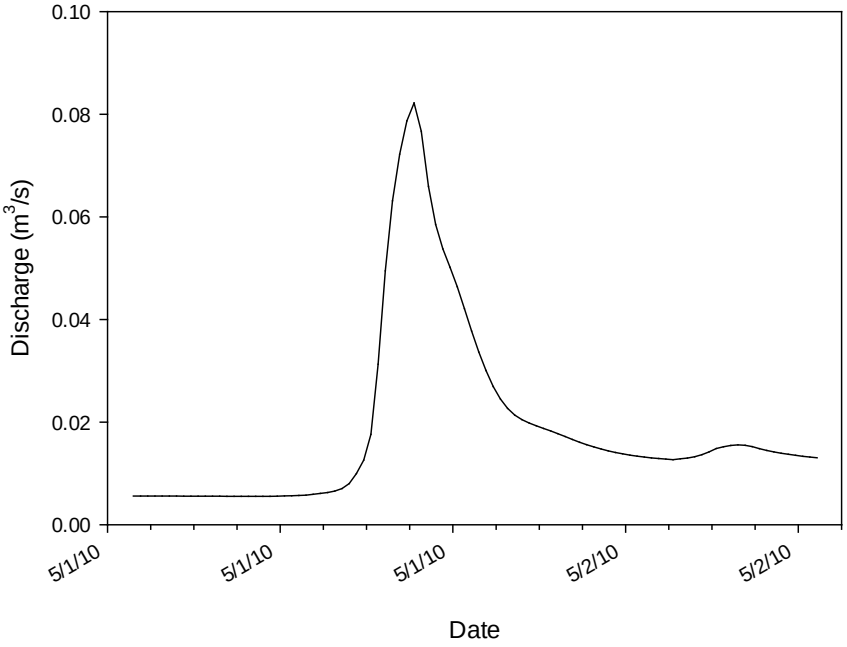

Figure E.4. Discharge from GC03 on May 1, 2010.

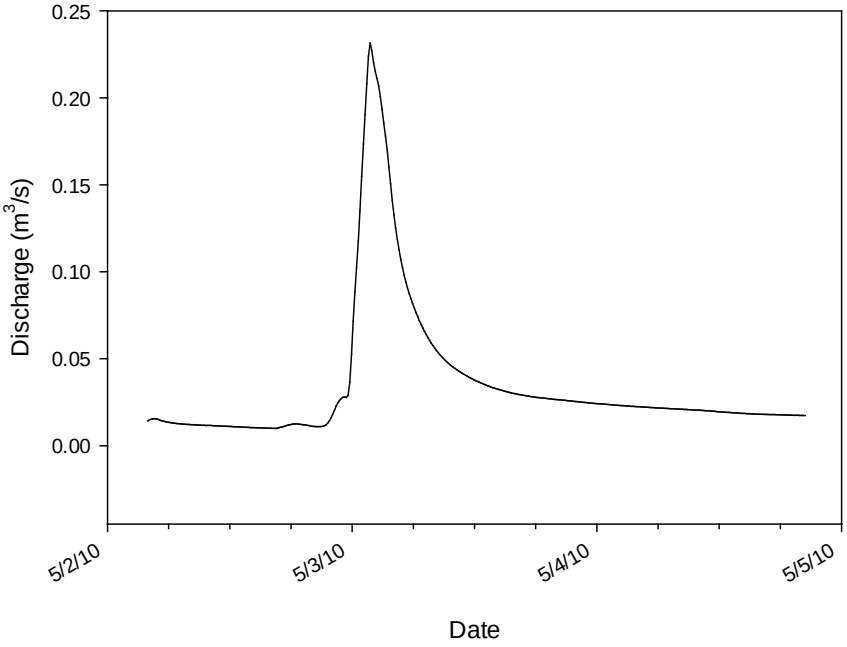

Figure E.5. Discharge from GC03 on May 2, 2010.

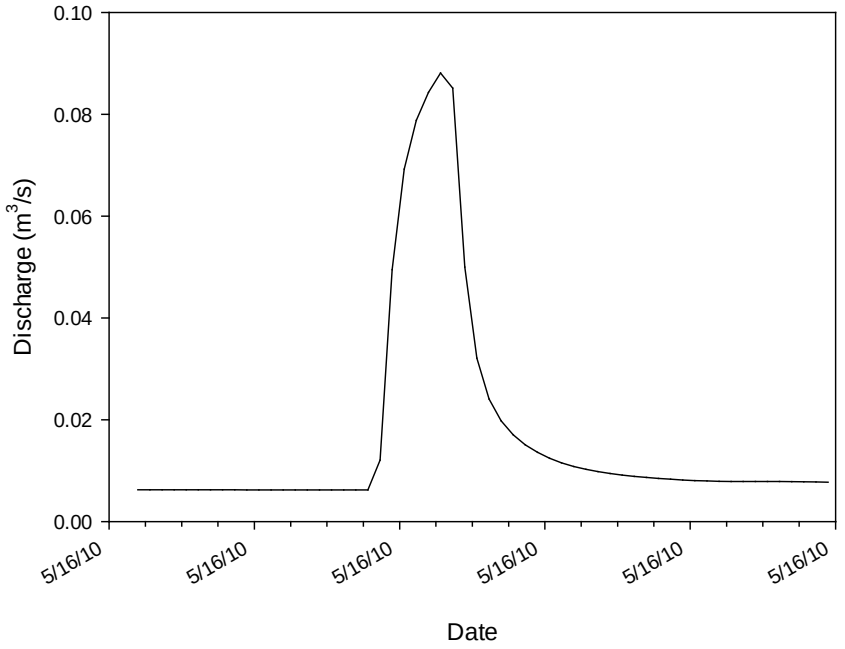

Figure E.6. Discharge from GC03 on May 14, 2010.

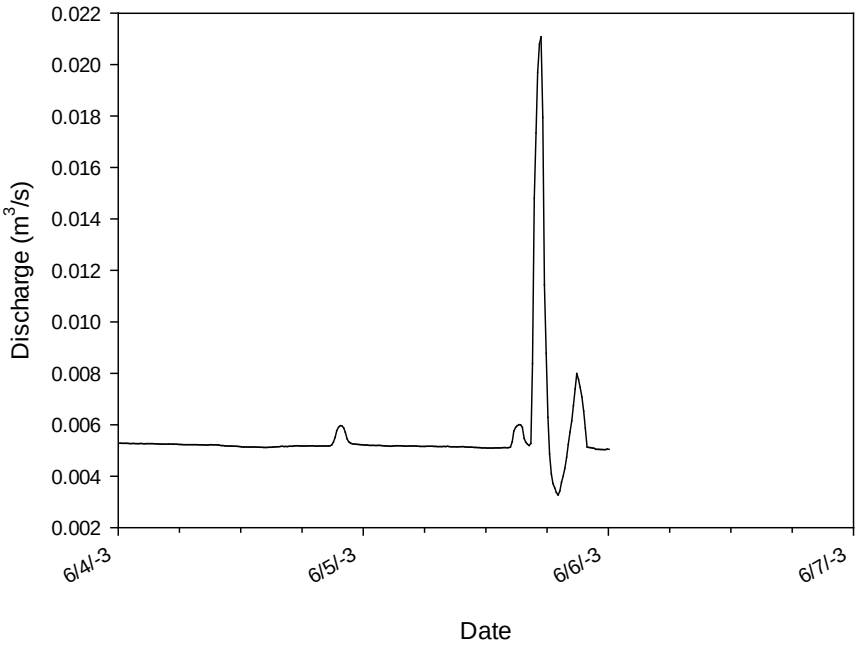

Figure E.7. Discharge from GC03 on June 4, 2010.

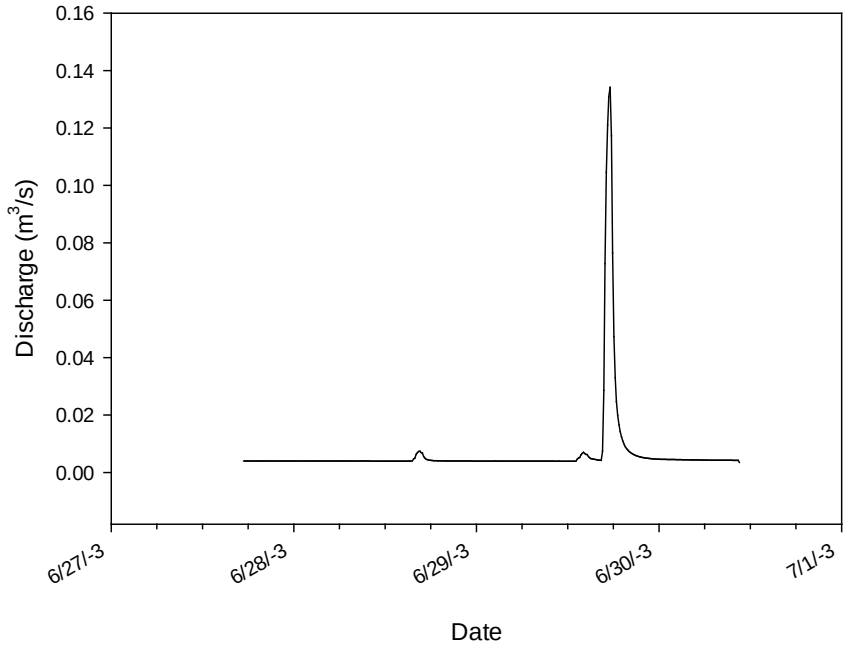

Figure E.8. Discharge from GC03 on June 28, 2010.

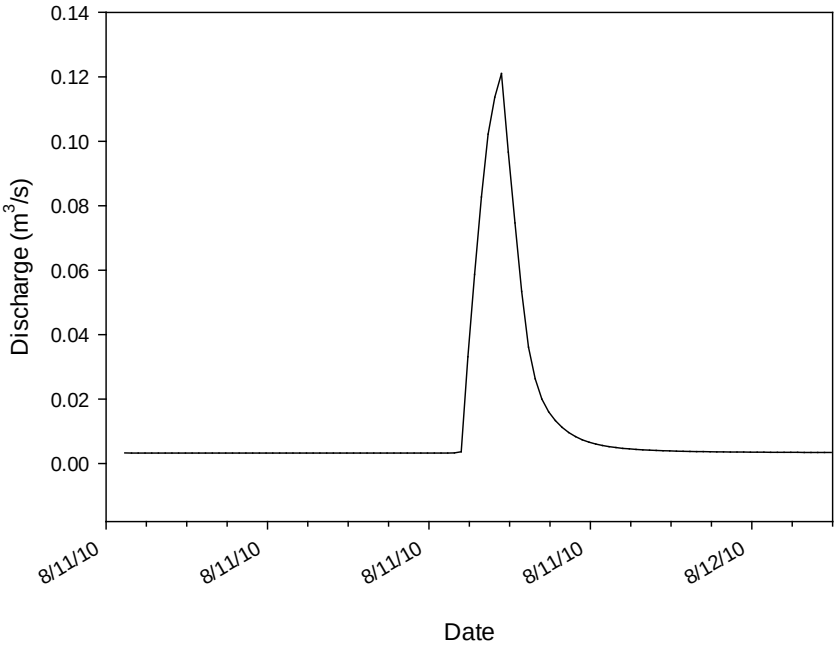

Figure E.9. Discharge from GC03 on August 11, 2010.

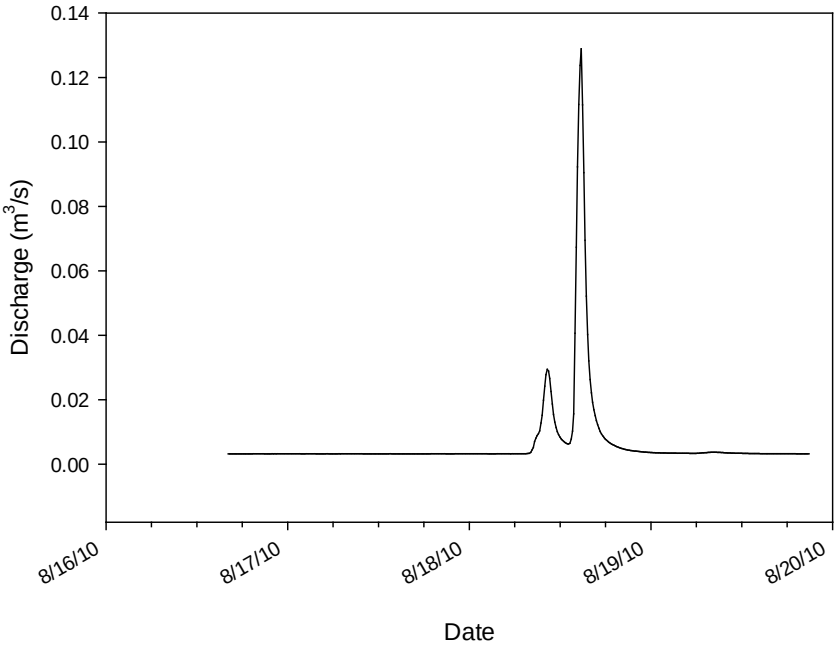

Figure E.10. Discharge from GC03 on August 18 2010.

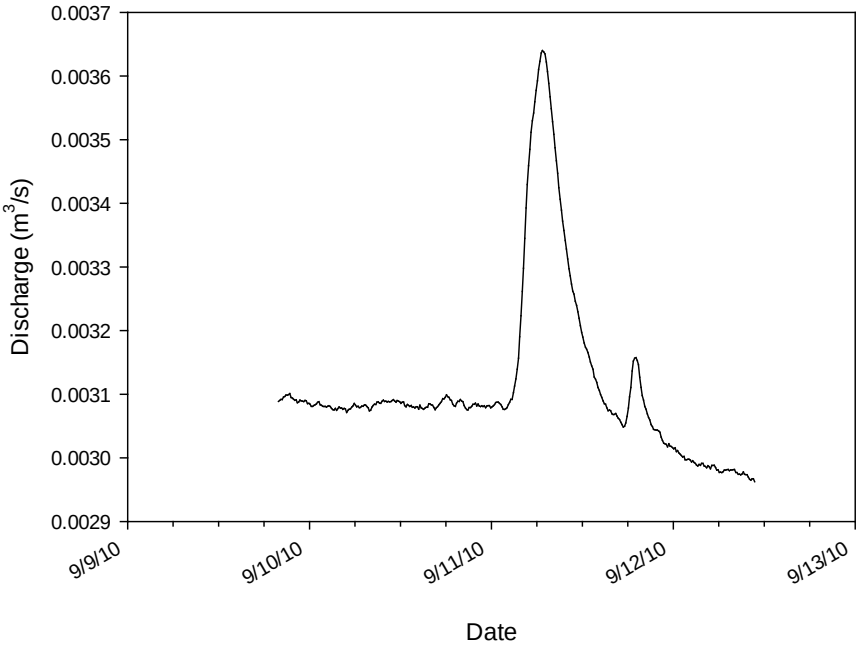

Figure E.11. Discharge from GC03 on September 11, 2010.

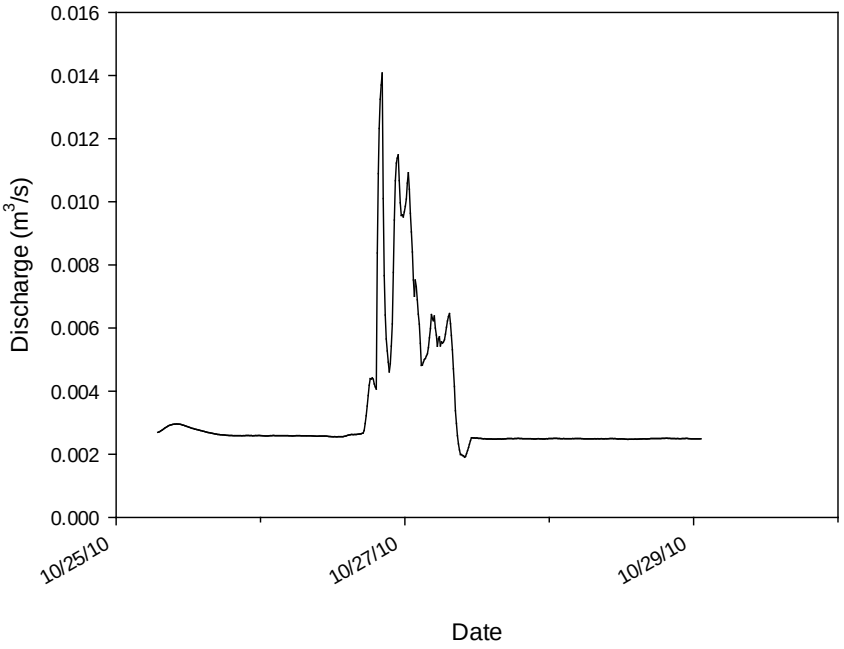

Figure E.12. Discharge from GC03 on October 26, 2010.

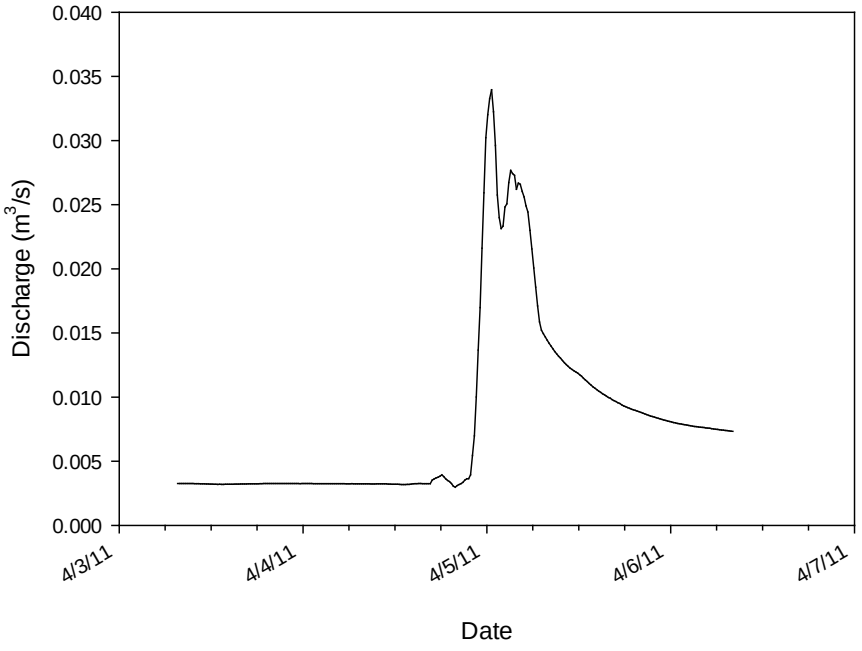

Figure E.13. Discharge from GC03 on April 2, 2011.

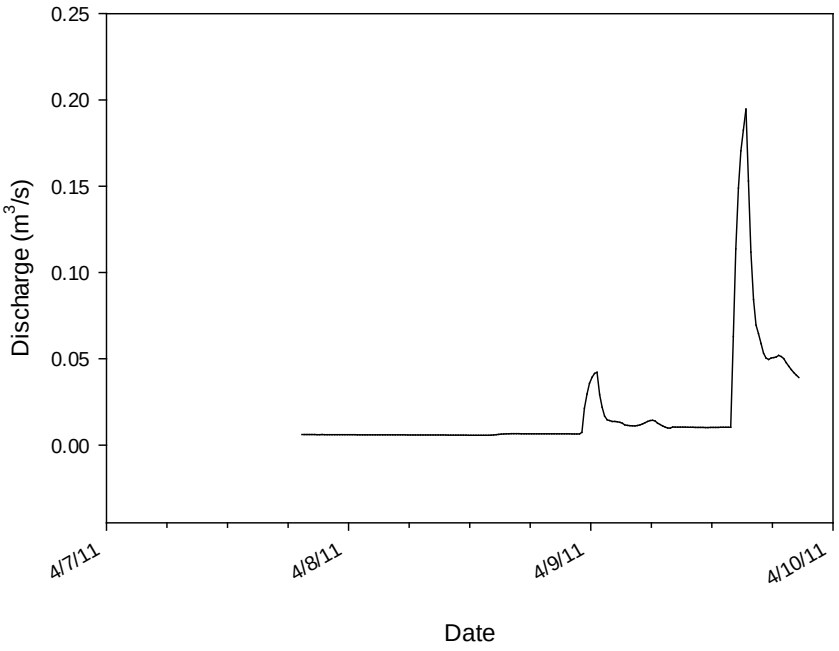

Figure E.14. Discharge from GC03 on April 8, 2011.

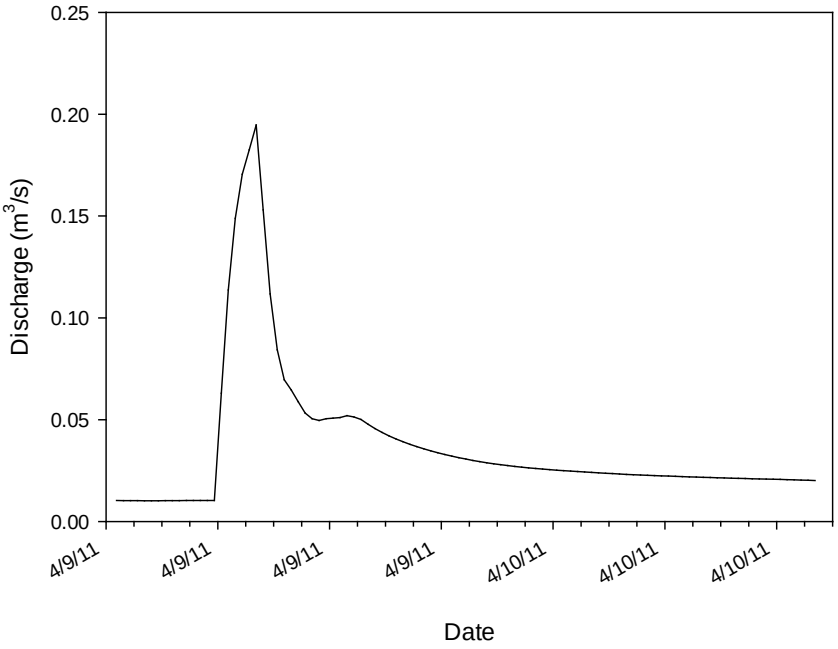

Figure E.15. Discharge from GC03 on April 8, 2011.

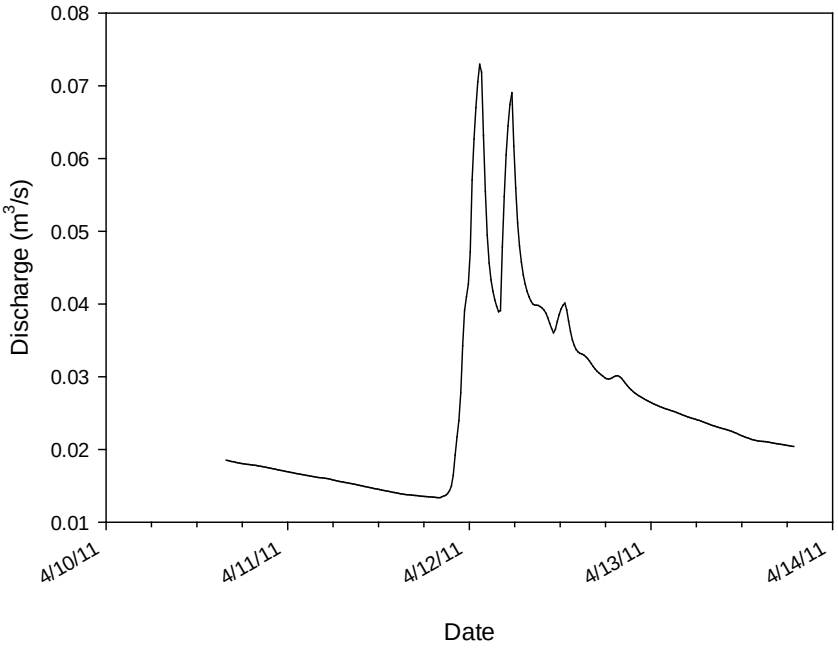

Figure E.16. Discharge from GC03 on April 10, 2011.

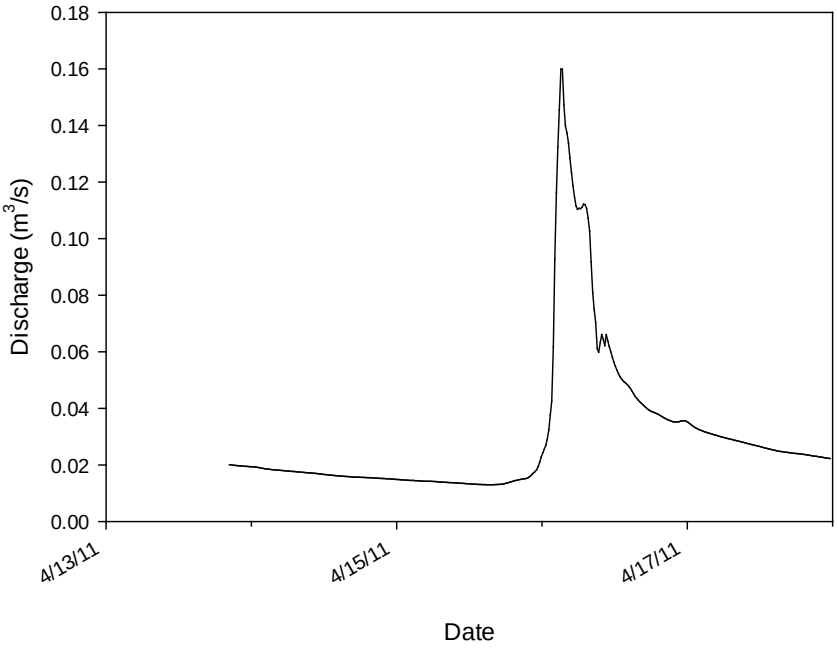

Figure E.17. Discharge from GC03 on April 14, 2011.

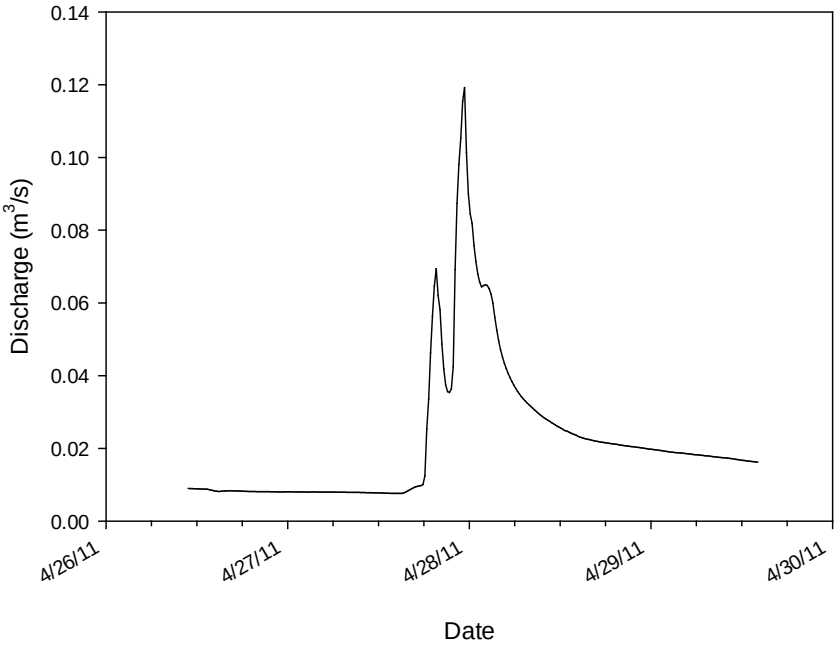

Figure E.18. Discharge from GC03 on April 26, 2011.

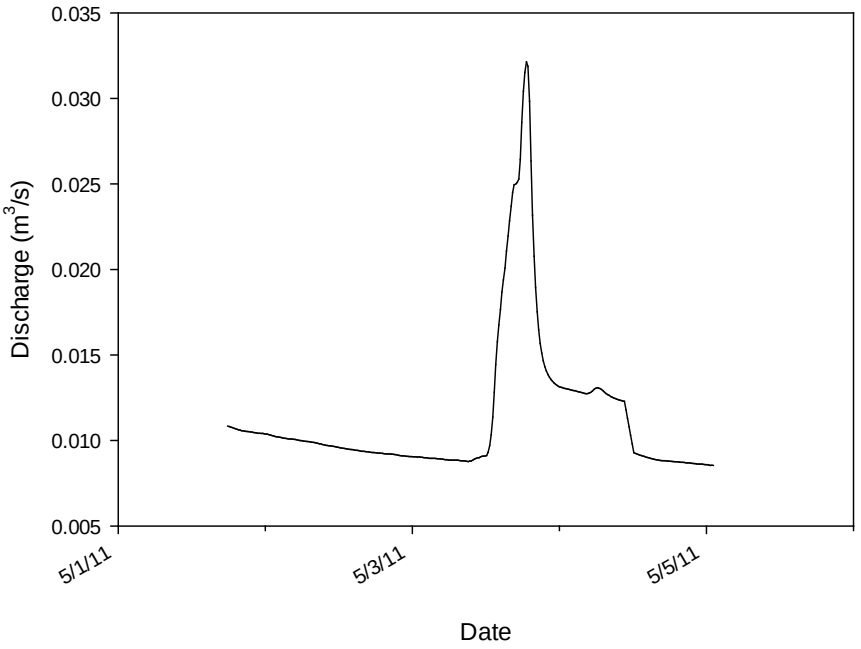

Figure E.19. Discharge from GC03 on May 2, 2011.

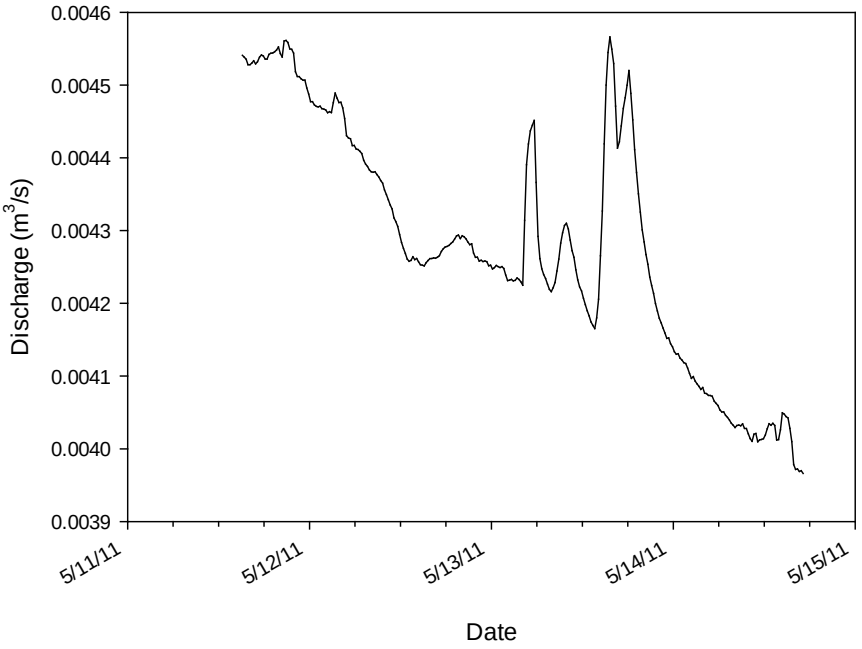

Figure E.20. Discharge from GC03 on May 12, 2011.

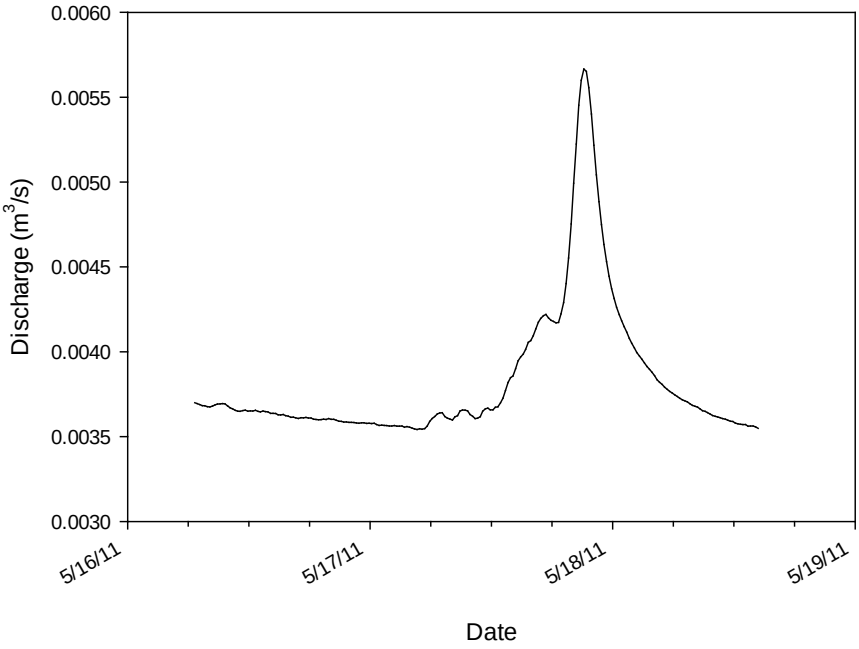

Figure E.21. Discharge from GC03 on May 16, 2011.

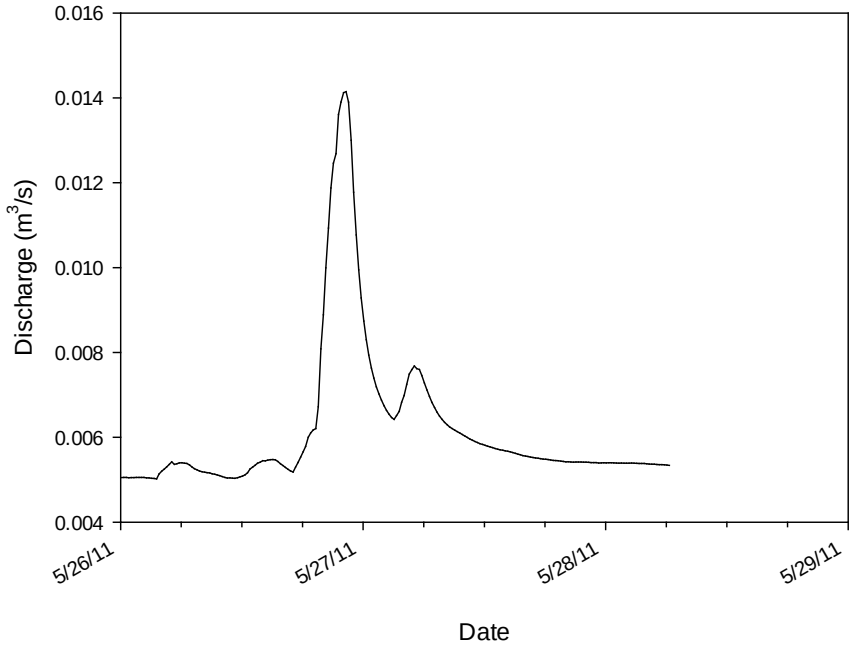

Figure E.22. Discharge from GC03 on May 25, 2011.

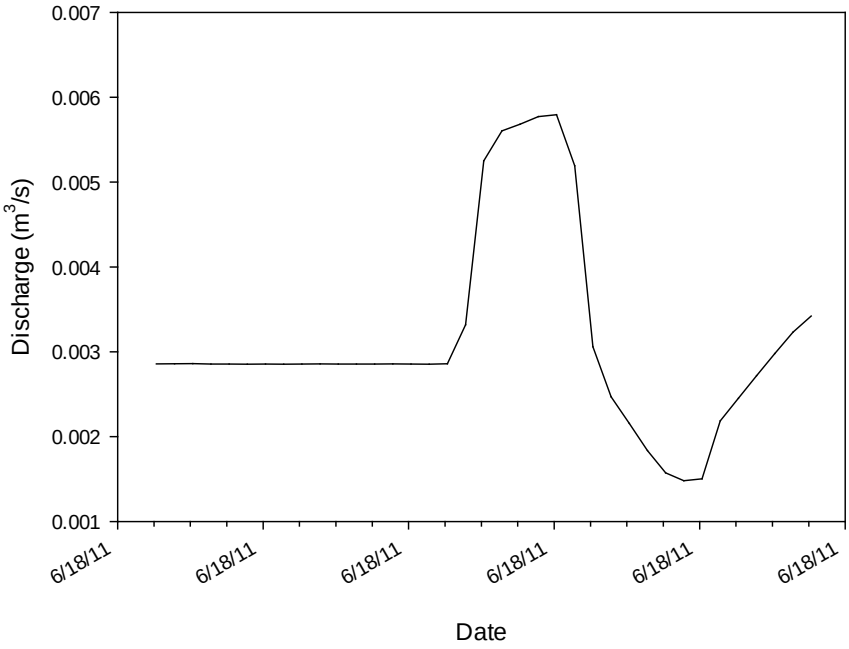

Figure E.23. Discharge from GC03 on June 17, 2011.

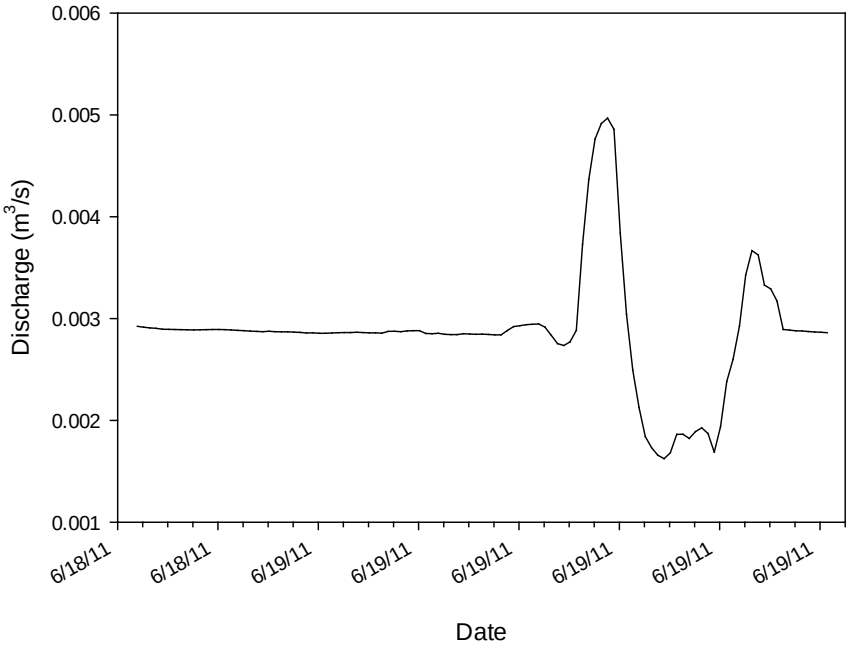

Figure E.24. Discharge from GC03 on June 18, 2011.

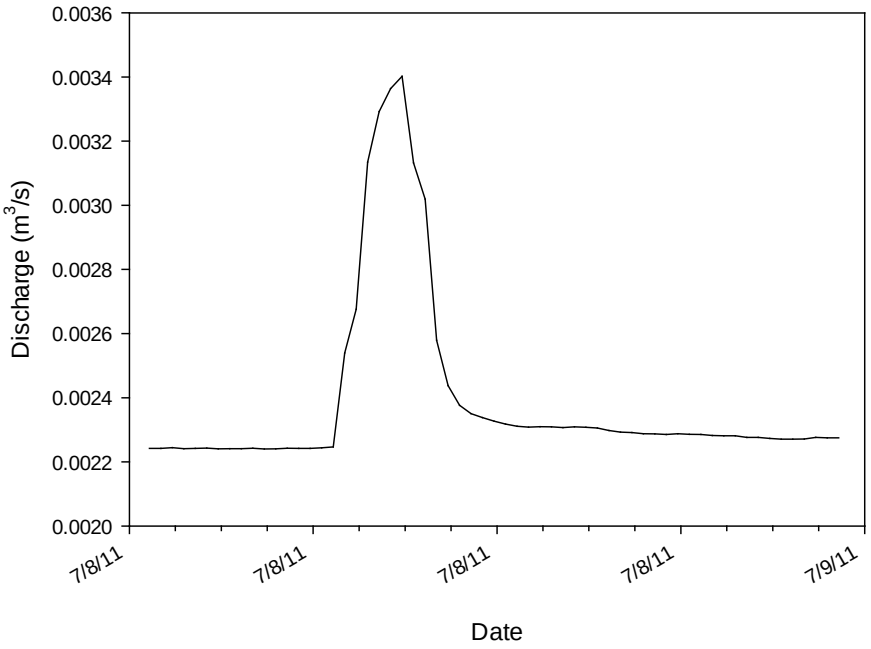

Figure E.25. Discharge from GC03 on July 11, 2011.

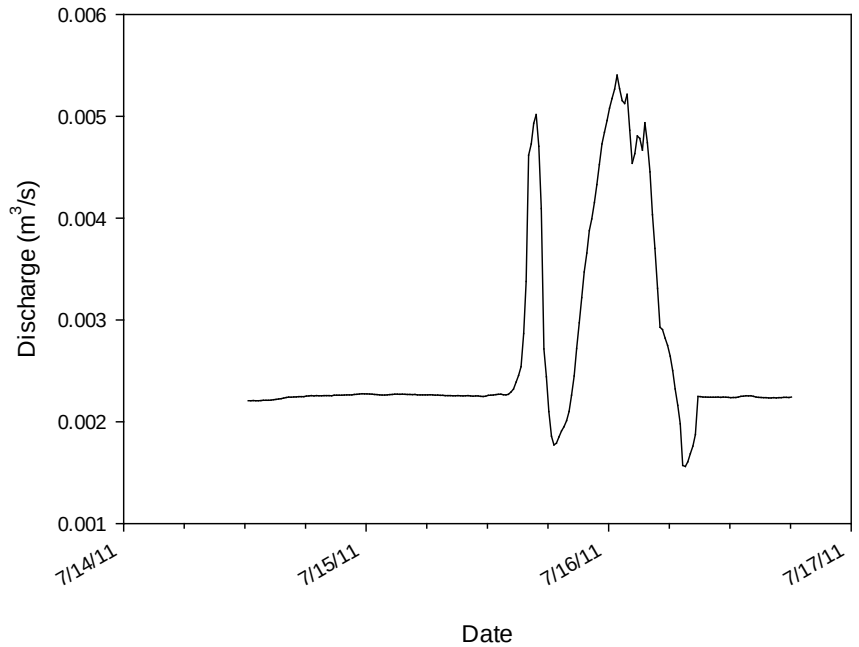

Figure E.26. Discharge from GC03 on July 14, 2011.

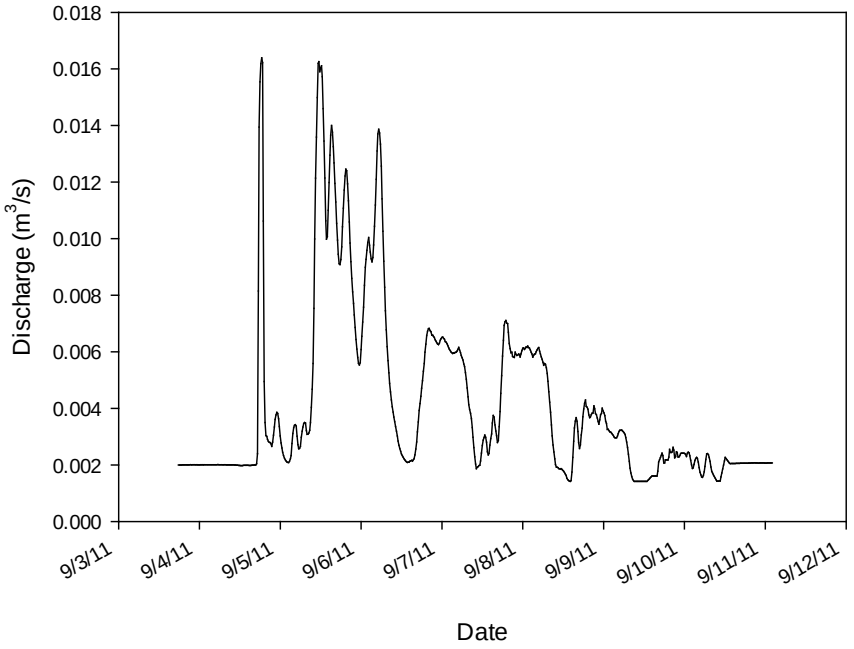

Figure E.27. Discharge from GC03 on September 3, 2011.

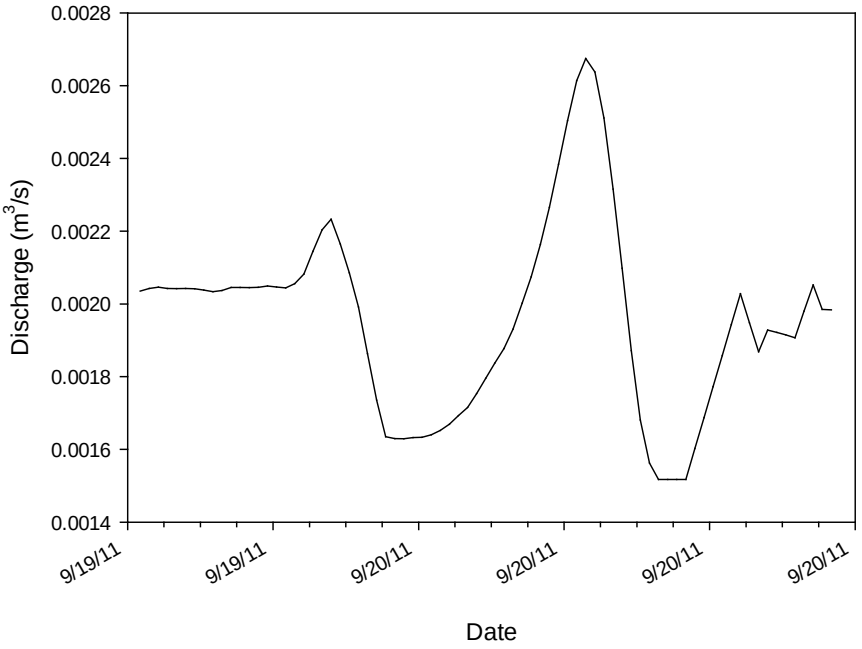

Figure E.28. Discharge from GC03 on September 20, 2011.

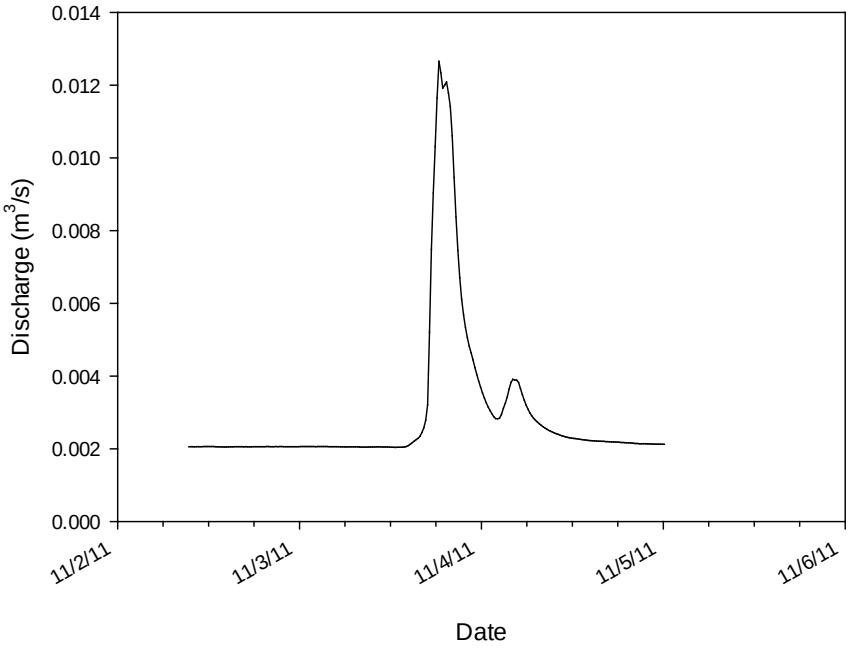

Figure E.29. Discharge from GC03 on November 2, 2011.

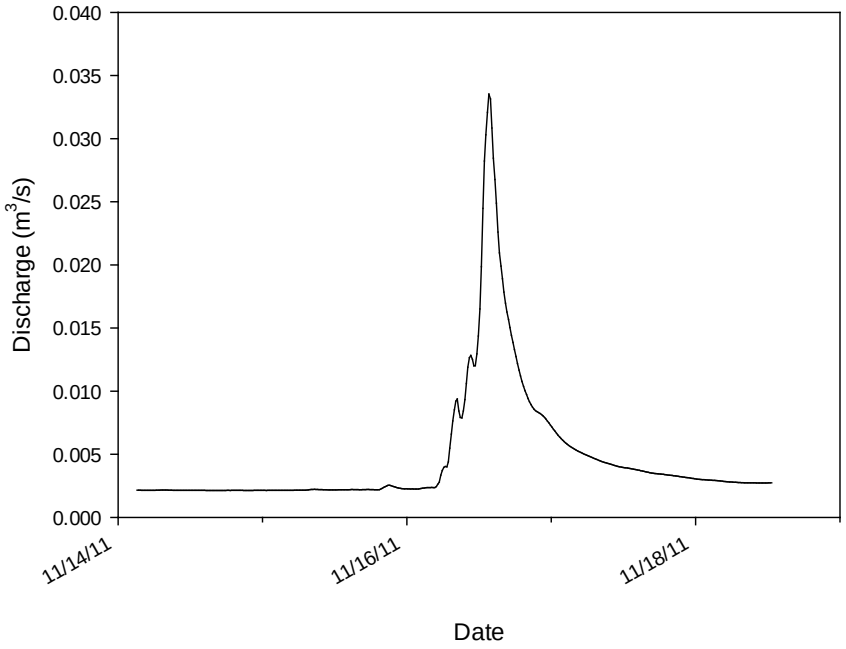

Figure E.30. Discharge from GC03 on November 15, 2011.

APPENDIX F: GC04 HYDROGRAPHS

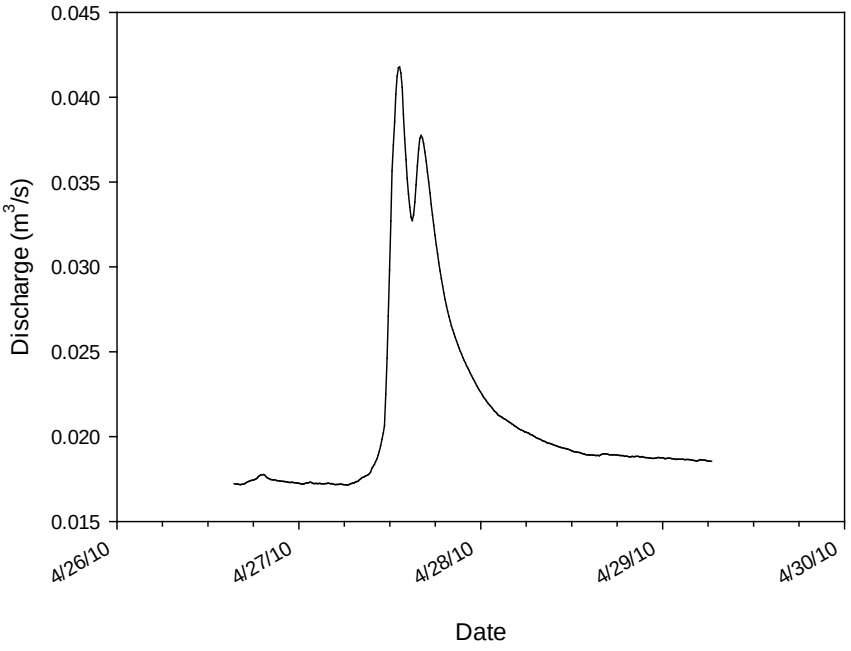

Figure F.1. Discharge from GC04 on April 27, 2010.

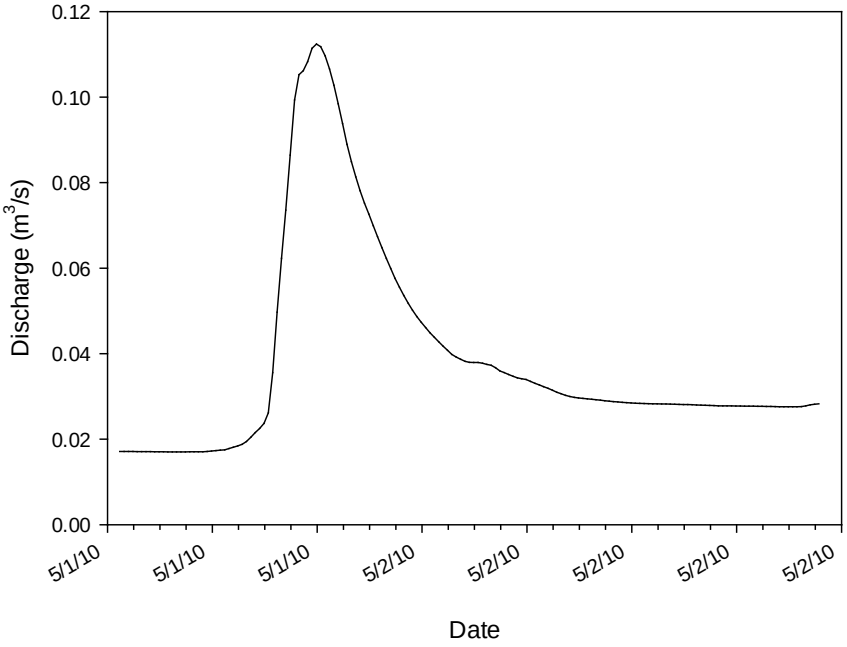

Figure F.2. Discharge from GC04 on May 1, 2010.

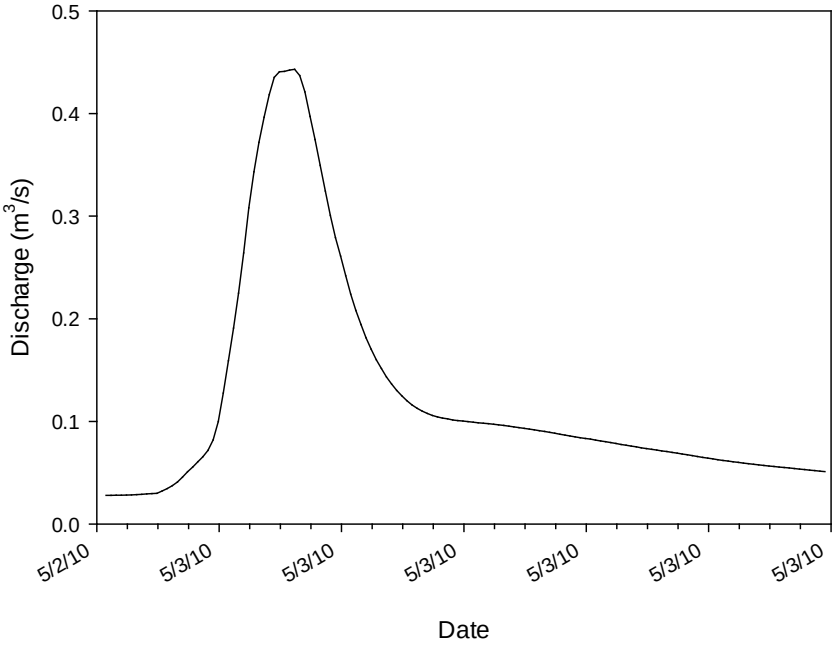

Figure F.3. Discharge from GC04 on May 2, 2010.

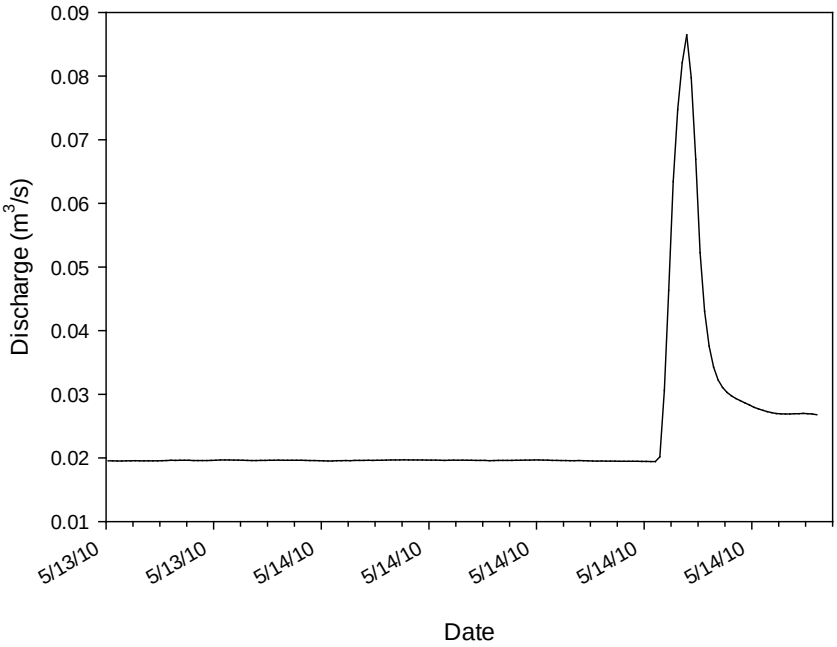

Figure F.4. Discharge from GC04 on May 14, 2010.

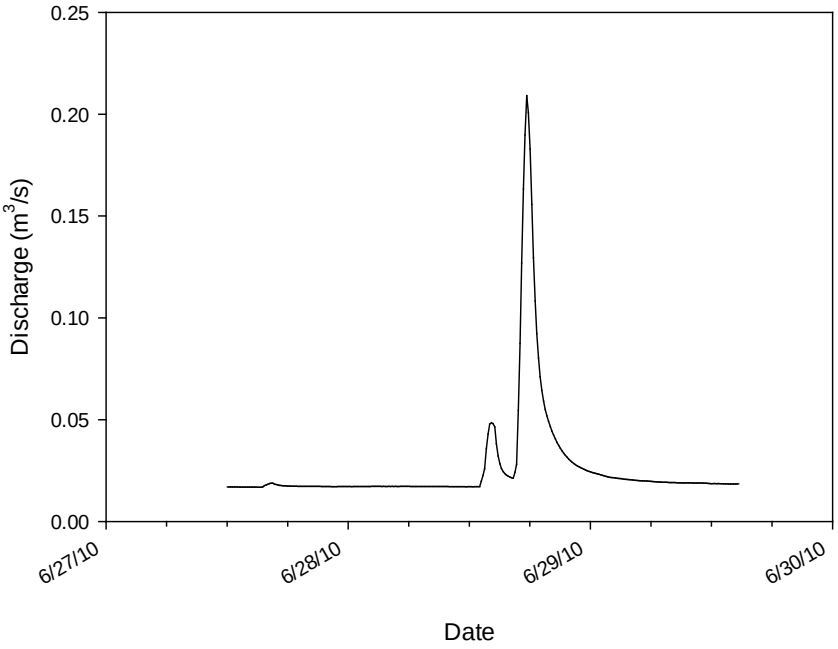

Figure F.5. Discharge from GC04 on June 28, 2010.

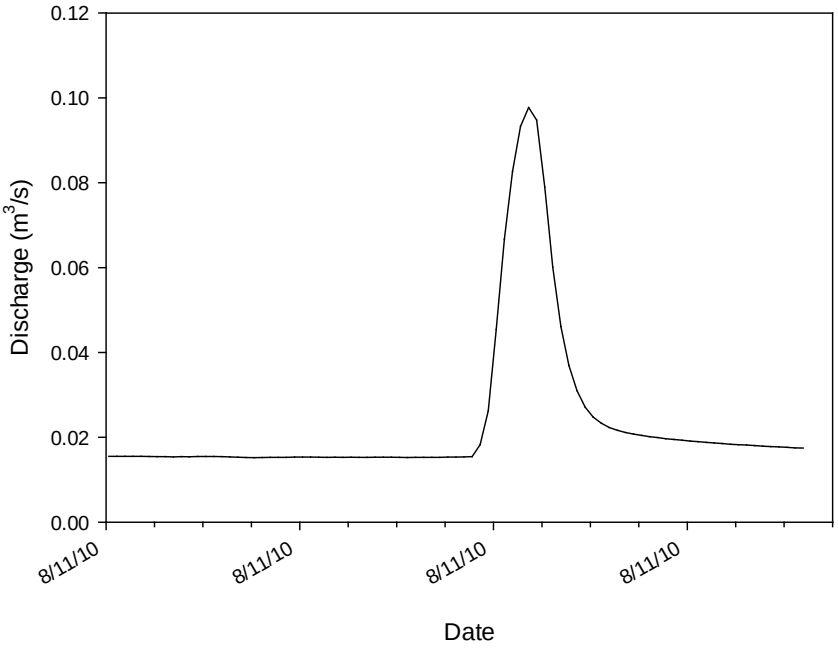

Figure F.6. Discharge from GC04 on May 14, 2010.

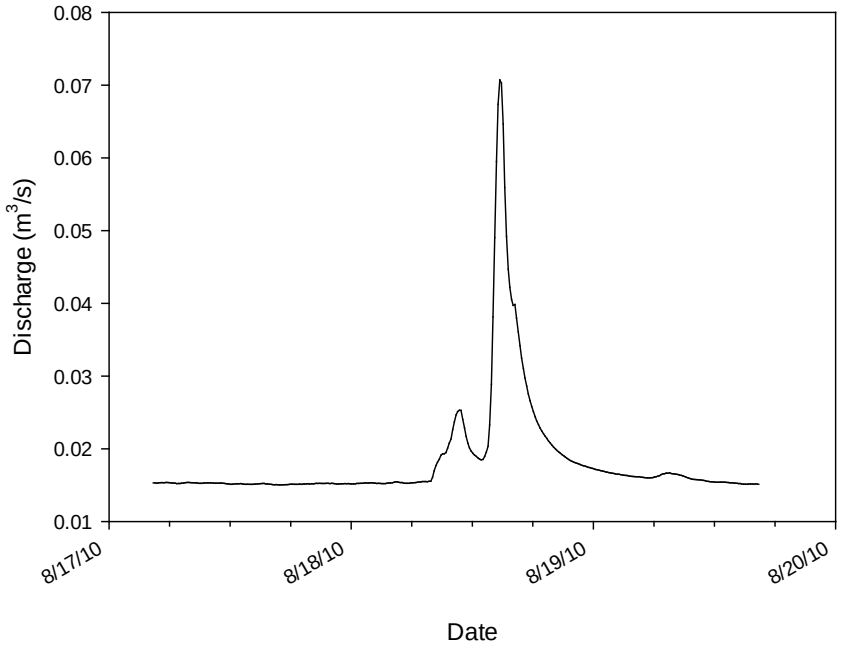

Figure F.7. Discharge from GC04 on August 18, 2010.

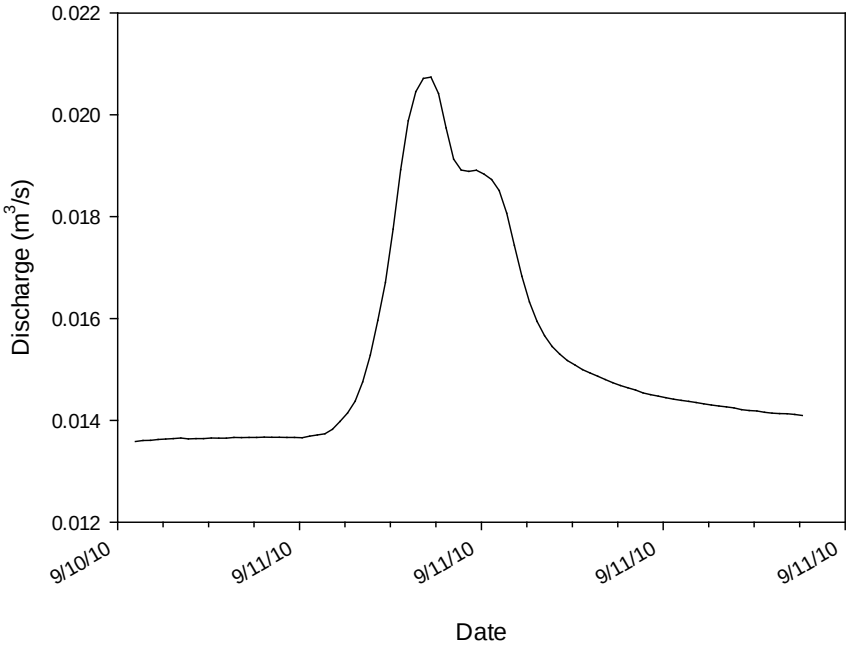

Figure F.8. Discharge from GC04 on September 11, 2010.

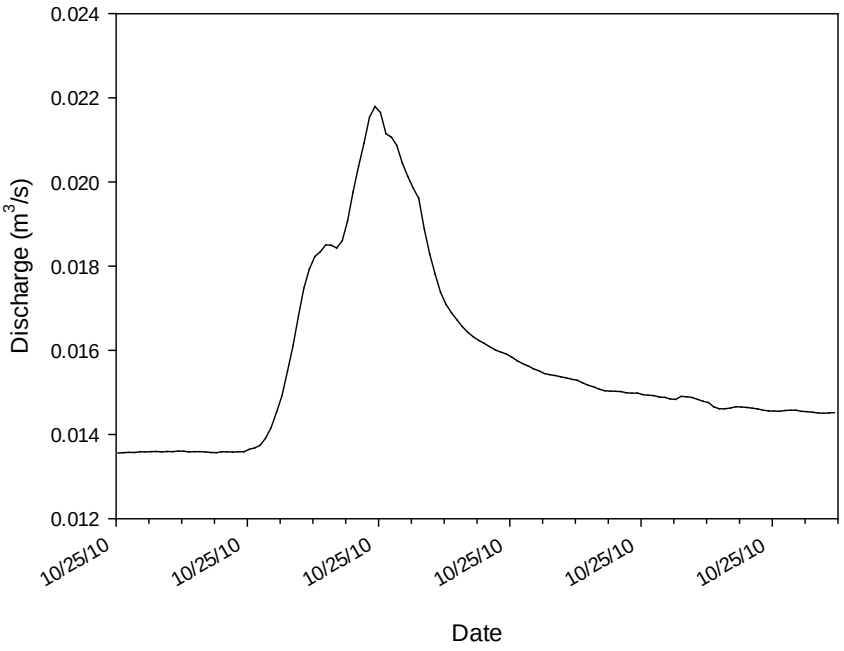

Figure F.9. Discharge from GC04 on October 25, 2010.

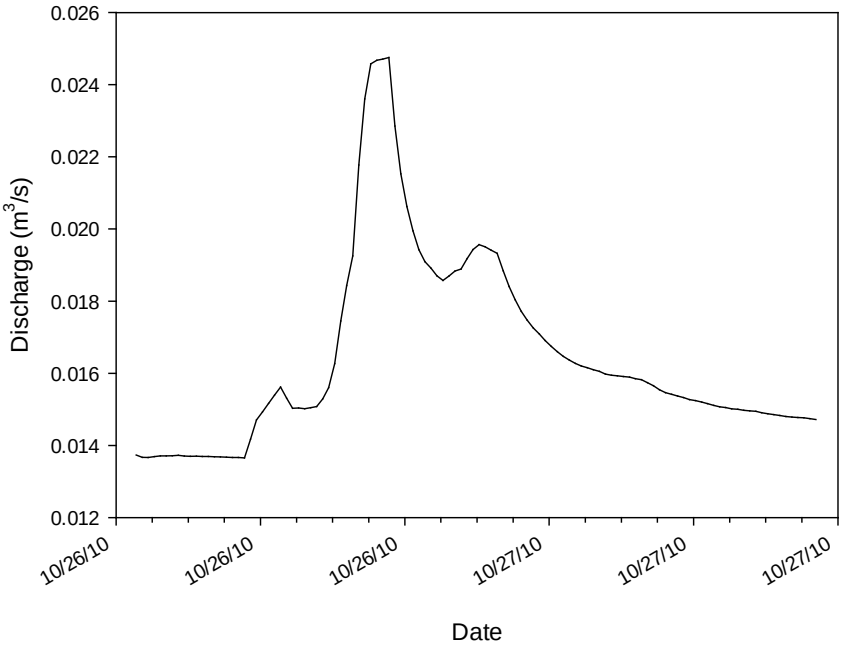

Figure F.10. Discharge from GC04 on October 26, 2010.

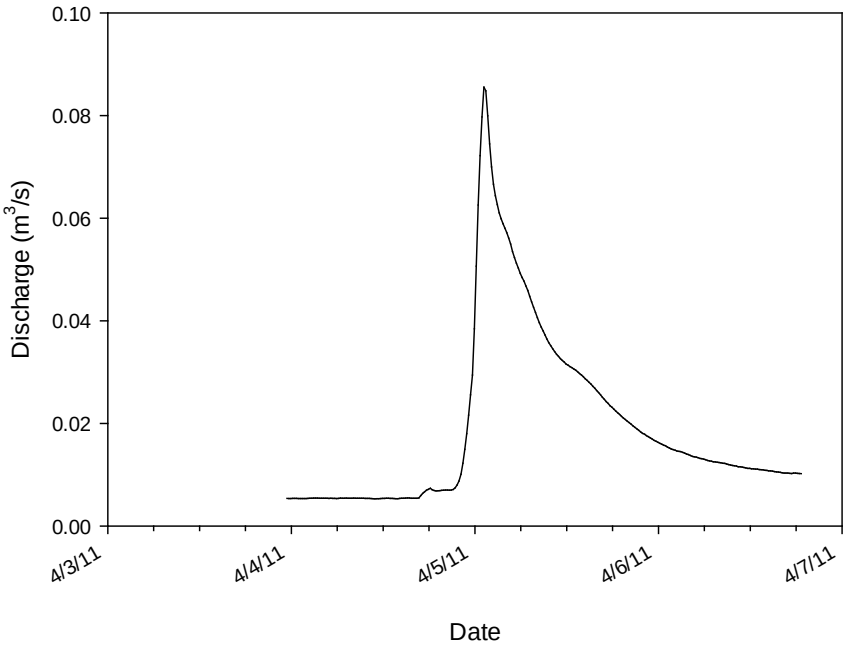

Figure F.11. Discharge from GC04 on April 2, 2011.

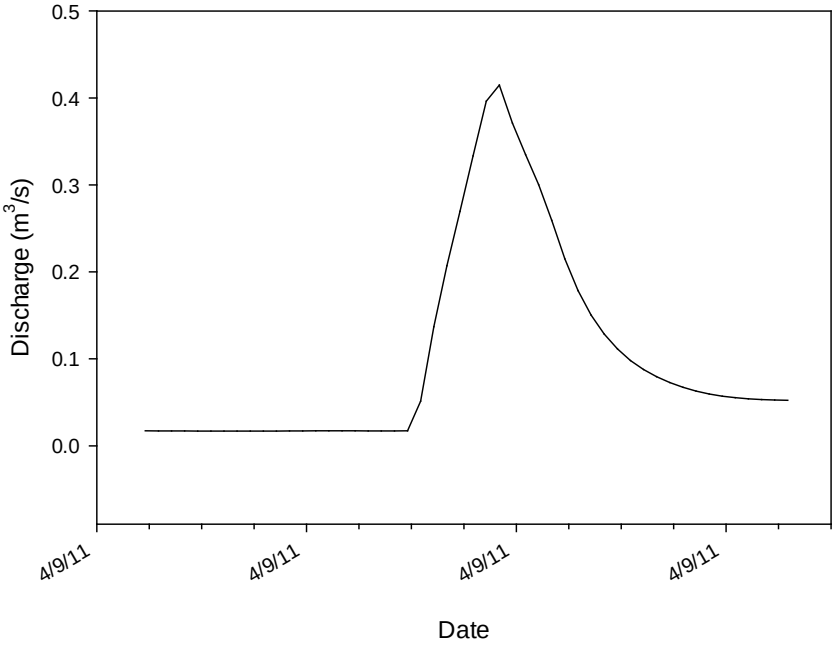

Figure F.12. Discharge from GC04 on April 8, 2011.

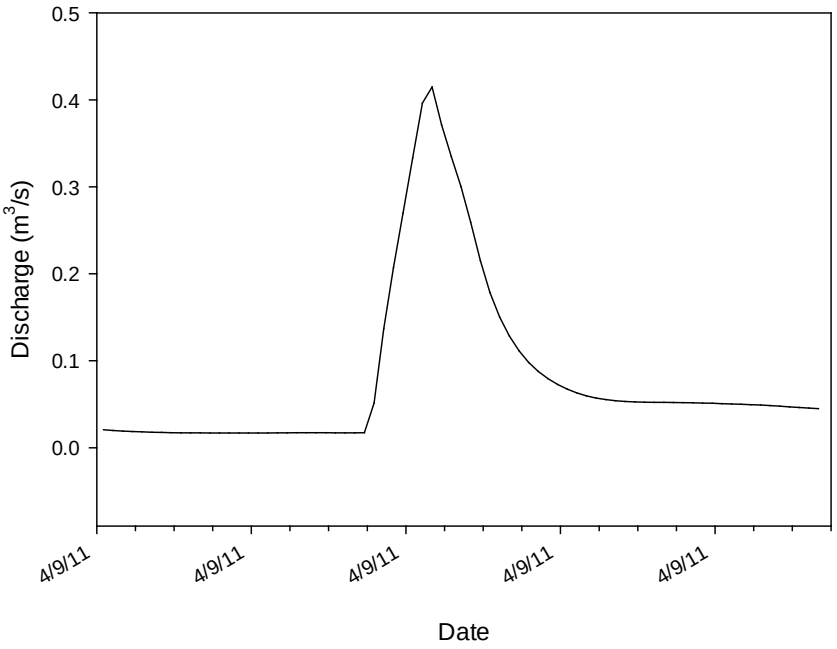

Figure F.13. Discharge from GC04 on April 8, 2011.

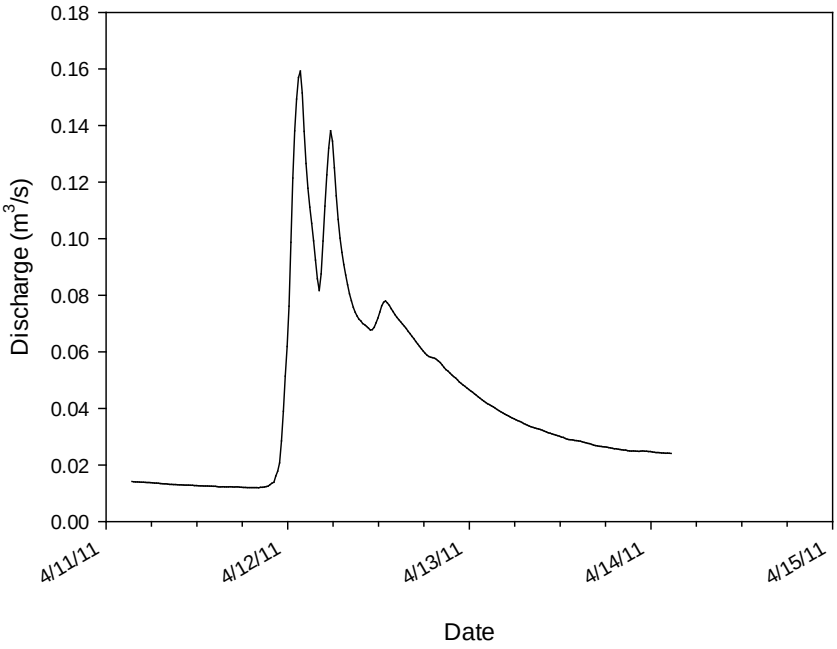

Figure F.14. Discharge from GC04 on April 10, 2011.

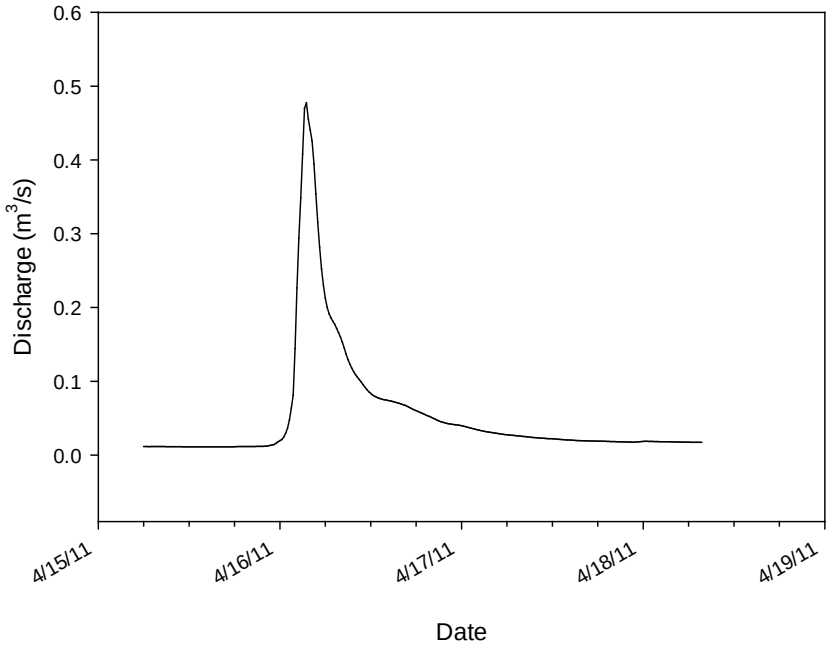

Figure F.15. Discharge from GC04 on April 14, 2011.

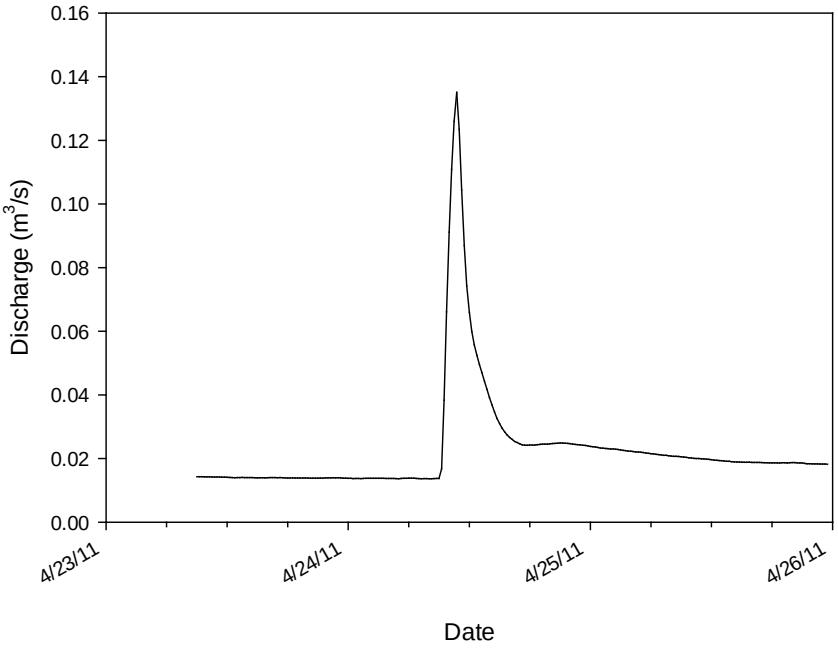

Figure F.16. Discharge from GC04 on April 23, 2011.

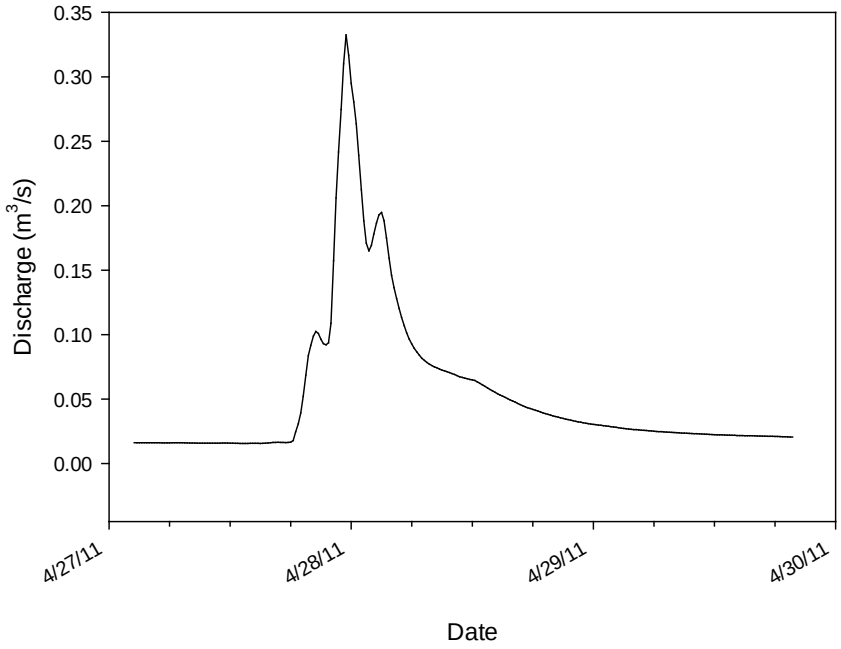

Figure F.17. Discharge from GC04 on April 26, 2011.

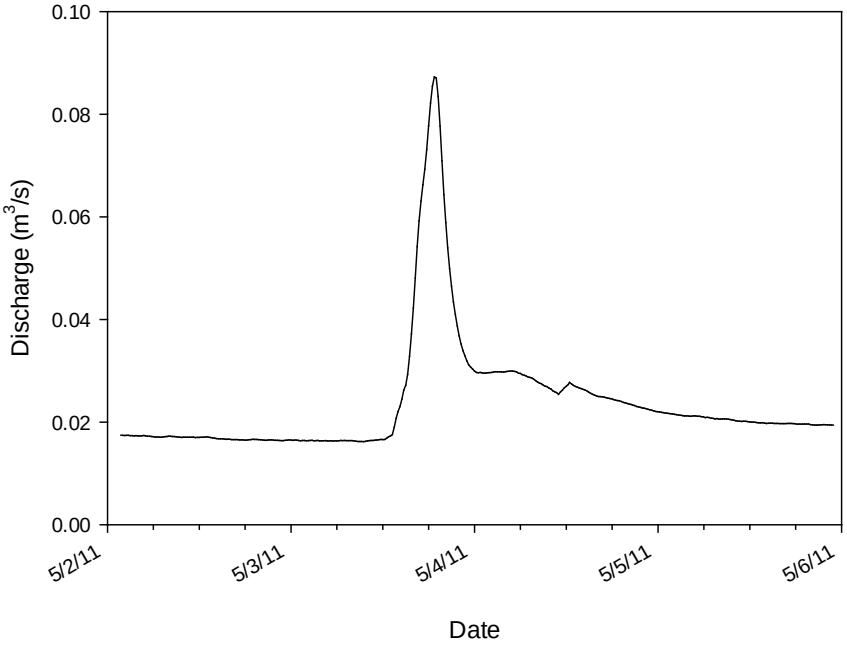

Figure F.18. Discharge from GC04 on May 2, 2011.

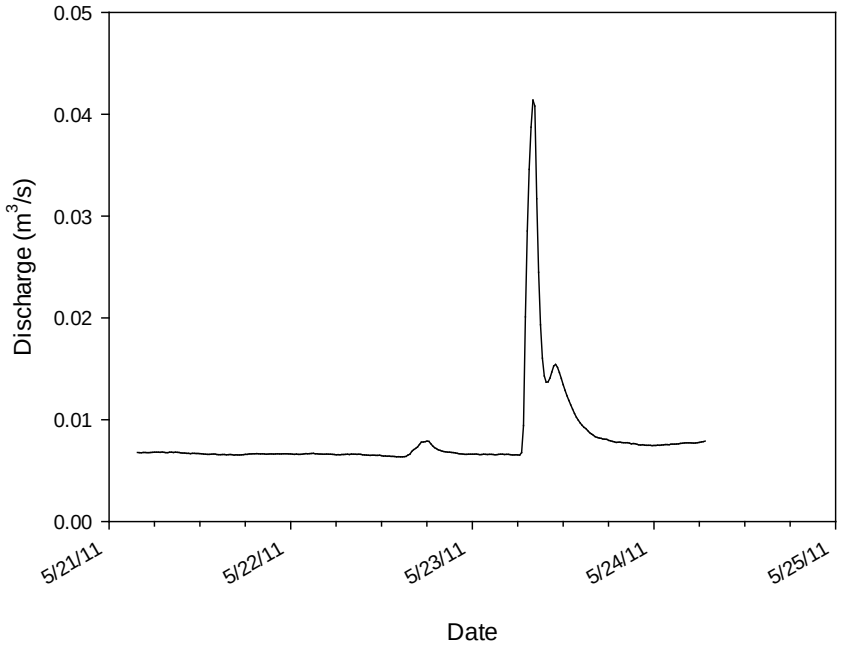

Figure F.19. Discharge from GC04 on May 22, 2011.

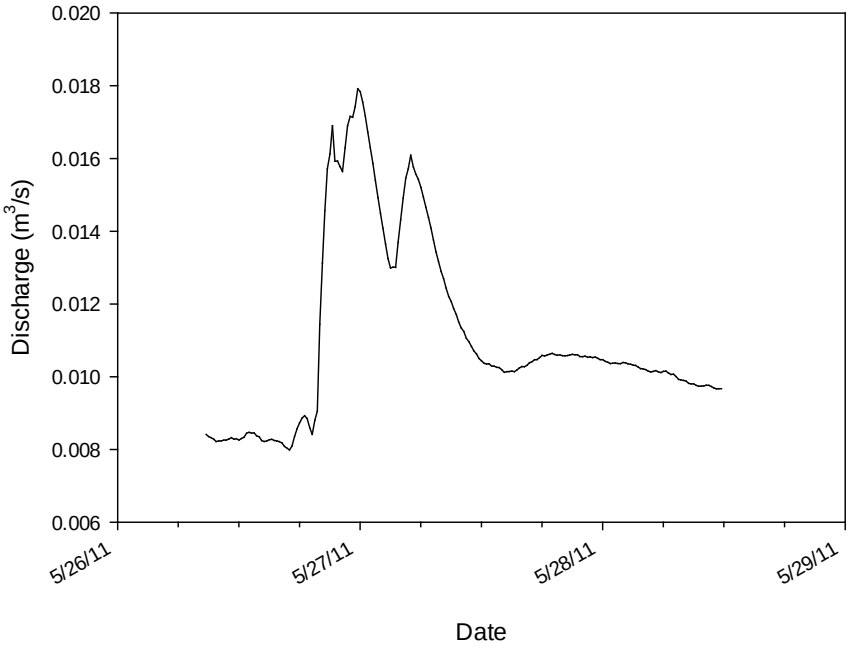

Figure F.20. Discharge from GC04 on May 25, 2011.

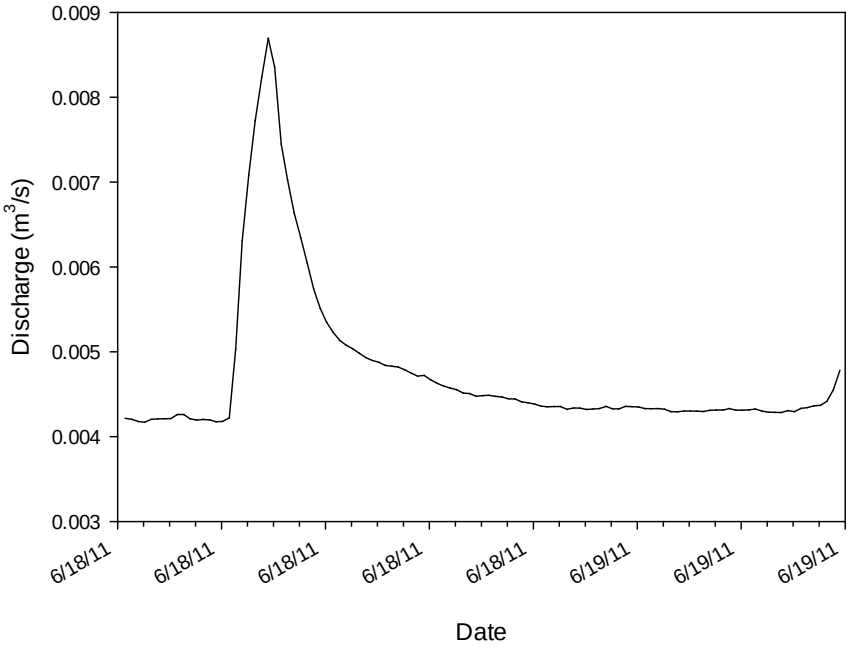

Figure F.21. Discharge from GC04 on June 17, 2011.

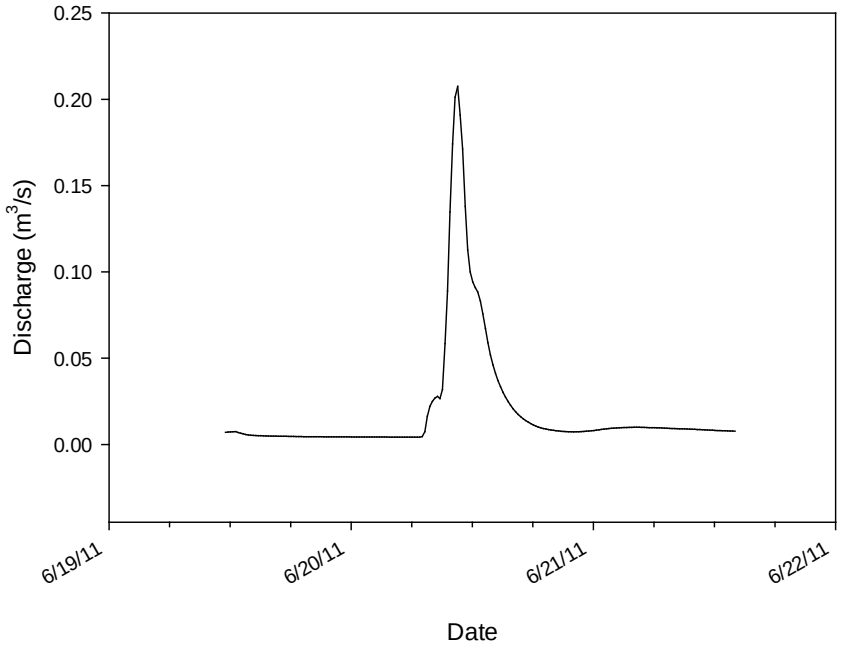

Figure F.22. Discharge from GC04 on June 18, 2011.

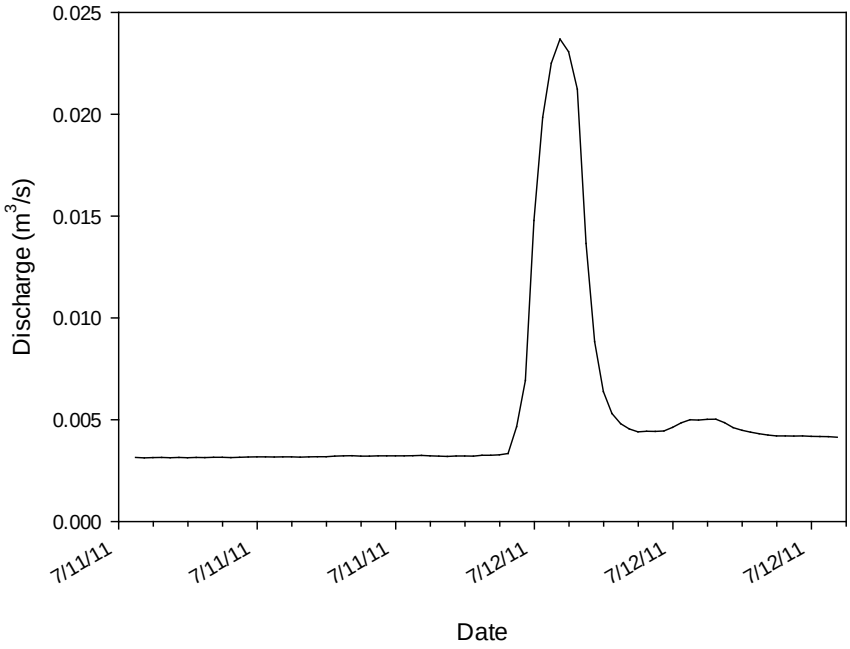

Figure F.23. Discharge from GC04 on July 11, 2011.

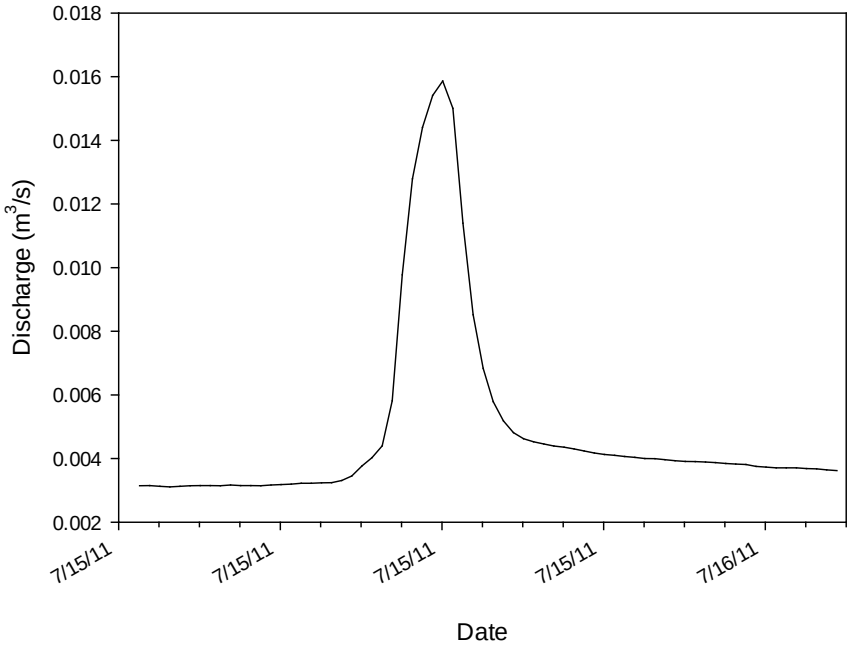

Figure F.24. Discharge from GC04 on July 14, 2011.

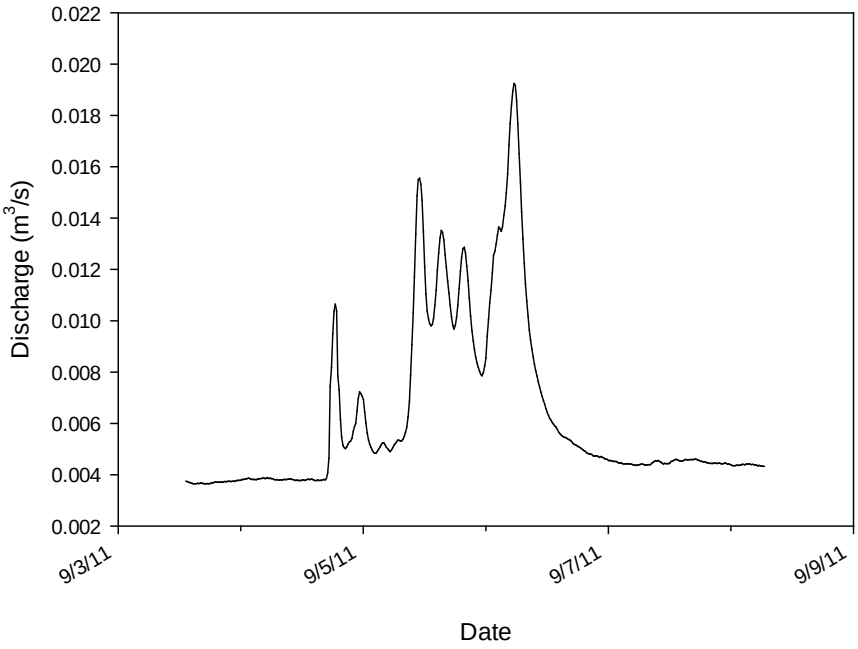

Figure F.25. Discharge from GC04 on September 3, 2011.

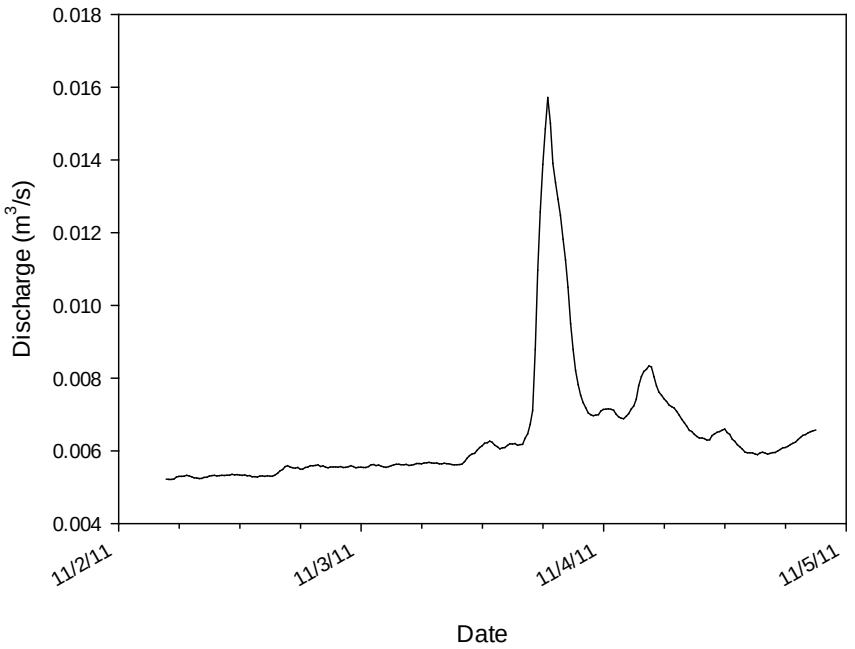

Figure F.26. Discharge from GC04 on November 2, 2011.

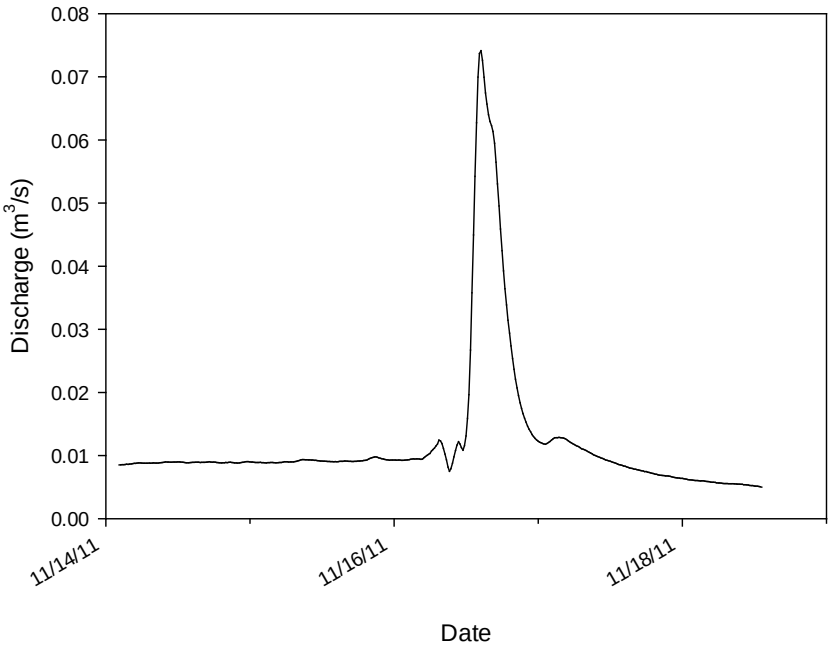

Figure F.27. Discharge from GC04 on November 15, 2011.

APPENDIX G: LMS HYDROGRAPHS

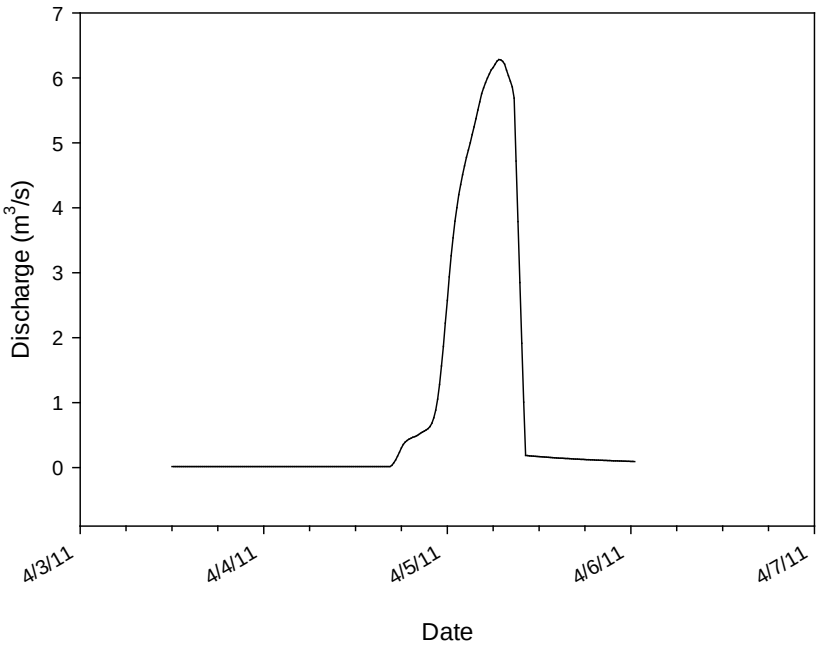

Figure G.1. Discharge from LMS on April 2, 2011.

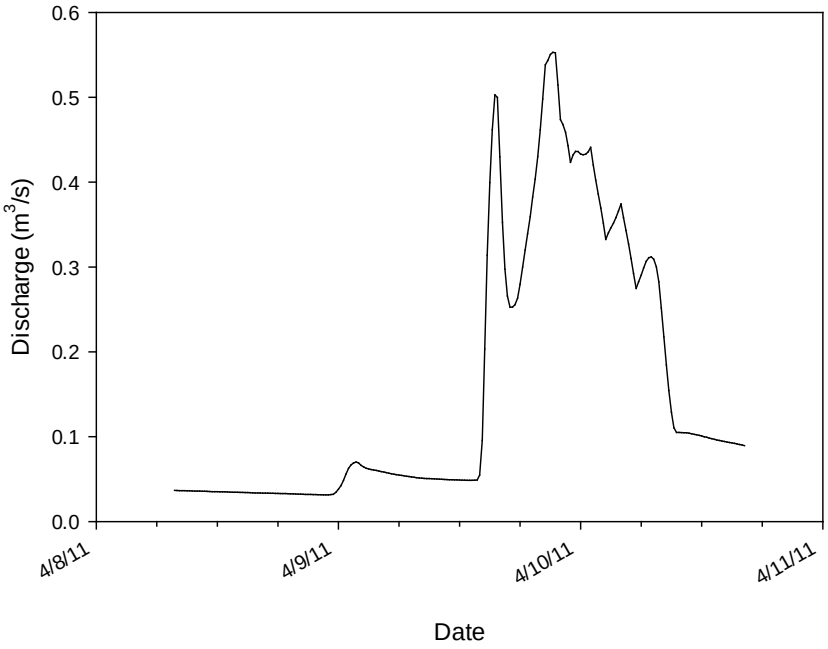

Figure G.2. Discharge from LMS on April 8, 2011.

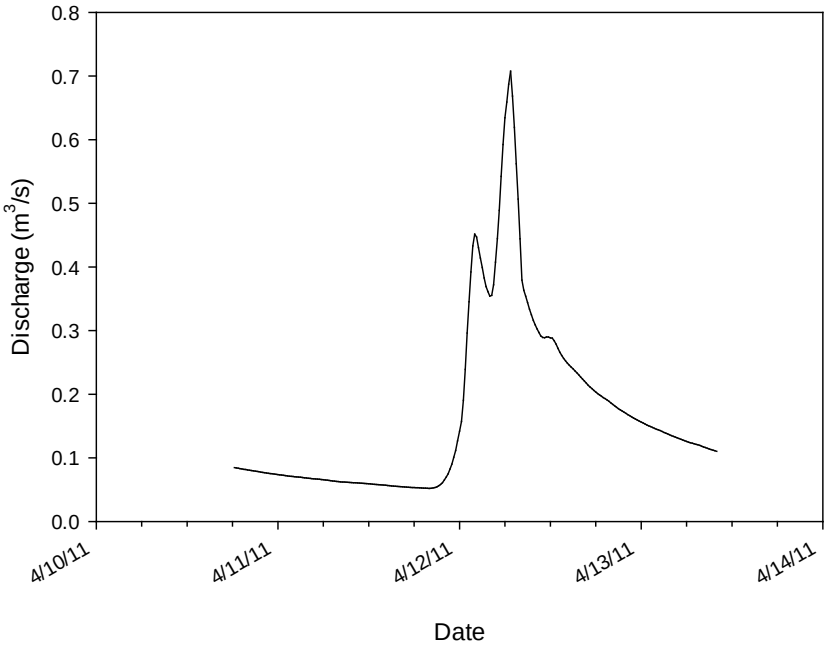

Figure G.3. Discharge from LMS on April 10, 2011.

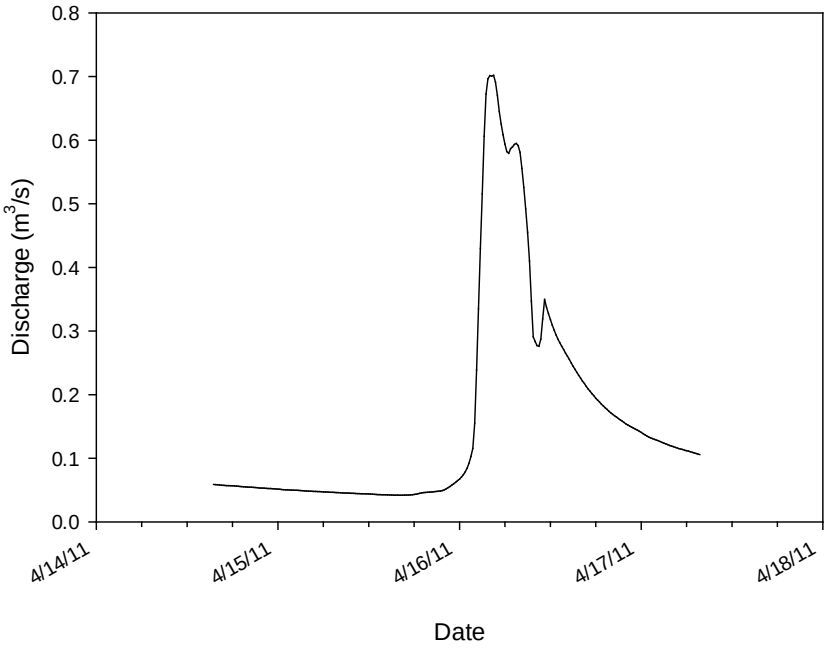

Figure G.4. Discharge from LMS on April 14, 2011.

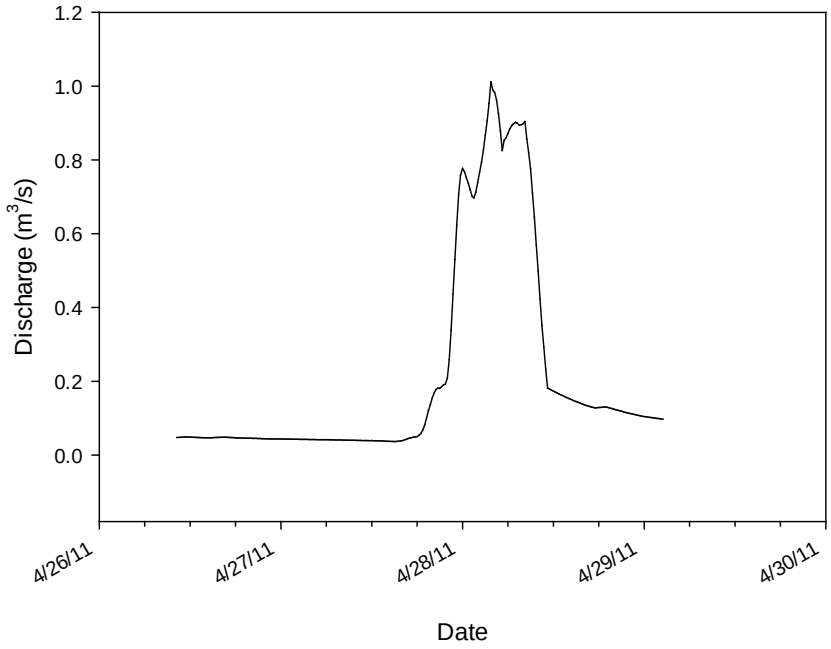

Figure G.5. Discharge from LMS on April 26, 2011.

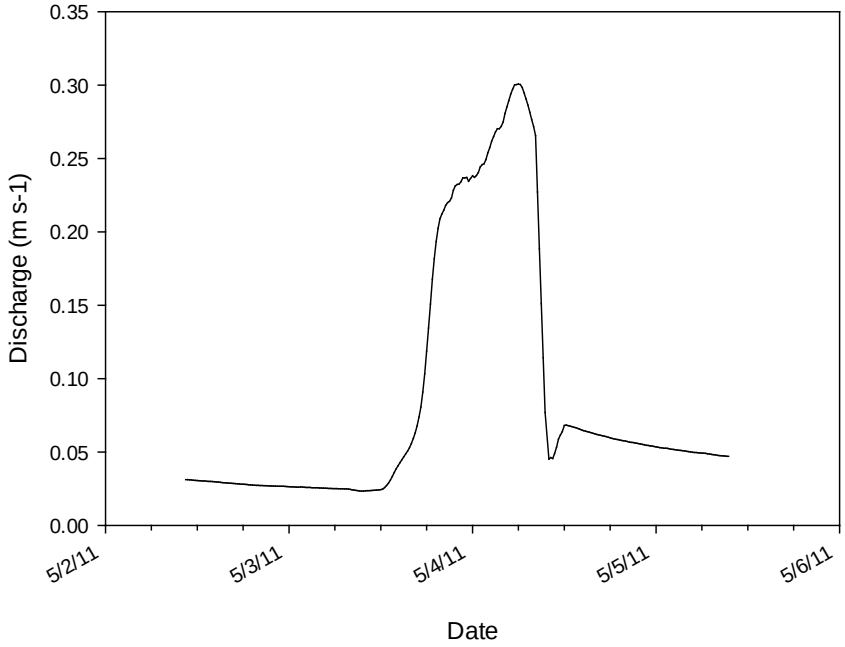

Figure G.6. Discharge from LMS on May 2, 2011.

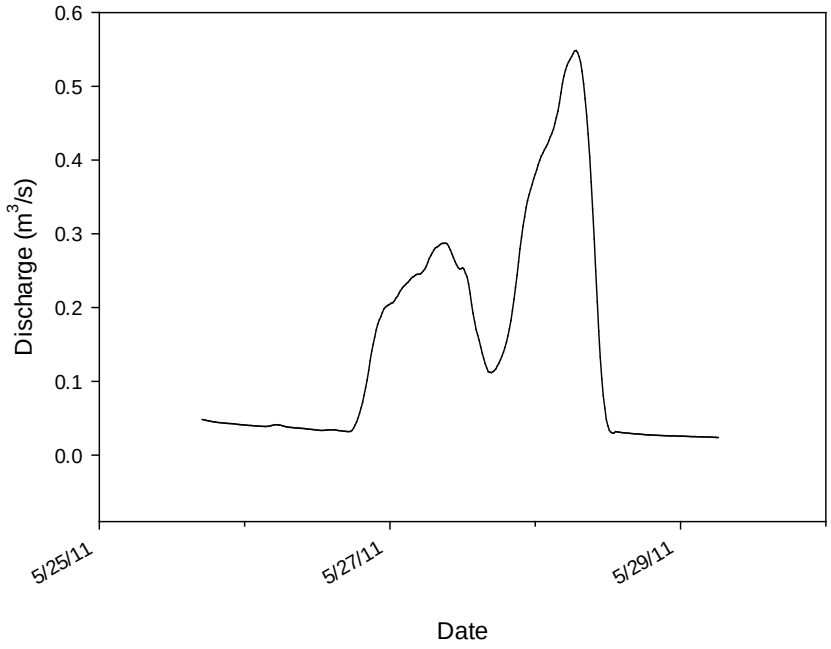

Figure G.7. Discharge from LMS on May 25, 2011.

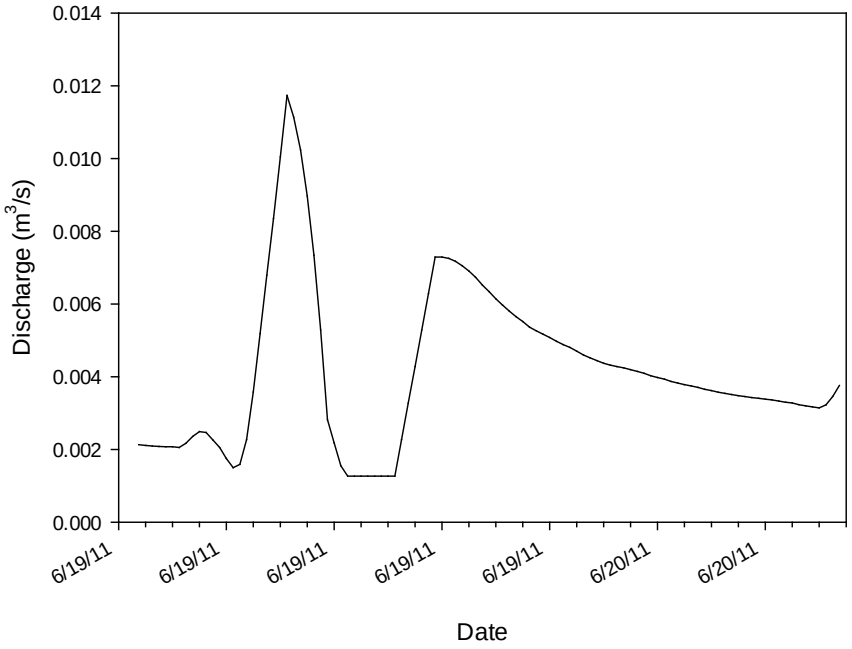

Figure G.8. Discharge from LMS on June 18, 2011.

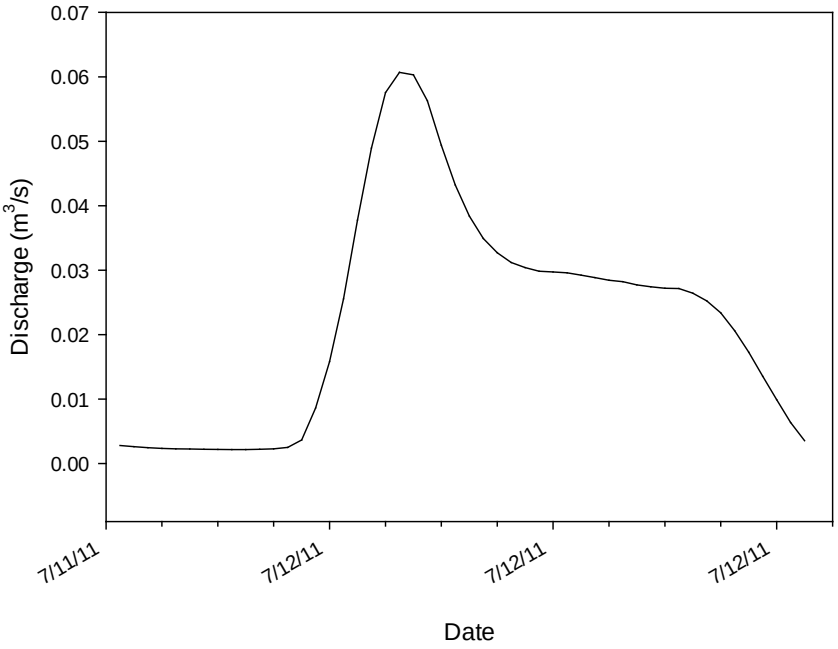

Figure G.9. Discharge from LMS on July 11, 2011.

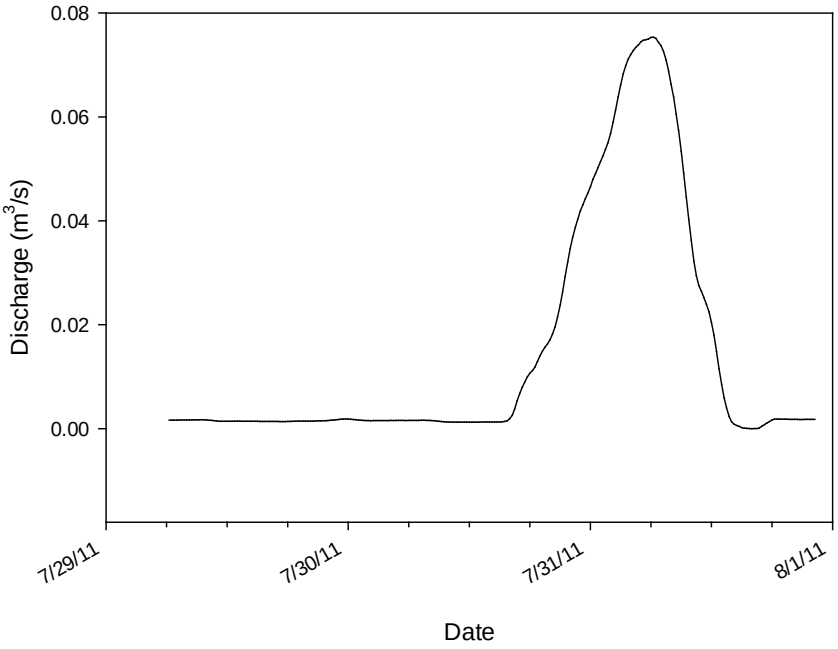

Figure G.10. Discharge from LMS on July 14, 2011.

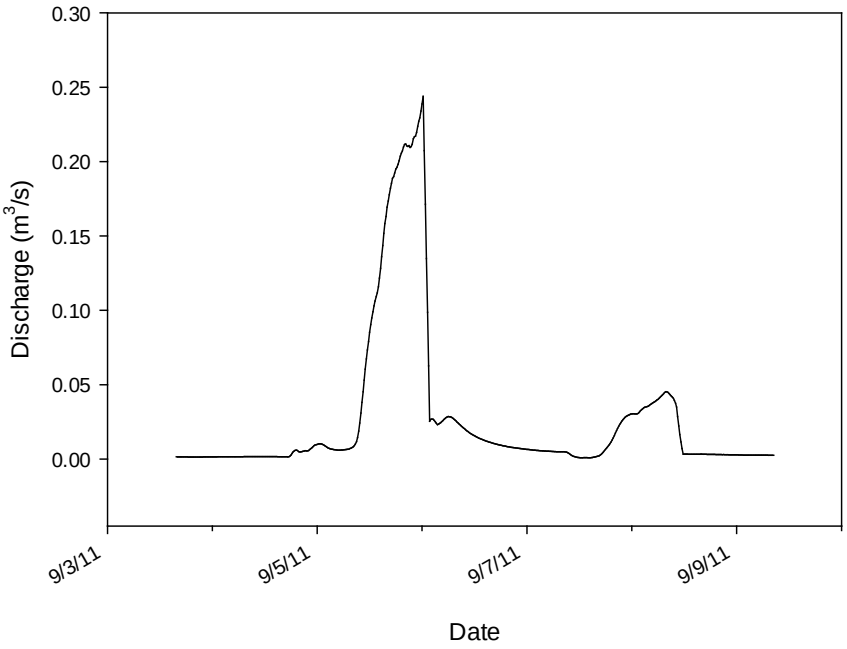

Figure G.11. Discharge from LMS on September 3, 2011.

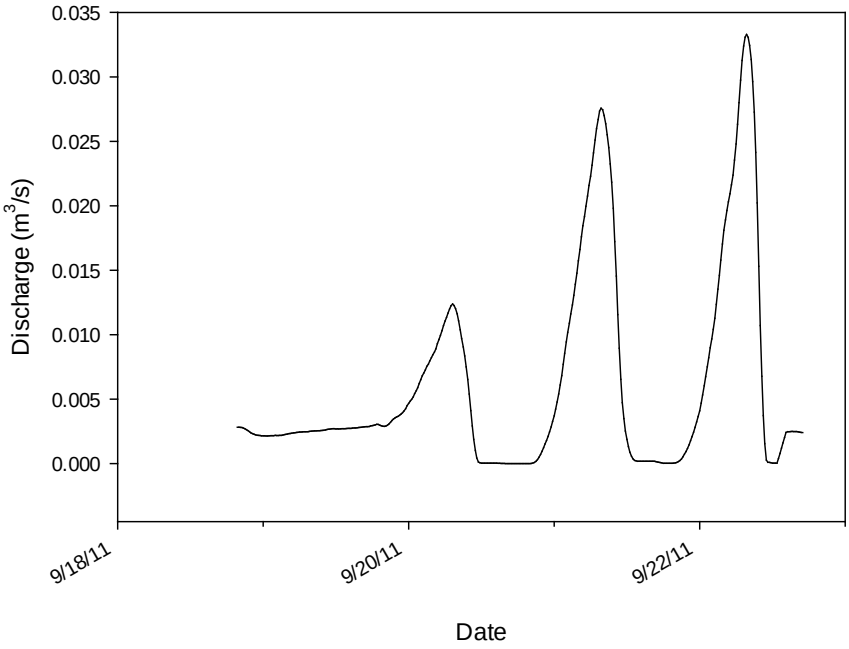

Figure G.12. Discharge from LMS on September 20, 2011.

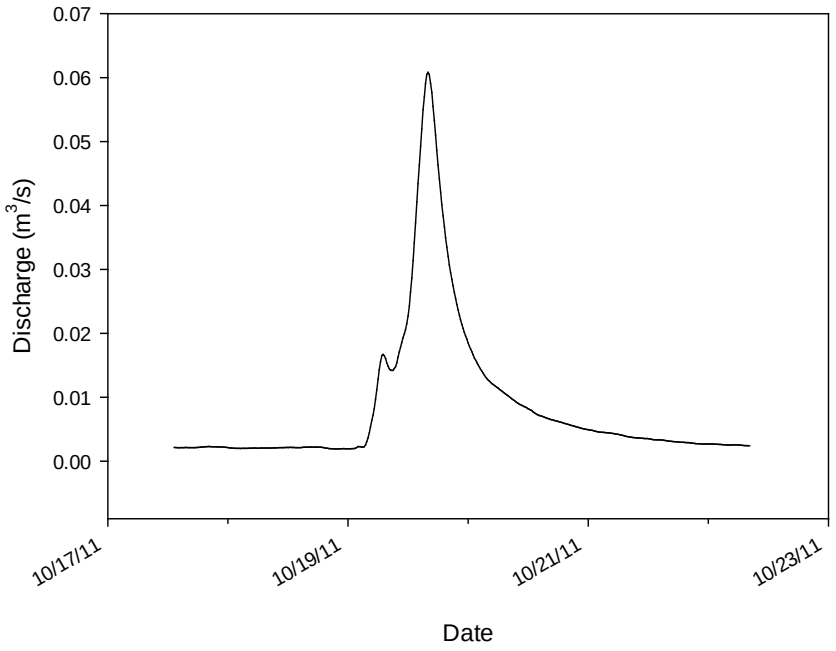

Figure G.13. Discharge from LMS on October 18, 2011.

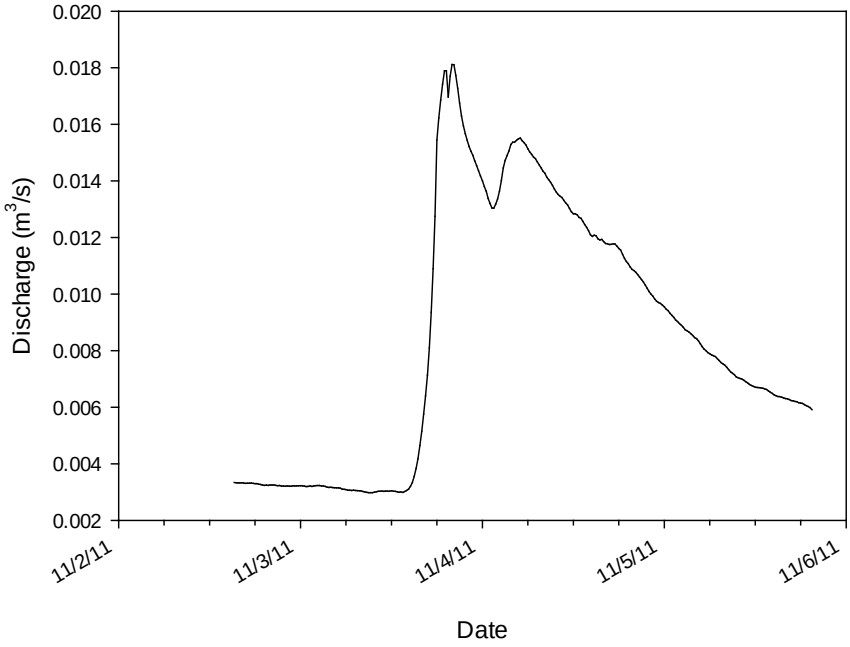

Figure G.14. Discharge from LMS on November 2, 2011.

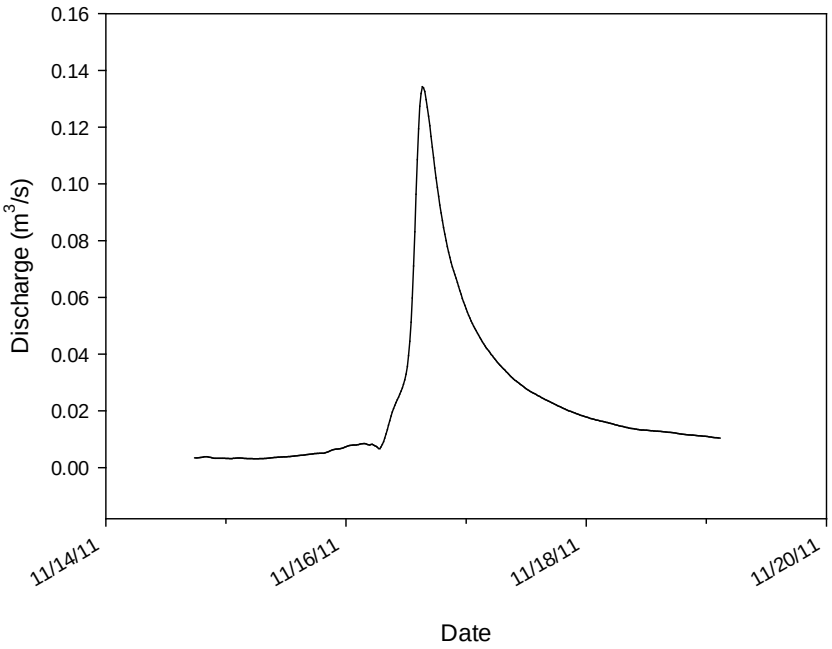

Figure G.15. Discharge from LMS on November 15, 2011.

REFERENCES

Agouridis, C.T. C.D. Barton, and R.C. Warner. 2011. UT to Laurel Fork: Guy Cove (Hollow Fill #9) stream restoration monitoring report. Monitoring year 3: 2011. Submitted to the U.S. Army Corps of Engineering, Louisville District.

Agouridis, C.T., C.D. Barton, and R.C. Warner. 2009. Recreating a headwater stream system on a head-of-hollow fill: a Kentucky case study. *In* Proceedings of Geomorphic Reclamation and Natural Stream Design at Coal Mines, Bristol, VA, April 27-30.

Ahearn, D.S., R.W. Sheibley, and R.A. Dahlgren. 2005. Effects of river regulation on water quality in the Lower Mokelumne River, California. River Research and Applications 21: 651-670.

Ahern, D.S., R.W. Sheibley, and R.A. Dahlgren. 2005. Effects of river regulation on water quality in the Lower Mokelumne River, California. River Research and Applications 21: 651-670.

Barton, C. 2011. Coal mining versus water quality: an electrifying issue. Water Resources IMPACT 13: 23-24.

Chapman, P.M., H. Bailey, and E. Canaria. 2000. Toxicity of total dissolved solids associated with two mine effluents to chironomid larvae and early life stages of rainbow trout. 2000. Environmental Toxicology and Chemistry 19: 210-214.

Cherry, M.A. 2006. Hydrochemical characterization of the headwater catchments in eastern Kentucky. M.S. Thesis, University of Kentucky, Lexington, KY.

Fogle, A.W., J.L. Taraba, and J.S. Dinger. 2003. Mass load estimation errors utilizing grab sampling strategies in a karst watershed. Journal of the American Water Resources Association 39: 1361-1372.

Fritz, K.M., S. Fulton, B.R. Johnson, C.D. Barton, J.D. Jack, D.A. Word, and R.A. Burke. 2010. Structural and functional characteristics of natural and constructed channels draining a reclaimed mountaintop removal and valley fill coal mine. Journal of the North American Benthological Society 29: 673-689.

Fritz, K.M., S. Fulton, B.R. Johnson, C.D. Barton, J.D. Jack, D.A. Word, and R.A. Burke. 2010. Structural and functional characteristics of natural and constructed channels draining a reclaimed mountaintop removal and valley fill coal mine. Journal of the North American Benthological Society 29: 673-689.

Grant, D.M. 1992. ISCO open channel flow measurement handbook, 3rd ed. ISCO, Inc., Lincoln, NE.

Haan, C.T. 1977. Statistical methods in hydrology. Iowa State University Press, Ames, IA.

Hayashi, M. 2004. Temperatur-electrical conductivity relation of water for environmental monitoring and geophysical data inversion. Environmental Monitoring and Assessment 96: 119-128.

Henjum, M.B., R.M. Hozalski, C.R. Wennen, W. Arnold, and P.J. Novak. 2010. Correlations between *in situ* sensor measurements and trace organic pollutants in urban streams. Journal of Environmental Monitoring 12: 225-233.

Jones, A.S., D.K. Stevens, J.S. Horsburgh, and N.O. Mesner. 2011. Surrogate measures for providing high frequency estimates of total suspended solids and total phosphorus concentrations. Journal of the American Water Resources Association 47: 239-253.

Kennedy, A.J., D.S. Cherry, and R.J. Currie. 2003. Field and laboratory assessment of a coal processing effluent in the Leading Creek watershed, Meigs County, Ohio. Archives of Environmental Contamination and Toxicology 44: 324-331.

Kimmel, W.G. and D.G. Argent. 2010. Stream fish community responses to a gradient of specific conductance. Water, Air, & Soil Pollution 206: 49-56.

Kirchner, J.W., X. Feng, C. Neal, and A.J. Robson. 2004. The fine structure of water-quality dynamics: the (high-frequency) wave of the future. Hydrological Processes 18: 1353-1359.

Kleinbaum, D.G., L.L. Kupper, A. Nizam, and K.E. Muller. 2008. Applied regression analysis and other multivariable methods. 4th ed. Duxbury, Belmont, CA.

Kobayashi, D., K. Suzuki, and M. Nomura. 1990. Diurnal fluctuations in stream flow and in specific electric conductance during drought periods. Journal of Hydrology 115: 105-114.

Kobayashi, D., K. Suzuki, and M. Nomura. 1990. Diurnal fluctuations in stream flow and in specific electric conductance during drought periods. Journal of Hydrology 115: 105-114.

Leib, B.G., J.D. Jabro, and G.R. Matthews. 2003. Field evaluation and performance comparison of soil moisture sensors. Soil Science 168: 396-408.

Lindberg, T.T., E.S. Barnhardt, R. Bier, A.M. Helton, R. B. Merola, A. Vengosh, and R.T. Di Giulio. 2011. Cumulative impacts of mountaintop mining on an Appalachian watershed. Proceedings of the National Academy of Sciences 108: 20929-20934.

Lindberg, T.T., E.S. Bernhardt, R.Bier, A.M. Helton, R.B. Merola, A. Vengosh, and R.T. Di Giulo. 2011. Cumulative impacts of mountaintop mining on an Appalachian watershed. Proceedings of the National Academy of Science 108: 20929-20934.

Maupin, T.P., C.T. Agouridis, C.D. Barton, and R.C. Warner. 2012. Laboratory evaluation of conductivity sensor accuracy and temporal consistency. *In:* Proceedings of the 2012 National Meeting of the American Society of Mining and Reclamation, Tupelo, MS, Sustainable Reclamation, June 8-15, 2012. R.I. Barnhisel (Ed.).

Merriam, E.R., J.T. Petty, G.T. Merovich, Jr., J.B. Fulton, and M.P. Strager. 2011. Additive effects of mining and residential development on stream conditions in a central Appalachian watershed. Journal of the North American Benthological Society 30: 399-418.

Messinger, T. 2003. Comparison of storm response of streams in small, unmined and valley-filled watersheds, 1999-2001, Ballard Fork, West Virginia. U.S. Geological Survey Water-Resources Investigations Report 02-4303, Charleston, WV.

Miguntanna, N.S., P. Egodawatta, S. Kokot, and A. Goonetilleke. 2010. Determination of a set of surrogate parameters to assess urban stormwater quality. Science of the Total Environment 408: 6251-6259.

Pond, G.J. 2012. Biodiversity loss in Appalachian headwater streams (Kentucky, USA): Plecoptera and Trichoptera communities. Hydrobiologia 679: 97-117.

Pond, G.J. 2010. Patterns of Ephemeroptera taxa loss in Appalachian headwater streams (Kentucky, USA). Hydrobiologia 641: 185-201.

Pond, G.J., M.E. Passmore, F.A. Borsuk, L. Reynolds, and C.J. Rose. 2008. Downstream effects of mountaintop coal mining: comparing biological conditions using family- and genus-level macroinvertebrate bioassessment tools. Journal of the North American Benthological Society 27: 717-737.

Pond, G.J., M.E. Passmore, F.A. Borsuk, L. Reynolds, and C.J. Rose. 2008. Downstream effects of mountaintop coal mining: comparing biological conditions using family- and genus-level macroinvertebrate Bioassessment tools. Journal of the North American Benthological Society 27: 717-737.

Ramos, P.M., J.M. Dias Pereira, H.M. Geirinhas Ramos, and A.L. Ribeiro. 2008. A four-terminal water-quality-monitoring conductivity sensor. IEEE Transactions on Instrumentation and Measurement 57: 577-583.

Rizzoni, G. 1993. Principles and applications of electrical engineering. Richard D. Irwin, Inc., Boston, MA.

SAS Institute. 2008. SAS user's guide. Version9. SAS Institute, Cary, NC.

Settle, S., A. Goonetilleke, and G. Ayoko. 2007. Determination of surrogate indicators for phosphorus and solids in urban stormwater: application of multivariate data analysis techniques. Water, Air, & Soil Pollution 182: 149-161.

Stubblefield, A.P., J.E. Reuter, R.A. Dahlgren, and C.R. Goldman. 2007. Use of turbidometry to characterize suspended sediment and phosphorus fluxes in the Lake Tahoe basin, California, USA. Hydrological Processes 21: 281-291.

Tchobanoglous, G., F.L. Burton, and H.D. Stensel. 2003. Wastewater Engineering: Treatment and Use, 4th ed. McGraw-Hill, New York, NY.

Tchobanoglous, G., F.L. Burton, and H.D. Stensel. 2003. Wastewater engineering: treatment and use, 4th ed. McGraw-Hill, New York, NY.

Tomlinson, M.S. and E.H. De Carlo. 2003. The need for high resolution time series data to characterize Hawaiian streams. Journal of the American Water Resources Association 39: 113-123.

[USEPA] United States Environmental Protection Agency. 2011b. Memorandum, improving EPA review of Appalachian surface coal mining operations under the Clean Water Act, National Environmental Policy Act, and the Environmental Justice Executive Order. Available at: http://www.epa.gov/owow/wetlands/guidance/pdf/appalachian_mtntop_mining_summary.pdf. Accessed August 30, 2011.

[USEPA] United States Environmental Protection Agency. 2005. Mountaintop mining/valley fills in Appalachia. Final programmatic environmental impact statement. U.S. Environmental Protection Agency, Region 3, Philadelphia, PA. Available online at: http://www.epa.gov/region3/mtntop/pdf/mtm-vf_fpeis_full-document.pdf.

[USEPA] United States Environmental Protection Agency. 2011. Memorandum, improving EPA review of Appalachian surface coal mining operations under the Clean Water Act, National Environmental Policy Act, and the Environmental Justice Executive Order. Available at: http://water.epa.goc/owow/wetlands/guidance/pdf/appalachia_mtntop_mining_summary.pdf. Accessed August 30, 2011.

[USEPA] United States Environmental Protection Agency. 2011a. The effects of mountaintop mines and valley fills on aquatic ecosystems of the Central Appalachian Coalfields. Office of Research and Development, National Center for Environmental Assessment, Washington, D.C. EPA/600/R-09/138F.

[USEPA] United States Environmental Protection Agency. 2012. National recommended water quality criteria. Available at: http://water.epa.gov/scitech/swguidance/standards/current/index.cfm. Accessed on January 10, 2012.

Wagner, R.J., H.C. Mattraw, G. F. Ritz, and B.A. Smith. 2006. Guidelines and standard procedures for continuous water-quality monitors: site selection, field operation, calibration, record computation, and reporting. United States Geological Survey, Techniques and Methods 1-D3, Reston, VA.

Wagner, R.J., H.C. Mattraw, G.F. Ritz, and B.A. Smith. 2006. Guidelines and standard procedures for continuous water-quality monitors: site selection, field operation, calibration, record computation, and reporting. Techniques and Methods 1-D3. U.S. Geological Survey, Reston, VA.

Wang, Z. and L.A. Goonewardene. 2004. The use of MIXED models in the analysis of animal experiments with repeated measures data. Canadian Journal of Animal Science 84: 1-11.

Wei, X. H. Wei, and R.C. Viadero. 2011. Post-reclamation water quality trend in a Mid-Appalachian watershed of abandoned mined lands. Science of the Total Environment 409: 941-948.

Whelan, A. and F. Regan. 2006. Antifouling strategies for marine and riverine sensors. Journal of Environmental Monitoring 8: 880-886.

Whelan, A. and F. Regan. 2006. Antifouling strategies for marine and riverine sensors. Journal of Environmental Monitoring 8: 880-886.

Wiley, J.B. and F.D. Brogan. 2003. Comparison of peak discharges among sites with and without valley fills for the July 8-9, 2001, flood in the headwaters of Clear Fork, Coal River Basin, mountaintop coal-mining region, southern West Virginia. U.S. Geological Survey Open-File Report 03-133, Charleston, WV.

Williamson, T.N. and C.G. Crawford. 2011. Estimation of suspended-sediment concentration from total suspended solids and turbidity data for Kentucky, 1978-1955. Journal of the American Water Resources Association 47: 739-749.

Yoder, R.E., D.L. Johnson, J.B. Wilkerson, and D.C. Yoder. 1998. Soil water sensor performance. Applied Engineering in Agriculture 14: 121-133.

VITA

DATE AND PLACE OF BIRTH

February 8, 1987 Lexington, Kentucky

EDUCATION

B.S. Biosystem and Agricultural Engineering, University of Kentucky, Lexington, Kentucky, May 2010

PROFESSIONAL EXPERIENCE

Graduate Research Assistant, Department of Biosystems and Agricultural Engineering, University of Kentucky, Lexington, Kentucky. May 2010 – Present. Advisor: Dr. C. T. Agouridis.

Sr. Engineering Aid. Lexington Fayette Urban County Government. May 2007 to August 2009

LICENSURE AND CERTIFICATION

Engineer In Training State of Kentucky (Certificate No.13907, May 8, 2010)

PROFESSIONAL SOCIETIES

American Society of Biosystem and Agricultural Engineers

PUBLICATIONS AND AWARDS:

Maupin, T., C.D. Barton, C.T. Agouridis, and R.C. Warner. 2012. Specific Conductivity Sensor Performance: Laboratory Evaluation. In: Proceedings of 2012 National Meeting of the American Society of Mining and Reclamation. Published by ASMR, 3134 Montavesta Rd., Lexington, KY 40502.

Selected to present at the NSF sponsored Graduate Student Water Research Conference held at Oklahoma State University in April 2012. Awarded Outstanding Graduate Student Oral Presentation Award.